Estratto da *Rendiconti della Scuola Internazionale di Fisica «E. Fermi»* - XXXV Corso

The General-Relativistic Theory of Stellar Structure and Dynamics (*).

K. S. THORNE (**)

Palmer Physical Laboratory, Princeton University - Princeton, N. J.

(*) Supported in part by U. S. Air Force Office of Scientific Research.

(**) NSF Postdoctoral Fellow. Present address: California Institute of Technology, Pasadena, Cal.

1. – Introduction.

Astrophysics and general relativity influenced each other very little during the long period between the first few years of relativity theory and about 1963. In fact, during that period the absence of any extensive experimental or observational phenomena in which general relativistic effects might be important tended to insulate Einstein's theory from all other branches of physics.

However, during the last three years a marked change has begun to occur: The discovery and investigation of quasi-stellar radio sources (***), of explosions in galactic nuclei (*•*), and of X-ray emission from supernova remnants (•**) have suggested to astrophysicists that strong gravitational fields might, after all, play an important role in astrophysical phenomena. At the same time, major advances in the techniques of radio and optical astronomy have enabled astronomers to begin to determine the cosmological structure of the universe (*••)—which structure is believed to be governed by general relativity—; and the development of powerful new experimental techniques has made possible new and improved tests of Einstein's theory (•**•). Because of these developments, strong

(***) See, *e.g.*, ROBINSON *et al.* (1965) and the lectures in this volume by E. M. BURBIDGE and A. R. SANDAGE.

(*•*) See, *e.g.*, BURBIDGE, BURBIDGE and SANDAGE (1963); also the lectures in this volume by E. M. BURBIDGE and A. R. SANDAGE.

(•*•) See, *e.g.*, the lectures in this volume by GIACCONI *et al.*

(*••) See, *e.g.*, the lectures in this volume by SANDAGE and by SCIAMA; also DICKE *et al.* (1965).

(•**•) See, *e.g.*, DICKE (1964), WEBER (1964), POUND and SNIDER (1964) and other references cited there, HILL and ZANONI (1966), SCHIFF (1960, 1966), FAIRBANK and EVERITT (1966), SHAPIRO (1964, 1966 *a*, *b*), ROSS and SCHIFF (1966).

gravitation physics as described by general relativity is rapidly becoming of interest to astrophysicists, and astrophysics is rapidly becoming of interest to relativists.

The present set of lectures is an attempt to facilitate the growing dialogue and co-operation between astrophysicists and relativists by presenting the general-relativistic theory of stellar structure and dynamics in a manner which, hopefully, will be intelligible to both, as well as to the uninitiated graduate student. As a result of this orientation neither a knowledge of the Newtonian theory of stellar structure, nor previous contact with general relativity are prerequisites for understanding these lectures—at least I hope they are not. All I have intended to assume of the reader is a strong background in the fundamentals of classical and modern physics, such as a student acquires in a four-year course of study at the university level.

The desire to not assume any general relativity as a prerequisite to reading these lectures has led me to employ a slightly novel—but, I believe, very powerful—approach to the derivation and discussion of the relativistic laws of stellar structure and dynamics. At no point in these lectures is tensor analysis or modern differential geometry used. Instead, the fundamental physical concepts of general relativity (*e.g.* the curvature of space-time), and a few basic results of the theory (*e.g.* red-shift in a static gravitational field) are introduced; and then these concepts and results are used, together with elementary considerations from theromodynamics and classical mechanics, as a complete basis for all further considerations. It must be emphasized that, although this « poor man's approach » to general relativity is extremely useful and powerful in the present context, it is so *only* because we restrict our attention to situations with spherical symmetry and thereby strongly limit the types of dynamical effects which are considered. (For example, spherically symmetric bodies cannot radiate gravitational waves.)

I make no apology to either the astrophysicist or the relativist for the omission of tensorial and differential-geometric tools from these lectures. The astrophysicist who is interested only in applying general relativity to stellar structure and dynamics has little or no need for the full formalism of relativity. On the other hand, this presentation of stellar theory will probably be clearer physically to a relativist who is familiar with differential geometry than would be a presentation couched in differential-geometric terms.

Throughout these lectures two distinct sets of physical units are employed: *standard* c.g.s. *units*, and *geometrized units*. Geometrized units are units in which Newton's gravitation constant, G, the speed of light, c, and Boltzmann's constant, k, are set equal to unity, and all quantities are expressed in terms of length. Quantities measured in geometrized units are distinguished from the corresponding cgs quantities by an asterisk; for example, the mass of the sun is $M_\odot = 1.989 \cdot 10^{33}$ g in c.g.s. units, or $M^*_\odot = GM_\odot/c^2 = 1.476$ km in geometrized

units. Table I shows how to convert quickly from one set of units to the other.

These lectures are divided into 6 major Sections: In Sect. **2** are presented the basic thermodynamic and gravitational concepts upon which the subsequent discussions are based. Section **3** contains a derivation and discussion of the general-relativistic equations of stellar structure, together with delineations and proofs of some fundamental properties of relativistic stellar models. Section **4** is a

TABLE I. – *The conversion from* c.g.s. *units to geometrized units* (*).

Quantity	cgs units	Geometrized units
Length	l (cm)	l (cm)
Time	t (s)	t^* (cm) $= ct = 2.997\,925 \cdot 10^{10}\, t$
Mass	M (g)	M^* (cm) $= GM/c^2 = 0.742 \cdot 10^{-28}\, M$
Energy	E (erg)	E^* (cm) $= GE/c^4 = 0.826 \cdot 10^{-49} E$
Density of mass	ϱ (g/cm^3)	ϱ^* (cm^{-2}) $= G\varrho/c^2 = 0.742 \cdot 10^{-28}\varrho$
Density of energy	ε (erg/cm^3)	ε^* (cm^{-2}) $= G\varepsilon/c^4 = 0.825 \cdot 10^{-49}\varepsilon$
Pressure	p (dyne/cm^2)	p^* (cm^{-2}) $= Gp/c^4 = 0.825 \cdot 10^{-49} p$
Temperature	T (°K)	T^* (cm) $= GkT/c^4 = 1.140 \cdot 10^{-65}\, T$
Entropy	S (erg/°K)	S^* (dimensionless) $= S/k = 7.243\ 5 \cdot 10^{15}\, S$
Luminosity	L (erg/s cm^2)	L^* (cm^{-2}) $= GL/c^5 = 2.755 \cdot 10^{-60} L$
Mass of sun	$M_\odot = 1.989 \cdot 10^{33}$ g	$M^*_\odot = GM_\odot/c^2 = 1.476$ km
Luminosity of sun	$L_\odot = 3.90 \cdot 10^{33}$ erg/s	$L^*_\odot = GL_\odot/c^5 = 1.07 \cdot 10^{-26}$ cm^{-2}
Nuclear density	$\varrho_{\text{nuc}} = 2 \cdot 10^{14}$ g/cm^3	$\varrho^*_{\text{nuc}} = G\varrho_{\text{nuc}}/c^2 = 1.48 \cdot 10^{-14}$ cm^{-2}
Quantum of angular momentum	$\hbar = 1.0544 \cdot 10^{-27}$ gcm^2/s	$\hbar^* = G\hbar/c^3 = 2.610 \cdot 10^{-66}$ cm^2

(*) Adapted from HARRISON, THORNE, WAKANO and WHEELER (1965).

development of the theory of the dynamical stability of relativistic stellar models. In Sect. **5** the tools developed in Sect. **3** and **4** are applied to configurations of matter near the endpoint of thermonuclear evolution (white dwarfs, neutron stars, hyperon stars); while in Sect. **6** those tools are applied to a wide class of hot, nondegenerate stellar models. Finally, Sect. **7** is a brief introduction to the theory of gravitational collapse to zero volume and infinite density.

If this written version of my lectures seems to overemphasize hot, nondegenerate stars as compared to configurations at the endpoint of thermonuclear evolution, it is because there is already in print a comprehensive monograph on configurations at the endpoint of thermonuclear evolution. That monograph—HARRISON, THORNE, WAKANO, and WHEELER (1965); cited henceforth as HTWW—is in large measure a companion to these lectures. Also closely related to these lectures are the review articles by ZEL'DOVICH and NOVIKOV (1964, 1965), and the brief, semipopular article of THORNE (1965*c*).

The form of these lectures and my point of view on the topics treated here have been influenced by a large number of people, foremost among whom are J. M. BARDEEN, J. P. WRIGHT, and *above all* J. A. WHEELER. I thank them.

2. – Thermodynamic and gravitational preliminaries.

2·1. *Separation of short-range and long-range forces* (*). – The structure and dynamics of a star are governed by an interplay between nuclear forces, electromagnetic forces, and gravitational forces. If it were necessary to describe the interactions between these three fundamental forces in precise mathematical detail, so complex a problem as the structure of a star could never be studied. The basic simplification which makes stellar theory possible is the clean separation of the short-range nuclear and electromagnetic forces from the long-range gravitational forces. By the phrase « clean separation of forces » we mean the following. In astrophysical situations the characteristic distance over which the gravitational force changes is many orders of magnitude greater than the microscopic scale at which nuclear and electromagnetic forces act. Consequently, the thermodynamic properties of matter and radiation, which describe the statistically averaged, macroscopic effects of nuclear and electromagnetic forces, are unaffected by gravitation. Gravitation is important only at the macroscopic scale, where, in cooperation with the thermodynamic properties of matter, it fixes the thermodynamic state (pressure, density, temperature).

Let us verify that short-range and long-range forces are, indeed, separated in astrophysical situations. There are several fundamental short-range lengths over which gravitational forces must be homogeneous in order for ordinary, « flat-space » thermodynamics to be valid. One fundamental short-range length is the $\sim 10^{-13}$ cm which characterizes nuclear forces. Another is the characteristic distance of action of strong electric forces, which is usually less than or of the order of the separation between atomic nuclei (**).

$$(2.1a)\quad l_{\text{s.r.}} \sim [(\text{density of total mass-energy})^*/(\text{nuclear rest mass})^*]^{-\frac{1}{3}} = (\varrho^*/\mu_{\text{N}}^*)^{-\frac{1}{3}}$$

(macroscopic charge neutrality). A third short-range length is the size of a sample of matter containing $\sim 10^{21}$ atomic nuclei (**),

$$(2.1b)\qquad l_{\text{s.r.}} \sim 10^7 (\varrho^*/\mu_{\text{N}}^*)^{-\frac{1}{3}} .$$

(*) For a more detailed exposition of these ideas see HTWW, p. 96.

(**) Formulae (2.1*a*), (2.1*b*) for the separation between nuclei and the size of a region containing 10^{21} nuclei break down at densities above $\sim 10^{14}$ g/cm^3 because of large Fermi kinetic energies and nuclear interaction energies. However, these formulae remain sufficiently accurate for present purposes up to $\sim 10^{30}$ g/cm^3.

(It is over such samples of matter that the statistical averaging which underlies thermodynamics takes place.) Finally, additional fundamental lengths are the characteristic « localizability distances »—the Compton wave lengths— of the particles which make up the matter. An upper limit on all of the short-range lengths is

$$(2.2)\qquad \left| \begin{array}{ll} l_{\text{s.r.}} \leqslant \begin{cases} 10^{7}(\varrho^{*}/\mu_{\text{N}}^{*})^{-\frac{1}{3}} & \text{if } \varrho \leqslant 10^{27}\ \text{g/cm}^{3} \\ \hbar/m_{e}c \sim 10^{-10}\ \text{cm} & \text{if } \varrho \geqslant 10^{27}\ \text{g/cm}^{3}, \end{cases} \\ \sim \begin{cases} 10^{4}\ \text{km} & \text{if } \varrho \sim 10^{-29}\ \text{g/cm}^{3}\ \text{(density of universe)}, \\ 0.1\ \text{cm} & \text{if } \varrho \sim 1\ \text{g/cm}^{3}\ \text{(density of water)}, \\ 10^{-6}\ \text{cm} & \text{if } \varrho \sim 10^{15}\ \text{g/cm}^{3}\ \text{(nuclear density)}, \\ 10^{-10}\ \text{cm} & \text{if } \varrho \gtrsim 10^{27}\ \text{g/cm}^{3}. \end{cases} \end{array} \right.$$

The characteristic size of inhomogeneities in a gravitational field is the radius of the space curvature which, according to general relativity, describes gravitation. In a region of space-time where the density of mass-energy is ϱ^{*}, this radius of curvature is (see, *e.g.* HTWW pp. 13 and 97)

$$(2.3)\qquad l_{\text{l.r.}} \sim \varrho^{*-\frac{1}{3}} \sim \begin{cases} \text{the Hubble radius} & \text{if } \varrho \sim 10^{-29}\ \text{g/cm}^{3}\ \text{(density of universe)}, \\ 10^{14}\ \text{cm} & \text{if } \varrho \sim 1\ \text{g/cm}^{3}\ \text{(density of water)}, \\ 10^{7}\ \text{cm} & \text{if } \varrho \sim 10^{15}\ \text{g/cm}^{3}\ \text{(nuclear density)} \\ 10^{-10}\ \text{cm} & \text{if } \varrho \sim 10^{49}\ \text{g/cm}^{3}. \end{cases}$$

So long as $l_{\text{l.r.}}$ is orders of magnitude greater than $l_{\text{s.r.}}$, *i.e.* so long as

$$(2.4)\qquad \varrho \ll 10^{49}\ \text{g/cm}^{3},$$

long-range gravitational forces can be cleanly separated from short-range forces. Condition (2.4) is satisfied with more than 20 orders of magnitude to spare in all conceivable astrophysical situations except one: the endpoint of gravitational collapse to a « general-relativistic singularity » (see Sect. **7**). Hence, throughout our discussion (except in analysing the endpoint of collapse) we can place great confidence in the clean separation of gravitational forces from the short-range forces which determine the construction and thermodynamic properties of matter.

2·2. *Thermodynamics, the science of short-range forces.*

2·2.1. Fundamental thermodynamic quantities. The macroscopic effects of short-range forces on the constitution of matter are described by the thermodynamic properties of matter. Throughout our discussion we shall restrict ourselves to matter which has the properties of a *perfect fluid*—*i.e.*,

nonviscous matter in which all stresses are zero except for an isotropic pressure. The basic thermodynamic quantities of interest to us will be:

a) *Pressure*, p (dyne/cm^2) or p^* (cm^{-2}) $= Gp/c^4$, as measured in a reference frame comoving with the matter. We shall assume that the pressure is always isotropic (negligible shear).

b) *Number density of baryons*, n (cm^{-3}) or $n^* = n$, as measured in a reference frame comoving with the matter. We shall often make use of the law of conservation of baryons.

c) *Average rest mass of a baryon*, μ_B (g) or μ_B^* (cm) $= G\mu_B/c^2$. The quantity μ_B depends upon the nuclear state of the matter: for a hydrogen gas μ_B is the mass of a hydrogen atom in its ground state; for a sample of pure ^{56}Fe, μ_B is 1/56 times the mass of a ^{56}Fe atom in its ground state. For a mixture of relativistically degenerate electron, proton, and neutron gases containing 8 neutrons for each proton and electron, μ_B is $(\frac{8}{9})\times$(rest mass of neutron)$+$ $+(\frac{1}{9})\times$(mass of hydrogen atom in its ground state). Whenever nuclear reactions occur, μ_B changes.

d) *Internal energy density of the matter*, ε (erg/cm^3) or ε^* (cm^{-2}) $= G\varepsilon/c^4$, as measured in a reference frame comoving with the matter. The internal energy includes all forms of energy except the rest mass of the baryons. For example, it includes atomic excitation energies, thermal kinetic energies, « zero-point » energies of compression, and photon energies.

e) *Density of total mass-energy*, ϱ (g/cm^3) or ϱ^* (cm^{-2})$=G\varrho/c^2$, as measured in a reference frame comoving with the matter. This includes rest mass-energy and internal energy

$$\varrho^* = \mu_B^* n + \varepsilon^* . \tag{2.5}$$

f) *Thermodynamic temperature of the matter*, $T(^\circ\mathrm{K})$ or $T^*(\mathrm{cm}) = G(kT)/c^4$, as measured in a reference frame comoving with the matter.

g) *Entropy per baryon*, s (erg/$^\circ$K) or s^*(dimensionless) $= s/k$, as measured in a reference frame comoving with the matter. The density of entropy is clearly ns (erg/$^\circ$K cm^3) or ns^* (cm^{-3}).

h) *Fractional nuclear abundances*, $Z_H, Z_{He}, Z_n, Z_\Lambda, \ldots . Z_k$ is the fraction of all baryons in a given sample of matter which are in the form k. The nuclear abundances must satisfy

$$\sum_k Z_k = 1 , \qquad \sum_k \mu_k Z_k = \mu_B , \tag{2.6}$$

where μ_k is the rest mass per baryon of the nuclear species k, and μ_B is the average baryonic rest mass.

i) *Nuclear chemical potentials*, $\bar{\mu}_k(g)$ or $\bar{\mu}_k^*(\mathrm{cm}) = G\bar{\mu}_k/c^2$. Let one baryon of species k be inserted into a sample of matter, along with enough internal energy to keep the sample's total entropy and volume constant. The total mass-energy added in this process is equal to $\bar{\mu}_k$, the chemical potential for baryons of type k.

In almost all astrophysical situations to be considered in these lectures nuclear burning occurs sufficiently slowly that nuclear reactions are *not* in thermodynamic equilibrium with other types of thermodynamic energy exchange. Consequently, when a sample of matter is subjected to a thermodynamic change of state the quantities p^*, n, ε^*, ϱ^*, T^*, and s^* change, but the average baryonic rest mass, μ_B^*, and the nuclear abundances remain fixed. Of the 6 parameters p^*, n, ε^*, ϱ^*, T^*, s^* which describe the thermodynamic state only 5—p^*, n, ϱ^*, T^*, s^*—are fundamental; the internal energy ε^* can always be expressed in terms of the other parameters through eq. (2.5).

In addition to the above thermodynamic parameters we shall be interested in the *adiabatic indices*, defined by (*)

$$\Gamma_1 \equiv (\partial \ln p^*/\partial \ln n)_{s^*} = (\varrho^* + p^*)\, p^{*-1}(\partial p^*/\partial \varrho^*)_{s^*}\,, \tag{2.7}$$

$$\Gamma_2 \equiv [1 - (\partial \ln T^*/\partial \ln p^*)_{s^*}]^{-1}\,, \tag{2.8}$$

$$\Gamma_3 \equiv 1 + (\partial \ln T^*/\partial \ln n)_{s^*} = 1 + (\varrho^* + p^*)\, T^{*-1}(\partial T^*/\partial \varrho^*)_{s^*}\,, \tag{2.9}$$

and in the *velocity of sound* (*)

$$v_s^* = [\Gamma_1 p^*/(\varrho^* + p^*)]^{\frac{1}{2}} = [(\partial p^*/\partial \varrho^*)_{s^*}]^{\frac{1}{2}}\,. \tag{2.10}$$

Note that because the velocity of sound can never exceed the velocity of light ($v_s^* \leqslant 1$), the pressure, p^*, can never exceed the density of mass-energy, ϱ^*.

2.2. Effects of special relativity on the laws of thermodynamics. By virtue of the separation of short-range and long-range forces, we need not take general relativity into account when discussing the thermodynamic properties of matter. Furthermore, so long as we carry out our thermodynamic analysis in reference frames which comove with the matter, we need not consider special relativity effects—with one exception. We must be careful to take into account the equivalence of mass and energy and the consequent inclusion

(*) The second equality in eq. (2.7) and that in (2.9) are straightforward consequences of the first law of thermodynamics—see eq. (2.14). Expression (2.10) for the velocity of sound has been derived within the framework of special relativity by TAUB (1948) and in general relativity by CURTIS (1950). The partial derivatives in eqs. (2.7)-(2.10) must be taken, not only with entropy held constant, but also with nuclear abundances held constant.

of the internal energy density, ε^*, in the total density of mass-energy, ϱ^*. (Cf. equation (2.5).)

To gain some insight into the manner in which the equivalence of mass and energy affects the formulae of thermodynamics, let us state the relationship between heat and entropy, and the first and second laws of thermodynamics in their correct relativistic forms: 1) If a small amount of heat $đQ^*$ is added quasi-statically to a small sample of matter containing δA baryons, then the entropy of the sample is increased by

$$\mathrm{d}(s^*\,\delta A) = (\delta A)\,\mathrm{d}s^* = đQ^*/T^* \,. \tag{2.11}$$

This formula is the same in relativity theory as in ordinary thermodynamics.

ii) During any quasi-static change in the state of our sample in which the total number of baryons, δA, is held fixed, but nuclear reactions may occur, the volume may change, and heat may be added

$$\begin{aligned}\mathrm{d}(\text{total mass-energy}) &\equiv \mathrm{d}(\varrho^*\,\delta A/n) = \\ &= -\,p^*\,\mathrm{d}(\text{volume}) + T^*\,\mathrm{d}(s^*\,\delta A) + \sum_k \bar{\mu}_k^*\,\mathrm{d}(\delta A Z_k) = \\ &= -\,p^*\,\mathrm{d}(\delta A/n) + T^*\,\delta A\,\mathrm{d}s^* + \sum_k \bar{\mu}_k^*\,\delta A\,\mathrm{d}Z_k \,,\end{aligned}$$

or, equivalently,

$$\mathrm{d}\varrho^* = [(\varrho^* + p^*)/n]\,\mathrm{d}n + T^* n\,\mathrm{d}s^* + \sum_k \bar{\mu}_k^* n\,\mathrm{d}Z_k \,. \tag{2.12}$$

These formulae for the first law of thermodynamics differ from the more familiar Newtonian formula

$$\mathrm{d}(\text{internal energy}) = -\,p\mathrm{d}(\text{volume}) + đQ + \sum_k \bar{\mu}_k\,\mathrm{d}(\text{number of type } k) \,,$$

because in relativistic theory we must allow for the possibility of changes in the rest mass-energies of the baryons. 3) For any change in the state of our sample which occurs in isolation

$$\mathrm{d}(\text{total entropy}) = (\delta A)\,\mathrm{d}s^* \geqslant 0; \tag{2.13}$$

and equality holds if and only if the change of state occurs reversibly. This formula for the second law of thermodynamics is the same as the corresponding nonrelativistic formula.

An important consequence of the relativistic first law (2.12) is an equation relating isentropic changes in the density of mass-energy to changes in baryon number density

$$(\partial\varrho^*/\partial n)_{s^*} = (\varrho^* + p^*)/n \,. \tag{2.14}$$

The more familiar nonrelativistic statement of this relation is the trivial formula

$$(\partial \varrho^*/\partial n)_{s^*} = \mu_B^* \qquad \text{(nonrelativistic limit)}.$$

Additional examples of changes forced onto the formulae of thermodynamics by the equivalence of mass and energy can be found in expression (2.7) and (2.9) for the adiabatic indices Γ_1 and Γ_2 in terms of ϱ^* and p^*, and in expression (2.10) for the velocity of sound in terms of Γ_1, ϱ^*, and p^*. The new, relativistic forms of these expressions are quite easily traced back through eq. (2.14) to the effect of the equivalence of mass and energy on the first law of thermodynamics.

All other formulae of thermodynamics can be put into relativistic form by going back to the foundations of thermodynamics, adding the law of the equivalence of mass and energy, and rederiving the formulae desired by the usual, nonrelativistic method. (See, *e.g.*, TOLMAN (1934*a*) for a partial development of the theory.)

2'2.3. Equations of state. Let us focus our attention on a small sample of matter located inside a static or dynamic star. The thermodynamic properties of that sample can be specified in either of two equivalent ways;

1) by giving the *fundamental equation*

$$\varrho^* = f(n, s^*, Z_1, Z_2, \ldots, Z_N) \tag{2.15}$$

for the material of which the sample is made, or

2) by giving $2 + N$ *equations of state* relating the «intrinsic variables», p^*, T^*, $\bar{\mu}_1^*, \ldots, \bar{\mu}_N^*$, to the «reduced extrinsic varables», ϱ^*, n, and s^*, and to the nuclear abundances, $Z_1, Z_2, \ldots, Z_N$ — *e.g.*

$$\left\{\begin{aligned} p^* &= g(\varrho^*, n, s^*, Z_1, \ldots, Z_N)\,, \\ T^* &= h(\varrho^*, n, s^*, Z_1, \ldots, Z_N)\,, \\ \bar{\mu}_k^* &= j_k(\varrho^*, n, s^*, Z_1, \ldots, Z_N)\,. \end{aligned}\right. \tag{2.16}$$

Once the fundamental equation or $2 + N$ equations of state have been given, the machinery of thermodynamics enables one to calculate all other desired thermodynamic properties of the sample of matter (see, *e.g.* CALLEN [1960]).

Any sample of matter has $1 + N$ thermodynamic degrees of freedom. From a knowledge of the equations of state of the sample, of the laws of thermodynamics, and of the nuclear abundances one can express any $4 + N$ of the parameters $(\varrho^*, n, s^*, p^*, T^*, Z_1, \ldots, Z_N, \bar{\mu}_1^*, \ldots, \bar{\mu}_N^*)$ as functions of the other $1 + N$ parameters.

2'2.4. Inertial mass per unit volume. In our analyses of stellar structure and dynamics we will need one more fundamental result from relativistic ther-

modynamics and mechanics; an expression for the inertial mass per unit volume of a perfect fluid in which p^*/ϱ^* is not small compared to unity. In order to obtain such an expression, consider in the framework of special relativity a perfect fluid which moves in the x-direction with velocity $v \ll c$ relative to an inertial observer. Focus attention on a fluid element of area A and thickness Δx. The momentum of this fluid element is the total mass-energy, m, which it carries past the observer multiplied by its velocity, v:

$$g = mv .$$

The mass m which passes the observer arises form *two* sources: the density of mass-energy, ϱ, of the fluid, and the work done on the rightward-moving fluid element by the pressure force acting on its left face

$$m = \varrho A\Delta x + \frac{1}{c^2} \times (\text{force on left face}) \times$$

$$\times (\text{distance through which force acts as fluid passes observer}) =$$

$$= \varrho A\Delta x + pA\Delta x/c^2 = (\varrho + p/c^2) A\Delta x .$$

Consequently, the momentum is

$$g = (\varrho + p/c^2)(A\Delta x) v .$$

Next suppose that the fluid element is initially at rest and that the external observer applies a force, F, to accelerate it up to velocity $v \ll c$ without changing its proper density and pressure. Then

$$F = \mathrm{d}g/\mathrm{d}t = (\varrho + p/c^2)(A\Delta x)\,\mathrm{d}v/\mathrm{d}t .$$

Consequently, the inertial mass of the fluid element is $(\varrho + p/c^2) A\Delta x$; or, equivalently,

$$(2.17) \qquad \begin{pmatrix} \text{inertial mass per unit volume of a perfect} \\ \text{fluid momentarily at rest with respect to} \\ \text{the inertial observer who measures it} \end{pmatrix} = (\varrho^* + p^*) .$$

At first sight this result might be disturbing since in Newtonian physics ϱ^* is *by definition* the inertial mass per unit volume. However, in relativity theory, as throughout modern physics, we define mass-energy *not* in terms of reaction to applied forces, but in terms of conservation laws. The density of mass-energy, ϱ^*, is that quantity which obeys the conservation law embodied in the first law of thermodynamics (2.12). In the Newtonian limit $(p/\varrho c^2 \ll 1)$

this quantity happens to be also the inertial mass per unit volume; but in relativity theory it is not.

We should note in passing that the inertial mass per unit volume is actually a tensorial quantity: For bodies in an anisotropic state of stress and with $v \ll c$, the acceleration, $\mathrm{d}\boldsymbol{v}/\mathrm{d}t$, produced by a force per unit volume, $\mathscr{F}$, which does not deform the body, satisfies (*)

$$\mathscr{F} = \varrho(\mathrm{d}\boldsymbol{v}/\mathrm{d}t) + \sum_{j,k=1}^{3} (T^{(0)}_{jk}/c^2)(\mathrm{d}v_j/\mathrm{d}t)\, \boldsymbol{e}_{[k]} . \tag{2.18}$$

Consequently, the inertial mass per unit volume, $\varrho + T^{(0)}_{xx}/c^2$, which resists acceleration in the x-direction differs from that, $\varrho + T^{(0)}_{yy}/c^2$, which resists acceleration in the y-direction. Only in the case of isotropic stresses is the inertial mass the same in all directions.

Although the inertial mass per unit volume is not equal to ϱ, the total inertial mass of any body of negligible self-gravitation (special-relativity limit) and zero velocity is given by

$$(\text{Total inertial mass}) = \int \varrho \, \mathrm{d}(\text{volume}) . \tag{2.19}$$

The stress gives no contribution to the total inertial mass because the equations of stress balance for a body not being deformed,

$$\sum_{j=1}^{3} \partial T^{(0)}_{kj}/\partial x^j = 0 ,$$

guarantee that the volume-integrated stress vanishes.

2·3. *General relativity, the science of long-range forces.*

2·3.1. Gravitation as geometry. According to general relativity the concepts of *gravitational field* and *curvature of space-time* are equivalent. From a knowledge of the curvature, or intrinsic geometry, of 4-dimensional space-time one can calculate the gravitational acceleration of any freely falling test particle as measured by an observer in an arbitrary state of motion near the test particle.

In our discussions of relativistic stellar models we shall find useful two quite different methods for describing the gravitational field. The first method is

(*) See, *e.g.*, the discussion of momentum density by TOLMAN (1934*a*), p. 65. Alternatively, this equation and the high-velocity generalization of it can be obtained by expressing the special-relativistic equations of motion $\sum_{\mu=0}^{3} (\partial T^{\mu}_{k}/\partial x^{\mu}) = 0$, in terms of the velocity, v^k, and the stresses $T^{(0)}_{jk}$ and density of mass-energy ϱ as measured in the rest frame of the body.

to construct a precisely-defined co-ordinate system in the stellar model, and to give the value relative to this co-ordinate system of the metric tensor, $g_{\mu\nu}$, as a function of the co-ordinates $(x^0 = t^*, x^1, x^2, x^3)$. (The value of $g_{\mu\nu}$ is such that the squared proper length of the co-ordinate displacement $[\mathrm{d}x^0, \mathrm{d}x^1, \mathrm{d}x^2, \mathrm{d}x^3]$ is

$$\mathrm{d}s^2 = \sum_{\mu,\nu} g_{\mu\nu}\,\mathrm{d}x^\mu \mathrm{d}x^\nu\,.) \tag{2.20}$$

The components of $g_{\mu\nu}$ play a role in relativity theory analogous to that of the gravitational potential, U, of Newtonian theory.

Although this first method of describing the gravitational field is very useful in mathematical analyses of stellar models, it has one serious deficiency: It is a co-ordinate-dependent description, whereas the gravitational field—or geometry of spacetime—is co-ordinate-independent. Our second method of describing the gravitational field avoids this deficiency by exhibiting the geometry of space-time pictorially. The pictorial tools of this method are «embedding diagrams», *i.e.* pictures of 3-dimensional spacelike hypersurfaces as they would look if extracted from the space-time manifold of the star and embedded, with one dimension suppressed, in our own 3-dimensional Euclidean space. By means of embedding diagrams we can describe the results of co-ordinate-dependent mathematical analyses in a co-ordinate-free manner. We shall first encounter embedding diagrams in Sect. 3·5.1.

2·3.2. Energy and pressure as the sources of curvature. In Einstein's theory of gravitation the curvature of spacetime is produced by the nongravitational stress-energy which moves through space-time. The equation which links curvature to stress-energy—*i.e.* to density of mass-energy, ϱ^*, pressure, p^*, and velocity of fluid—is

$$(\text{Einstein curvature tensor}) = 8\pi(G/c^4) \times (\text{stress-energy tensor}). \tag{2.21}$$

This equation is the analogue of the Newtonian equation

$$\nabla^2(\text{gravitational potential}) = 4\pi G \times (\text{mass density})\,. \tag{2.22}$$

We shall be concerned here with eq. (2.21) only as it is applied in particular co-ordinate systems to particular situations.

2·3.3. Proper reference frames. There is sometimes considerable confusion in general-relativistic situations over the reference frames in which such quantities as density of mass-energy, fluid velocity and acceleration, and photon energy are measured. In order to avoid such confusion, let us introduce the concept of *proper reference frame.*

Consider an observer who moves along some arbitrary path, or « world line », through space-time, Let such an observer use physical rods and clocks, which he carries with himself, to perform measurements in his own neighborhood (within a distance small compared to the radii of curvature of space-time (*)). The results of such measurements will be called the values of the measured quantities relative to the observer's proper reference frame.

In more mathematical terms, the observer's proper reference frame is formed by an orthonormal tetrad which keeps its time-leg tangent to the observer's world line and which, for definiteness, is Fermi-Walker transported along the world line (see SYNGE (1960), pp. 13-15).

The reference frame to which the thermodynamic quantities and laws of Sect. 2·2. are referred is the proper reference frame of an observer who comoves with the matter being studied. The laws of physics in this comoving proper frame are those of flat space-time (special relativity) as augmented by an inertial (or, according to the equivalence principle, gravitational; or, in more intuitive terms, centrifugal) acceleration. This inertial acceleration is caused by deviations of the motion of the origin of the comoving frame from a freely falling, or geodesic path.

2·3.4. The Newtonian approximation. In studying a particular astrophysical situation it would be a great waste of time and effort to use Einstein's geometric theory of gravitation if Newtonian theory would yield the same results. For this reason it is important to delineate those circumstances under which Newtonian theory is a good approximation to general relativity. We refer the reader to EINSTEIN (1965), pp. 85-90, for a beatiful and coincise demonstration that Newtonian theory and general relativity theory are equivalent if the following three conditions are satisfied throughout the system under study:

a) The system is small compared with the radii of curvature of space-time (*); or equivalently (cf. eq. (2.3)), the maximum density of mass-energy, $\varrho^*_{\max}$, and the linear dimensions, l, over which the density of mass-energy is large satisfy

$$l \ll (\varrho^*_{\max})^{-\frac{1}{2}}; \tag{2.23}$$

or, equivalently, the Newtonian gravitational potential, U, satisfies

$$U/c^2 \ll 1 \tag{2.24}$$

everywhere.

(*) By « radii of curvature of space-time » we mean (physical components of 4th rank Riemann curvature tensor as measured in the observer's proper frame)$^{-\frac{1}{2}}$.

b) The pressure and density of mass-energy satisfy

$$p^*/\varrho^* = p/\varrho c^2 \ll 1 \tag{2.25}$$

everywhere in the system.

c) The macroscopic velocity, v, of the matter relative to the Newtonian co-ordinate system is everywhere small compared to the speed of light

$$(v/c)^2 \ll 1 \,. \tag{2.26}$$

When these conditions are satisfied the discrepancy between the results of a Newtonian analysis and a general-relativistic analysis is usually of the order of the maximum of the dimensionless quantities U/c^2, $p/\varrho c^2$, and v^2/c^2. However, there are exceptions to this «rule-of-thumb»: If a particular phenomenon depends critically, in Newtonian theory, upon the difference between two quantities; and if that difference is of order U/c^2 or $p/\varrho c^2$ or v^2/c^2 smaller than the two quantities, then general-relativistic effects can play a crucial role in the phenomenon. An important example of such a situation is the phenomenon of general-relativistic instabilities in hot stellar models (see Sect. 4·3.1).

2·3.5. The post-Newtonian approximation. The Newtonian theory of gravitation is obtained from general relativity by expanding Einstein's equations in powers of U/c^2, $p/\varrho c^2$, $\varepsilon/\varrho c^2$, and v^2/c^2; and keeping only the zero-order terms. A more accurate approximation to general relativity—the *post-Newtonian approximation*—results from keeping both zero-order and first-order terms in the expansion. The resultant equations are very useful for studying general-relativistic effects in systems for which U/c^2, $p/\varrho c^2$, and v^2/c^2 are everywhere small.

The post-Newtonian approximation to general relativity has been developed in full generality for perfect fluids by CHANDRASEKHAR (1965*a*, *b*); and it has been independently developed in restricted form for application to problems of stellar structure, stability, and collapse by FOWLER (1964, 1966). We shall briefly describe Chandrasekhar's formulation since results obtained from it will play an important role in some of the later Sections.

To orient ourselves let us briefly review the Newtonian theory of perfect fluids. In Newtonian theory we describe the gravitational field by a single gravitational potential, $U(\boldsymbol{x})$; and we describe the fluid by (in the notation of CHANDRASEKHAR (1965*a*, *b*) except that our ϱ_0 is his ϱ) its density of rest mass,

$$\varrho_0 \equiv \mu_B n \,, \tag{2.27}$$

its pressure, p, its temperature, T, its internal energy per unit rest mass,

$$\Pi \equiv \varepsilon/\varrho_0 \,, \tag{2.28}$$

and its three components of velocity, v_x, v_y, v_z. These eight quantities (U, $\varrho_0, p, T, \Pi, v_x, v_y, v_z$) are tied together by eight relations: One gravitational source equation

$$\nabla^2 U = -4\pi G\varrho_0 , \tag{2.29}$$

one equation of continuity

$$\partial\varrho_0/\partial t + \nabla\cdot(\varrho_0 \boldsymbol{v}) = 0, \tag{2.30}$$

three equations of motion

$$(\partial/\partial t)(\varrho_0 v_j) + \sum_k (\partial/x_k)(\varrho_0 v_k v_j) = -\partial p/\partial x_j + \varrho_0 \partial U/\partial x_j , \tag{2.31}$$

two thermodynamic equations of state, and the demand that the motion be adiabatic.

In Chandrasekhar's analogous post-Newtonian theory the gravitational field is described *not* by a single potential function, U, but by 3 scalar potentials (U, Φ, χ) and the three components (U_1, U_2, U_3) of a vector potential. The orders of magnitude of the five new potentials are

$$\begin{cases} \Phi/c^4 \leqslant [\text{maximum } (U/c^2, v^2/c^2, p/\varrho_0 c^2)]^2 \equiv O(1/c^4) , \\ (\partial^2\chi/\partial t\partial x_j)/c^3 \leqslant [\text{maximum } (U/c^2, v^2/c^2, p/\varrho_0 c^2]^{\frac{3}{2}} \equiv O(1/c^3) , \\ U_j/c^3 \leqslant [\text{maximum } (U/c^2, v^2/c^2, p/\varrho_0 c^2)]^{\frac{3}{2}} \equiv O(1/c^3) . \end{cases} \tag{2.32}$$

The six post-Newtonian gravitational potentials are related to the metric tensor of general relativity by (*)

$$\begin{cases} g_{00} = 1 - 2U/c^2 + (2U^2 - 4\Phi)/c^4 + O(1/c^6) , \\ g_{0j} = 4U_j/c^3 - (\partial^2\chi/\partial t\partial x_j)/2c^3 + O(1/c^5) , \\ g_{jk} = -(1 + 2U/c^2)\delta_{jk} + O(1/c^4) . \end{cases} \tag{2.33}$$

Why are some components of the metric (2.33) expanded in powers of « $1/c$ » to order 4, some to order 3, and some only to order 2? Why are we not consistent? Each component is expanded just far enough to guarantee that in the equations of motion of the fluid all terms of order « $1/c^2$ » are included.

(*) The arbitrariness in $g_{\mu\nu}$ associated with the arbitrariness of co-ordinate systems is here partially removed by the co-ordinate condition $\frac{1}{2}(\partial/\partial t)\left(\sum_\alpha h_\alpha^\alpha\right) - \sum_\alpha \partial h_0^\alpha/\partial x_\alpha = 0$, where $h_{\mu\nu}$ is the deviation of $g_{\mu\nu}$ from the Minkowskian metric: $h_{\mu\nu} = g_{\mu\nu} - \eta_{\mu\nu}$.

The physics of Chandrasekhar's post-Newtonian approximation is contained in 13 equations which relate the 6 gravitational quantities (U, Φ, χ, U_1, U_2, U_3) and the 7 fluid quantities (ϱ_0, p, T, Π, v_x, v_y, v_z) to each other. Of these 13 basic equations 6 are gravitational source equations analogous to the Newtonian eq. (2.29), one is an equation of continuity analogous to (2.30), three are equations of motion analogous to (2.31), two are the thermodynamic equations of state, and one is the demand that the motion be adiabatic. We refer the reader to CHANDRASEKHAR (1965*a*) (eqs. (6), (7), (9)–(12)) for the precise forms of these equations.

In general-relativity theory there is considerable difficulty with the definitions of energy, momentum, and angular momentum and with the corresponding conservation laws. Roughly speaking, the difficulty results from interchanges of energy and momentum between the gravitational field and the fluid, and from the nonlocalizability of the gravitational field energy-momentum. Such difficulties are *not* encountered in the post-Newtonian approximation because there cannot be gravitational radiation in this approximation. Gravitational radiation couples to the fluid only in higher orders of the expansion in « $1/c$ » than are included here. As a result, rest mass, total energy, momentum, and angular momentum are well defined in the post-Newtonian approximation and satisfy local as well as global conservation laws. Expressions for these 4 conserved quantities are given in CHANDRASEKHAR (1965*a*) (eqs. (13)–(16)), and the conservation laws are proved in CHANDRASEKHAR (1965*b*). CHANDRASEKHAR also gives post-Newtonian forms of the tensor and scalar virial theorems.

The post-Newtonian approximation as developed by CHANDRASEKHAR is sufficiently simple that any astrophysical problem ever solved numerically in Newtonian theory can now be solved without too much more effort in post-Newtonian theory. The results of several such post-Newtonian analyses will play important roles in later Sections (**3**˙6.2, **4**˙1, **4**˙4).

2˙4. *Summary.* – The principal results of Sect. **2** are these: 1) In all astrophysical situations except the endpoint of gravitational collapse long-range gravitational forces can be separated from the short-range forces which determine the structure and properties of matter. 2) The effect of short-range forces on the properties of matter can be described in a comoving proper reference frame by the parameters and laws of classical thermodynamics plus the law of the equivalence of mass and energy. 3) The gravitational field is described by the general-relativistic curvature of space-time. Alternatively, if U/c^2, v^2/c^2, and $p/\varrho c^2$ are all small compared to unity, Newtonian or post-Newtonian gravitational potentials can be used to describe the gravitational field. 4) The coupling between the long-range gravitational field and the matter whose thermodynamic properties are determined by short-range forces is described by Einstein's field equations (2.21) or, in the Newtonian and post-Newtonian ap-

proximations, by the source equations of the gravitational field plus the equations of motion of the fluid.

With these thermodynamic and gravitational preliminaries completed, we are now prepared to turn our attention to the structure of equilibrium stellar configurations.

3. – Equilibrium stellar configurations.

3·1. *Parameters describing the structure of nonrotating stellar models.*

3·1.1. Description of the gravitational field. To give an analytic description of the gravitational field of a nonrotating star, we must first construct a precisely defined co-ordinate system and then give, relative to that co-ordinate system, the metric tensor, $g_{\mu\nu}$, which determines the geometry of space-time (cf. Sect. 2·3.1). Nonrotating, equilibrium stellar configurations are necessarily spherically symmetric. Consequently, we can use as our three space co-ordinates the familiar spherical co-ordinates (r, θ, φ); r being such that $4\pi r^2$ is the surface area of a sphere about the center of the star, and (θ, φ) being angular coordinates on that sphere. Our time co-ordinate, t, is chosen such that *a*) the geometry of space-time is independent of t; and *b*) very far from the star (at $r \to \infty$) co-ordinate time, t, is identical to the proper time measured by the clock of an observer at rest with respect to the star.

These conditions determine our co-ordinate system uniquely, except for trivial rotations about the center of the star. With respect to this co-ordinate system the metric tensor which describes the gravitational field can be put into the form

$$(3.1) \quad ds^2 = \sum_{\mu,\nu} g_{\mu\nu} dx^\mu dx^\nu = e^{2\Phi} dt^2 - (1 - 2m^*/r)^{-1} dr^2 - r^2(d\theta^2 + \sin^2\theta\, d\varphi^2) .$$

(See, *e.g.*, TOLMAN (1934), Sect. **95**.) Hence the geometry of space-time depends upon two gravitational potentials, $\Phi(r)$ and $m^*(r)$. These potentials always satisfy $\Phi(\infty) = m^*(0) = 0$ (The gravitational potential Φ of eq. (3.1) is not to be confused with the potential Φ of post-Newtonian theory (Sect. 2·3.5).)

We shall see in Sect. 3·2.2 that $m^*(r)$ can be thought of as the mass inside a radius r. As for $\Phi(r)$, it plays in general relativity a role analogous to that of the gravitational potential, U, of Newtonian theory. In fact, a comparison of equation (2.33) with the expression

$$g_{00} = e^{2\Phi} \approx 1 + 2\Phi + O(\Phi^2)$$

reveals that $-U/c^2$ is the Newtonian limit of Φ. For this reason $\Phi(r)$ is sometimes called the « Newtonian potential » of general relativity.

3'1.2. $\Phi(r)$ as a governor of energy red-shift. Just as U provides us with an equation governing the rate of change of the kinetic energy of a particle moving in a Newtonian gravitational field

$$\tfrac{1}{2} m_0 v^2 - m_0 U = \text{const}\,, \tag{3.2}$$

so Φ is the basis for a general-relativity energy equation. At each point on the orbit of a particle (or photon) let an observer fixed with respect to the star $((r, \theta, \varphi) = \text{const})$ measure the particle's total energy, E, in his own proper reference frame. (By total energy, E, we mean $E = h\nu$ for a photon, and $E = (\text{rest mass plus kinetic energy}) = m_0/(1 - v^2)^{\frac{1}{2}}$ for a material particle.) Then the energies measured by observers at different points in the star are related by

$$E e^{\Phi} = \text{const}\,. \tag{3.3}$$

This equation is valid for particles or photons falling freely inside the star as well as outside it. In fact, eq. (3.3) is valid for particles or photons falling in *any static gravitational field* of the form

$$\mathrm{d}s^2 = e^{2\Phi}\,\mathrm{d}t^2 + \sum_{i,j=1}^{3} g_{ij}\,\mathrm{d}x^i\,\mathrm{d}x^j\,. \tag{3.4}$$

(See *e.g.* LANDAU and LIFSHITZ (1962), Sect. **89**.)

Equation (3.2), which is the Newtonian limit of eq. (3.3), is usually called « the equation of energy conservation »; the energy which is conserved is the sum of the kinetic energy, $\frac{1}{2} m_0 v^2$, and the potential energy, $- m_0 U$. In general relativity, however, it is more convenient to avoid introducing the concept of potential energy and to regard eq. (3.3) as an « energy red-shift » equation. The energy which is red-shifted as a particle or photon climbs out of a gravitational field is E, and the amount by which this energy is red-shifted in moving from point A to point B is

$$[E(B) - E(A)]/E(A) = \exp[\Phi(A) - \Phi(B)] - 1\,. \tag{3.5}$$

3'1.3. Description of thermodynamic structure. The thermodynamic structure of an equilibrium stellar configuration will be described in these lectures by giving the radial distribution of the following thermodynamic parameters: density of mass-energy, ϱ^*; pressure, p^*; number density of baryons, n; internal energy density, ε^*; entropy per baryon, s^*, temperature, T^*; average baryonic rest mass, μ_{B}^*; nuclear abundances, $Z_1, \ldots, Z_N$; nuclear chemical potentials, $\bar{\mu}_1^*, \ldots, \bar{\mu}_N^*$; number of baryons inside a radius r, $a(r)$; total luminosity, L_r^*; neutrino luminosity, $L_r^{(\nu)*}$; radiative absorption coefficient,

$\varkappa_R^*$; thermal conductivity, λ_c^*; rate of change of nuclear abundances, $\alpha_1^*, \ldots, \alpha_N^*$; rate of thermonuclear energy generation, q^*; and rate of energy release into neutrinos, $q_{(\nu)}^*$. All of these quantities were defined in Sect. 2·2 except the following: *The number of baryons inside a radius r, a(r)*, is a very useful parameter for identifying shells of matter in successive configurations of an evolutionary sequence. In the language of hydrodynamics, a is a Lagrangian radial co-ordinate. We shall sometimes use a rather than r as the independent radial co-ordinate. *The radial luminosity*, L_r^*, is the total mass-energy carried by photons, by neutrinos, by conduction, and by convection outward across a sphere of co-ordinate radius r in unit time, as measured in the proper frame of an observer located at r and at rest with respect to the star. *The neutrino luminosity* $L_r^{(\nu)*}$ is that portion of L_r^* due to neutrinos. *The radiative absorption coefficient*, $\varkappa_R^*$, multiplied by the density of mass-energy, ϱ^*, is the fractional attenuation per unit proper distance of the intensity (watt/cm² s) of a beam of light in the absence of gravitational fields

$$\mathrm{d}I/I = -\varkappa_R^* \varrho^* \mathrm{d}(\text{proper distance}) \qquad \text{(no gravitation)}. \tag{3.6}$$

The light beam is assumed to have the average spectral distribution of the radiation at point r. *The thermal conductivity*, λ_c, is the proportionality constant which, in the absence of a gravitational field, relates the energy flux by heat conduction to the temperature gradient.

$$\boldsymbol{Q} = -\lambda_c \nabla T \qquad \text{(no gravitation)}. \tag{3.7}$$

The rates of change of nuclear abundances, $\alpha_1^*, \ldots, \alpha_N^*$, are defined by

$$\alpha_k^* = \mathrm{d}Z_k/\mathrm{d}\,(\text{time as measured in proper frame of observer at rest in star}). \tag{3.8}$$

The nuclear abundances change as a result of nuclear reactions. Because $Z_1 + \ldots + Z_N = 1$, we always have

$$\alpha_1^* + \ldots + \alpha_N^* = 0\,. \tag{3.9}$$

The rate, q, of thermonuclear energy generation* is the rate per baryon, as measured by an observer at rest in the star, at which rest mass-energy is converted into internal energy by thermonuclear reactions

$$q^* = -\mathrm{d}\mu_{\mathrm{B}}^*/\mathrm{d}\,(\text{proper time}) = -\alpha_1^*\mu_1^* - \ldots - \alpha_N^*\mu_N^*\,. \tag{3.10}$$

The rate of energy release into neutrinos, $q_{(\nu)}^*$, is the rate per baryon at which internal energy is converted into outgoing neutrinos. (We view nuclear reactions

as an exchange of energy between rest mass, $\mu_B^* n$, and internal energy, ε^*, followed by the conversion of some of the internal energy into neutrinos and photons.)

3·2. *Equations of stellar structure.* – The structure of a star which contains N different types of baryons can be described by the $16 + 3N$ functions of radius (Φ, m^*, a, ϱ^*, p^*, n, ε^*, s^*, T^*, L_r^*, $L_r^{(\nu)*}$, $\varkappa_\varrho^*$, λ_c^*, q^*, $q_{(\nu)}^*$, μ_B^*, Z_1, ..., Z_N, $\bar{\mu}_1^*$, ..., $\bar{\mu}_N^*$, α_1^*, ..., α_N^*). These $16 + 3N$ functions are governed by $16 + 3N$ equations of stellar structure:

I) *Differential equations of stellar structure*:

a) Baryon number equation:

$$\mathrm{d}a/\mathrm{d}r = 4\pi r^2 (1 - 2m^*/r)^{-\frac{1}{2}} n \,, \qquad a(0) = 0 \,, \tag{3.11-1}$$

b) Mass equation:

$$\mathrm{d}m^*/\mathrm{d}r = 4\pi r^2 \varrho^* \,, \qquad m^*(0) = 0 \,, \tag{3.11-2}$$

c) TOV equation of hydrostatic equilibrium:

$$\frac{\mathrm{d}p^*}{\mathrm{d}r} = \frac{-(\varrho^* + p^*)(m^* + 4\pi r^3 p^*)}{r(r - 2m^*)} \,, \tag{3.11-3}$$

d) Source equation for Φ:

$$\frac{\mathrm{d}\Phi}{\mathrm{d}r} = \frac{m^* + 4\pi r^3 p^*}{r(r - 2m^*)} \,, \qquad \Phi(\infty) = 0 \,, \tag{3.11-4}$$

e) Equations of thermal equilibrium:

$$\frac{\mathrm{d}(L_r^* e^{2\Phi})}{\mathrm{d}r} = \frac{4\pi r^2 n e^{2\Phi}}{(1 - 2m^*/r)^{\frac{1}{2}}} \left\{ q^* - \left[e^{-\Phi} \frac{\mathrm{d}}{\mathrm{d}t}\left(\frac{\varepsilon^*}{n}\right) - \frac{p^*}{n^2} e^{-\Phi} \frac{\mathrm{d}n}{\mathrm{d}t} \right]_{a=\text{constant}} \right\} = \tag{3.11-5}$$

$$= \frac{-4\pi r^2 n e^{\Phi}}{(1 - 2m^*/r)^{\frac{1}{2}}} \left\{ T^* \left(\frac{\mathrm{d}s^*}{\mathrm{d}t}\right)_{a=\text{constant}} + \sum_k \bar{\mu}_k^* \left(\frac{\mathrm{d}Z_k}{\mathrm{d}t}\right)_{a=\text{constant}} \right\},$$

$$\frac{\mathrm{d}(L_r^{(\nu)*} e^{2\Phi})}{\mathrm{d}r} = \frac{4\pi r^2 n e^{2\Phi}}{(1 - 2m^*/r)^{\frac{1}{2}}} q_{(\nu)}^* \,. \tag{3.11-6}$$

f) Equation of energy transport:

i) If convective transport is negligible beside conductive plus radiative transport (temperature gradient subadiabatic)

$$\begin{cases} \dfrac{\mathrm{d}(Te^{*\Phi})}{\mathrm{d}r} = -\dfrac{3}{16\sigma^*} \dfrac{\varkappa^* \varrho^*}{T^{*3}} \dfrac{(L_r^* - L_r^{(\nu)*}) e^{\Phi}}{4\pi r^2} \left(1 - \dfrac{2m^*}{r}\right)^{-\frac{1}{2}} , \\ \dfrac{1}{\varkappa^*} = \dfrac{1}{\varkappa_R^*} + \dfrac{1}{\varkappa_c^*} , \qquad \varkappa_c^* = \dfrac{16\sigma^* T^{*3}}{3\varrho^* \lambda_c^*} . \end{cases} \tag{3.11-7a}$$

ii) If conductive and radiative transport are negligible beside convection, and if convection proceeds efficiently (adiabatic approximation)

$$\frac{\mathrm{d}T^*}{\mathrm{d}r} = \frac{\Gamma_2 - 1}{\Gamma_2} \frac{T^*}{p^*} \frac{\mathrm{d}p^*}{\mathrm{d}r} \,. \tag{3.11-7b}$$

Procedure for choosing between (3.11-7*a*) and (3.11-7*b*): Calculate temperature gradient from (3.11-7*a*); if it is subadiabatic then the assumption of no convection was correct; but if it is superadiabatic then convection is important and (3.11-7*b*) should be used.

II) *Gas characteristic relations*:

a) Thermodynamic relations:

(3.11-8) → $4 + N$ algebraic thermodynamic relations linking the

(3.11-11 + N) fundamental thermodynamic quantities (ϱ^*, p^*, n, s^*, T^*, $Z_1, \ldots, Z_N, \bar{\mu}_1^*, \ldots, \bar{\mu}_N^*$).

$$\varrho^* = \mu_{\mathrm{B}}^* n + \varepsilon^* \,, \tag{3.11-12 + N}$$

$$\mu_{\mathrm{B}}^* = \sum_k Z_k \mu_k^* \,. \tag{3.11-13 + N}$$

b) Opacity relation:

$$\varkappa_R^* = \varkappa_R^*(\varrho^*, T^*, Z_1, \ldots, Z_N) \,. \tag{3.11-14 + N}$$

c) Conductivity relation:

$$\lambda_c^* = \lambda_c^*(\varrho^*, T^*, Z_1, \ldots, Z_N) \,. \tag{3.11-15 + N}$$

d) Equations of thermonuclear energy generation:

$$q^* = -\sum_k \alpha_k^* \mu_k^* \,, \tag{3.11-16 + N}$$

$$q_{(\nu)}^* = q_{(\nu)}^*(\varrho^*, T^*, Z_1, \ldots, Z_N) \,, \tag{3.11-17 + N}$$

(3.11-18 + N) → (3.11-16 + $2N$) $\alpha_k^* = \alpha_k^*(\varrho^*, T^*, Z_1, \ldots, Z_N)$, $k = 1, \ldots, N-1$,

(3.11-17 + $2N$) → (3.11-16 + $3N$) $(\mathrm{d}Z_k/\mathrm{d}t)_{a=\mathrm{const}} = e^{\Phi} \alpha_k^*$ $k = 1, \ldots, N$.

Let us examine the origin, the significance, and the Newtonian limits of these equations.

3·2.1. Baryon number. The baryon number eq. (3.11-1) states that the number of baryons inside radius r is

$$a(r) = \int_0^r (\text{baryon number density})\, \mathrm{d}(\text{proper volume}) = \tag{3.12}$$

$$= \int_0^r n 4\pi r^2 (1 - 2m^*/r)^{-\frac{1}{2}} \mathrm{d}r \,.$$

3'2.2. Mass equation. The mass eq. (3.11-1) arises from Einstein's field eq. (2.21) (see *e.g.* TOLMAN (1934*a*), Sect. **95**). Its form suggests that we interpret $m^*(r)$ as the *total mass–energy inside radius* r, including rest mass-energy, internal energy, and (negative) gravitational potential energy. $m^*(r)$ is split into its three parts as follows

$$(3.13)\quad m^*(r) = (\text{rest mass-energy}) + (\text{internal energy}) +$$

$$+ (\text{gravitational potential energy}) = \int_0^r \mu_B^* n \, \mathrm{d}(\text{proper volume}) +$$

$$+ \int_0^r \varepsilon^* \, \mathrm{d}(\text{proper volume}) - \int_0^r \varrho^* [1 - (1 - 2m^*/r)]^{\frac{1}{2}} \, \mathrm{d}(\text{proper volume}) .$$

(To derive the second equality, combine the mass eq. (3.11-2) with the two-way split (2.5) of ϱ^* into rest mass plus internal energy, and with the expression

$$\mathrm{d}(\text{proper volume}) = 4\pi r^2 (1 - 2m^*/r)^{-\frac{1}{2}} \mathrm{d}r$$

for the proper volume of a spherical shell of co-ordinate thickness $\mathrm{d}r$.) In the Newtonian limit the three-way split (3.13) takes the familiar form

$$(3.13')\quad m(r)c^2 = \int_0^r \mu_B n c^2 \, \mathrm{d}(\text{proper volume}) + \int_0^r \varepsilon \, 4\pi r^2 \, \mathrm{d}r + \int_0^r \mu_B n (-Gm/r) 4\pi r^2 \, \mathrm{d}r .$$

Although it is very useful to give the title «total mass-energy inside radius r» to $m^*(r)$ (*), and although the rest mass-energy, $\int \mu_B^* n \, \mathrm{d}(\text{proper volume})$, is a useful quantity (**), the internal energy and gravitational potential energy of eq. (3.13) are *not particularly* useful except in the Newtonian and post-Newtonian approximations.

The value of m^* at the surface of the star,

$$(3.14)\quad M^* \equiv m^*(R) = \int_0^R 4\pi r^2 \varrho^* \, \mathrm{d}r ,$$

is the total gravitating mass as measured by an observer who applies Kepler's

---

(*) See *e.g.* the remainder of Sect. **3**, as well as HTWW Chapters 2 and 3 and Appendix B; and THORNE (1965*b*), Chapter 5.

(**) See *e.g.* Sect. **3**'5.3 and **4**'2.4, as well as BARDEEN (1965) and TOOPER (1966).

laws to planets in large orbits about the star (cf. Sect. 3·4.1). The difference between this total mass-energy and the total rest mass-energy,

$$M_0^* \equiv \int_0^R \mu_B^* \, n 4\pi r^2 (1 - 2m^*/r)^{-\frac{1}{2}} \, dr \,, \tag{3.15}$$

is the negative of the binding energy, $-E_B^*$:

$$E_B^* \equiv M_0^* - M^* \,. \tag{3.16}$$

Binding energy and rest mass play an important role in the supermassive stellar models of FOWLER (1964, 1966) and BARDEEN (1964, 1965, 1966).

3·2.3. TOV equation of hydrostatic equilibrium. The TOV (TOLMAN [1934*a*], [1939], OPPENHEIMER and VOLKOFF (1939]) equation (3.11-3), like the mass equation (3.11-2), arises from Einstein's field equations. It expresses the fact that the buoyant force per unit volume, as measured in the proper reference frame of an observer fixed in the star,

$$\boldsymbol{F}^*_{\text{buoyant}} = -\, dp^*/d(\text{proper radial distance})\, \boldsymbol{e}_r = -\,(1 - 2m^*/r)^{\frac{1}{2}} (dp^*/dr) \boldsymbol{e}_r \,, \tag{3.17a}$$

precisely balances the gravitational force per unit volume,

$$\boldsymbol{F}^*_{\text{grav}} = \frac{-(\varrho^* + p^*)(m^* + 4\pi r^3 p^*)}{r^2 (1 - 2m^*/r)^{\frac{1}{2}}} \, \boldsymbol{e}_r \,. \tag{3.17b}$$

(Here $\boldsymbol{e}_r$ is a unit vector in the radial direction.)

The TOV equation of hydrostatic equilibrium (3.11-3) differs from its Newtonian counterpart

$$-F^*_{\text{buoy}} = dp^*/dr = F^*_{\text{grav}} = -\varrho^* m^*/r^2 \tag{3.18}$$

in several key ways: 1) In place of the density of mass-energy, ϱ^*, appears density plus pressure, $(\varrho^* + p^*)$. This is a consequence of the relativistic role of $(\varrho^* + p^*)$ as inertial mass per unit volume (cf. Sect. 2·2.4), plus the equivalence of inertial and gravitational forces (Einstein's equivalence principle). 2) In place of the mass, m^*, appears the expression $m^* + 4\pi r^3 p^*$. The additional term proportional to p^* results in one of the most important of all nonlinear gravitational effects, *multiplicative regeneration of pressure* (see Sect. 3·5.2). 3) In the denominator of the TOV equation (3.11-3) is a factor $(1 - 2m^*/r)$ which does not appear in the Newtonian equation (3.18). This factor prevents the mass inside a radius r, $m^*(r)$, from ever being as large as $r/2$ (cf. Sect. 3·5.1);

and it is closely related to the evolution of an event horizon in gravitational collapse (cf. Sect. **7**).

3'2.4. Source equation for Φ. The source equation (3.11-4), like eqs. (3.11-2)–(3.11-3) arises from Einstein's field equations (see, *e.g.*, TOLMAN [1943*a*] Sect. **95**); and like the TOV equation (3.11-3), it can be rewritten in a form which expresses the hydrostatic balance between gravitational force and pressure-buoyant force:

$$(3.19)\quad \boldsymbol{F}^*_{\text{grav}} = -(\varrho^* + p^*)(1 - 2m^*/r)^{\frac{1}{2}}(\mathrm{d}\Phi/\mathrm{d}r)\boldsymbol{e}_r = -\boldsymbol{F}^*_{\text{buoy}} = (1 - 2m^*/r)^{\frac{1}{2}}(\mathrm{d}p^*/\mathrm{d}r)\boldsymbol{e}_r .$$

Note that the relativistic expression (3.19) for the gravitational force per unit volume, when rewritten in words, takes a form familiar from Newtonian theory

$$(3.20)\quad \boldsymbol{F}^*_{\text{grav}} = -(\textit{inertial mass per unit volume}) \times \mathrm{d}\Phi/\mathrm{d}(\textit{proper radial distance})\boldsymbol{e}_r .$$

This is another aspect of the close analogy between the general-relativity potential Φ and the gravitational potential U of Newtonian theory (cf. Sect. **3**'1.1 and **3**'1.2).

3'2.5. Thermal equilibrium. The energy which a star radiates is supplied from its rest mass by nuclear burning, from its gravitational and internal energy by quasistatic contraction, or from both sources by both processes. Equation of thermal equilibrium (3.11-5) expresses the energy balance which occurs during this conversion of mass-energy from one form to another.

To derive eq. (3.11-5) consider a spherical shell of the star inside of which there are a baryons and which itself contains δa baryons. During a co-ordinate time interval $\mathrm{d}t$ the internal energy of this shell changes by

$$(3.21)\quad \mathrm{d}(\text{internal energy}) =$$
$$= (\text{rest mass-energy converted to internal energy by nuclear reactions}) +$$
$$+ \begin{pmatrix}\text{work done on shell by gravitational forces to}\\ \text{change its volume during quasistatic contraction}\end{pmatrix} -$$
$$- (\text{energy radiated away, conducted away, or convected away}).$$

By virtue of definition (3.10) the amount of rest mass converted to internal energy is $q^*\,\delta a e^{\Phi}\,\mathrm{d}t$. During quasi-static contraction the shell under consideration changes its volume by an amount $\mathrm{d}(\delta a/n)$, and the work done on the shell to produce this change is $-p^*\mathrm{d}(\delta a/n)$. The rate, as measured by a clock fixed in the shell, at which the shell radiates, conducts and convects away energy is

$$(3.22)\quad L^*_r(r + \delta r)\exp\left[2[\Phi(r + \delta r) - \Phi(r)]\right] - L^*_r(r) = (\mathrm{d}L^*_r/\mathrm{d}r + 2L^*_r\,\mathrm{d}\Phi/\mathrm{d}r)\,\delta r .$$

One of the factors of $\exp[\Phi(r+\delta r)-\Phi(r)]$ accounts for the gravitational redshift which the transported energy undergoes as it crosses the shell (cf. Sect. 3·1.2.), while the other accounts for time dilation between the inner and outer surfaces of the shell. Consequently, the total energy carried away from the shell in co-ordinate time dt is

$$(dL_r^*/dr + 2L_r^* d\Phi/dr)\,\delta r e^{\Phi}\,dt\,.$$

These results enable us to rewrite the equation of energy balance (3.21) as

$$d(\varepsilon^*\,\delta a/n) = q^*\,\delta a e^{\Phi}\,dt - p^*\,d(\delta a/n) - (dL_r^*/dr + 2L_r^*\,d\Phi/dr)\,\delta r\,e^{\Phi}\,dt\,. \tag{3.23}$$

When expanded and rearranged this becomes the equation of thermal equilibrium (3.11-5). The alternative form (second equality) of the equation of thermal equilibrium (3.11-5) follows from the relation

$$q^* - e^{-\Phi}(d/dt)(\varepsilon^*/n) - p^* e^{-\Phi}(d/dt)(1/n) = -e^{-\Phi}[(d/dt)(\varrho^*/n) + p^*(d/dt)(1/n)] =$$
$$= -e^{-\Phi}\,T^*(ds^*/dt) - \sum_k \mu_k^*(dZ_k/dt)$$

(cf. the first law of thermodynamics, eq. (2.12)).

From the above derivation it is evident that *the time derivatives in the equation of thermal equilibium must be taken with baryon number, a, held fixed; not with radius, r, held fixed.* How these time derivatives are handled in practice will be discussed in Sect. 3·4.3.

It should be mentioned that the equation of thermal equilibrium (3.11-5) can be derived directly from the general-relativity law of local energy conservation, $\sum_{\mu,\nu} u_\mu T^{\mu\nu}{}_{;\nu} = 0$ (see BARDEEN [1965], or MISNER and SHARP [1965, 1966]).

In addition to the general equation of thermal equilibrium (3.11-5), we have equation (3.11-6) which expresses the law of energy balance for neutrinos alone. Neutrinos have their own, separate equation of thermal equilibrium because once a neutrino is produced it escapes freely from the equilibrium configuration without ever being converted into any other form of energy. Equation (3.11-6) can be derived in the same way as was (3.11-5).

3·2.6. Energy transport. In general, energy is transported from the hot interior of a star toward its cool surface by a combination of diffusing photons, escaping neutrinos, heat conduction in the stellar material, and convective motions of the stellar material. In any particular situation a careful analysis of the processes of energy transport yields three basic equations: the equations of thermal equilibrium (3.11-5, 6)—which are expressions for the gradient of the energy flux—; and the equation of energy transport (3.11-7), which is an expression for the temperature gradient.

The analysis of energy transport for stellar models in which convection contributes roughly the same energy flux as conduction plus photon diffusion is very difficult and has not yet been carried out in general relativity. Fortunately, in most situations of physical interest either convection is negligible beside conduction plus radiation, or conduction plus radiation is negligible beside convection. We consider these two cases below.

3'2.7. Energy transport by conduction, photon diffusion, and neutrino escape. When convective transport is absent or negligible, the equation of energy transport takes the form (3.11-7*a*). We will derive this equation in three steps: *First*, we will obtain a relation between temperature gradient and photon energy flux; *second*, we will obtain a similar relation between temperature gradient and conduction energy flux; *third*, we will combine these relations to obtain eq. (3.11-7*a*).

a) *Photon energy transport.* The theory of radiative transport in general relativity has been developed independently by BARDEEN (1965), by MISNER and SHARP (1965, 1966), by HÄMEEN-ANTTILA and ANTTILA (1966), and, in greatest detail, by LINDQUIST (1966). For the interior of a star, where photon transport is diffusive, this theory yields the following *equation of radiative transport*:

$$\frac{\mathrm{d}(T^* e^{\Phi})}{\mathrm{d}r} = -\frac{3}{16\sigma^*}\frac{\varkappa_R^* \varrho^*}{T^{*3}}\frac{L_r^{(R)*} e^{\Phi}}{4\pi r^2}\left(1-\frac{2m^*}{r}\right)^{-\frac{1}{2}}. \tag{3.24}$$

Here $L_r^{(R)*}$ is that portion of the luminosity, L_r^*, which is due to photon diffusion; σ^* is the Stefan-Boltzmann constant (cf. eq. (3.28)); and the other quantities have the meanings given in Sect. **3**'1.

One can give a physical derivation of eq. (3.24) without going into the details of transport theory. At any point inside the star the electromagnetic radiation consists of two parts—a large, isotropic part; and a very much smaller, purely radial part which accounts for the photon luminosity $L_r^{(R)*}$. Consider the gradient in the radial component of the (almost isotropic) radiation pressure. It arises from two sources—gravitational attraction of the photon gas toward the center of the star; and interaction of the radiation with matter. The gravitational attraction must be balanced by a pressure gradient

d(radiation pressure)/d(proper radial distance) =

= — (inertial mass per unit volume of photon gas) $\mathrm{d}\Phi$/d(proper radial distance);

or, equivalently,

$$(\mathrm{d}p_R^*/\mathrm{d}r)_{\mathrm{grav}} = -(\varrho_R^* + p_R^*)\,\mathrm{d}\Phi/\mathrm{d}r \tag{3.25}$$

(cf. Sect. 3·2.4). Of all interactions between matter and radiation only absorption of the excess radial component, $L_r^{(R)*}$, is anisotropic and can thus contribute to the radiation pressure gradient. The drop in radiation pressure over a co-ordinate interval dr due to absorption is the mass-energy absorbed from the radial beam per unit proper time and per unit area by the matter in the shell of thickness dr:

$$(dp_R^*)_{\text{absorption}} = -\varkappa_R^* \varrho^* (L_r^{(R)*}/4\pi r^2)(1-2m^*/r)^{-\frac{1}{2}} dr. \tag{3.26}$$

Consequently, the total gradient of the radiation pressure (sum of (3.25) and (3.26)) is:

$$dp_R^*/dr = -(\varrho_R^* + p_R^*)\, d\Phi/dr - \varkappa_R^* \varrho^* (L_r^{(R)*}/4\pi r^2)(1-2m^*/r)^{-\frac{1}{2}}\,. \tag{3.27}$$

Now, the (very nearly isotropic) radiation pressure, p_R^*, and the density of radiation energy, ϱ_R^*, are related to the temperature, T^*, of the matter by

$$\varrho_R^* = 3p_R^* = 4\sigma^* T^{*4}\,, \tag{3.28}$$

where σ^* is the Stefan-Boltzmann constant. By combining equations (3.27) and (3.28), and rearranging, one obtains the equation of radiative energy transport (3.24).

b) Conductive energy transport. The portion, $L_r^{(c)*}$, of the total luminosity L_r^*, which is due solely to heat conduction is related to the temperature gradient by the equation of conductive energy transport

$$\frac{d(T^* e^{\Phi})}{dr} = -\frac{L_r^{(c)*} e^{\Phi}}{4\pi r^2 \lambda_c^*}\left(1-\frac{2m^*}{r}\right)^{-\frac{1}{2}}. \tag{3.29}$$

This equation can be derived from the following considerations: In the Newtonian approximation the conductive luminosity is related to the temperature gradient by the equation of conductive energy transport

$$dT^*/dr = -\lambda_c^{*-1} \times (\text{energy flux}) = -L_r^{(c)*}/4\pi r^2 \lambda_c^*\,. \tag{3.30}$$

The relativistic generalization of this equation must be obtainable by insertion of the general-relativity « correction factors » e^{Φ} and $(1-2m^*/r)^{\frac{1}{2}}$ in appropriate places. The factor $(1-2m^*/r)^{\frac{1}{2}}$ is always used to convert differential radial co-ordinate intervals, dr, to proper radial distances, $(1-2m^*/r)^{-\frac{1}{2}}dr$. Hence, eq. (3.30) when corrected for the effects of $(1-2m^*/r)^{\frac{1}{2}}$ reads

$$dT^*/d(\text{proper radial distance}) \equiv (1-2m^*/r)^{\frac{1}{2}}\, dT^*/dr = -L_r^{(c)*}/4\pi r^2 \lambda_c^*\,. \tag{3.30'}$$

The second correction factor, e^{Φ}, must be inserted in such a manner as to account for the red-shift of the energy which is being conducted upward through the star. A factor of e^{Φ} to some power, k, will appear inside the radial derivative; and another factor, $e^{k'\Phi}$, will appear outside the radial derivative

$$(3.30'') \qquad (1-2m^*/r)^{\frac{1}{2}} e^{k'\Phi}\, \mathrm{d}(T^* e^{k\Phi})/\mathrm{d}r = -L_r^{(c)*}/4\pi r^2 \lambda_c^* .$$

We have chosen our normalization of Φ in such a manner that $\Phi(\infty) = 0$. However, just as Newtonian gravitation theory is unaffected by the addition of a constant to the gravitational potential, $U \to U +$ constant, so the laws of general relativity are unaffected by the corresponding transformation $\Phi \to \Phi +$ const. Such a transformation merely corresponds to an expansion or contraction of the *co-ordinate* time scale (cf. eq. (3.1)). The demand that the equation of conductive transport (3.30'') be invariant under the transformation $\Phi \to \Phi +$ const tells us that $k' = -k$.

To determine the correct value of $k = -k'$, consider a hot star which is surrounded by an insulator that prevents energy from flowing into or out of it. Inside the star photon diffusion will attempt to create a temperature distribution of $T^* e^{\Phi} =$ const (cf. eq. (3.24)), while heat conduction will attempt to create the distribution $T^* e^{k\Phi} =$ const. (cf. eq. (3.30'')). Consequently, if $k > 1$, photons will carry energy at a finite rate from the center of the star to the surface, and heat conduction will recycle the energy back to the center. The result will be a finite heat flow from a hot region to a cold region by one route and back by another with no increase in entropy—a violation of the second law of thermodynamics. Since $k < 1$ would lead to a similar violation of the second law, k must be precisely 1, and k' must be -1 (*). By setting $k = -k' = 1$ in eq. (3.30') and rearranging, we obtain the general-relativity equation (3.29) for heat conduction in a star.

c) Combined photon, conduction, and neutrino transport. We have now completed the first two steps in our derivation of the transport equation (3.11-7*a*). We have obtained the eqs. (3.24) and (3.29) which govern photon diffusion and heat conduction whenever there are no mass motions in the star (negligible convection). Before constructing the combined transport equation (3.11-7*a*), it is useful to rewrite the equation of conductive transport in a form identical to the equation of radiative transport

$$(3.29') \qquad \frac{\mathrm{d}(T^* e^{\Phi})}{\mathrm{d}r} = -\frac{3}{16\sigma^*} \frac{\varkappa_c^* \varrho^*}{T^{*3}} \frac{L_r^{(c)*} e^{\Phi}}{4\pi r^2} \left(1 - \frac{2m^*}{r}\right)^{-\frac{1}{2}} .$$

Evidently the conductive absorption coefficient $\varkappa_c^*$ which appears here is related

(*) This proof that $k = 1$ is due to P. J. E. PEEBLES (private communication).

to the thermal conductivity λ_c^* by

$$\varkappa_c^* = (16\sigma^* T^{*3})/(3\varrho^* \lambda_c^*) . \tag{3.31}$$

By combining the conduction eq. (3.29′) with the equation of radiative transport (3.24), and by noting that because convection is negligible

$$L_r^{(R)*} + L_r^{(c)*} = L_r^* - L_r^{(v)*} ,$$

we obtain the transport equation (3.11-7*a*).

3˙2.8. Convective energy transport. In general relativity, as in Newtonian theory, a layer of a star is unstable against convection if and only if its temperature gradient is superadiabatic:

$$\text{Instability against convection} \Leftrightarrow \tag{3.32}$$

$$\Leftrightarrow (-\mathrm{d}T^*/\mathrm{d}r) - (1 - 1/\Gamma_2)(T^*/p^*)(-\mathrm{d}p^*/\mathrm{d}r) > 0 .$$

Here Γ_2 is the adiabatic index of eq. (2.8).

This condition for convective instability can be derived in general relativity theory by a physical argument analogous to the Newtonian argument of SCHWARZSCHILD (1958), pp. 44-46: (*)

Consider a particular configuration of hydrostatic and thermal equilibrium. Displace a small element of fluid at radius r_A upward through a small coordinate distance Δr, to $r_B = r_A + \Delta r$. As it is displaced let the fluid element expand adiabatically until it reaches the same pressure as its new surroundings. Then release the displaced fluid element and see in what direction the sum of the gravitational and buoyant forces acts. If the fluid falls back toward its original position, the star is stable against convection in the neighborhood of r_A; if it continues to rise, the star is unstable against convection. The forces per unit volume acting on the displaced fluid element, as seen by an observer at rest at r_B, are (cf. Sect. **3**˙2.4)

$$\boldsymbol{F}^* = \boldsymbol{F}^*_{\text{grav}} + \boldsymbol{F}^*_{\text{buoyant}} = \tag{3.33}$$

$$= [-(\varrho^*_{fe} + p^*)(1 - 2m^*/r)^{\frac{1}{2}}(\mathrm{d}\Phi/\mathrm{d}r)\,\boldsymbol{e}_r]_B + [-(1 - 2m^*/r)^{\frac{1}{2}}(\mathrm{d}p^*/\mathrm{d}r)\,\boldsymbol{e}_r]_B .$$

(*) For a considerably more rigorous relativistic derivation of (3.32) see THORNE (1966). For a post-Newtonian discussion see CHANDRASEKHAR (1965*d*). BONDI (1964) seems to have been the first to notice that convective instability is unaffected by general relativity.

Here $\varrho^*_{\rm fe}$ is the density of mass-energy of the displaced fluid element,

$$\varrho^*_{\rm fe} = \varrho^*_A + [(\varrho^* + p^*)(\mathrm{d}p^*/\mathrm{d}r)/\Gamma_1 p^*]_A \Delta r; \tag{3.34}$$

and the subscripts « A » and « B » indicate quantities evaluated at r_A and r_B. By combining expressions (3.33), (3.34), and (3.19), we obtain for the proper acceleration of the displaced fluid element relative to the surrounding medium

$$\boldsymbol{a} = \frac{\boldsymbol{F}}{\varrho^*_{\rm fe} + p^*} = -\frac{(1-2m^*/r)^{\frac{1}{2}}}{(\varrho^* + p^*)\Gamma_1 p^*}\left(\frac{-\mathrm{d}p^*}{\mathrm{d}r}\right)\Delta r S(r)\boldsymbol{e}_r\,, \tag{3.35}$$

where $S(r)$, the relativistic Schwarzschild discriminant, is

$$S(r) = \mathrm{d}p^*/\mathrm{d}r - \Gamma_1 p^*(\varrho^* + p^*)^{-1}\,\mathrm{d}\varrho^*/\mathrm{d}r\,. \tag{3.36}$$

If $S(r)$ is positive (subadiabatic temperature gradient), the displaced fluid element is accelerated back toward r_A and the star is stable against convection; but if $S(r)$ is negative (superadiabatic temperature gradient), the displaced fluid element is accelerated on upward, away from r_A, and the star is unstable against convection. Hence, criterion (3.32) for convective instability, which is, equivalent to $S(r) < 0$, is proved.

It should not be surprising that the condition for convective instability is the same in general-relativity theory as in Newtonian theory. Convective instability is a purely local phenomenon; it occurs locally and it is governed entirely by the local values of the thermodynamic variables and their gradients. Consequently, it cannot be affected by nonlinearities in the gravitational field, which act only over finite distances.

Whenever photon, conduction, and neutrino energy transport alone would produce a superadiabatic temperature gradient, convection breaks out and drives the temperature gradient down to adiabatic or near-adiabatic (*). In the adiabatic approximation, which is usually valid, the temperature and pressure gradients are related by eq. (3.11-7*b*); and they are related to the density gradients by

$$\mathrm{d}\varrho^*/\mathrm{d}r = (\varrho^* + p^*)\,n^{-1}\,\mathrm{d}n/\mathrm{d}r\,, \tag{3.37a}$$

$$\mathrm{d}T^*/\mathrm{d}r = (\Gamma_3 - 1)(T^*/n)\,\mathrm{d}n/\mathrm{d}r = (\Gamma_3 - 1)\big(T^*/[\varrho^* + p^*]\big)\,\mathrm{d}\varrho^*/\mathrm{d}r\,, \tag{3.37b}$$

$$\mathrm{d}p^*/\mathrm{d}r = \Gamma_1(p^*/n)\,\mathrm{d}n/\mathrm{d}r = \Gamma_1\big(p^*/[\varrho^* + p^*]\big)\,\mathrm{d}\varrho^*/\mathrm{d}r\,. \tag{3.37c}$$

(*) See *e.g.*, SCHWARZSCHILD (1958), p. 47. For a Newtonian discussion of those rare circumstances in which convection does not produce an adiabatic temperature gradient, see KIPPENHAHN (1963).

Here Γ_1 and Γ_3 are the adiabatic indices of eqs. (2.7) and (2.9). A stellar model in which the gradients are adiabatic is often called *isentropic* because it has constant entropy per baryon,

$$ds^*/dr = 0 \,. \tag{3.37d}$$

This completes our discussion of energy transport in relativistic stellar models. We have considered transport only for the cases in which convective transport is negligible beside radiation plus conduction (eq. (3.11-7*a*)), and for the case in which radiation plus conduction is negligible beside convection, and convection proceeds efficiently (eq. (3.11-7*b*) or, equivalently, any one of eq. (3.37)). It is interesting to note that in neither case does the neutrino luminosity $L_r^{(\nu)*}$ have a direct influence on the temperature gradient. This is because once neutrinos are emitted they never interact again with the star.

3˙2.9. Thermodynamic relations. As was discussed in Sect. 2˙2.3, once the equations of state of the stellar material have been specified, the laws of thermodynamics fix any $4+N$ of the quantities (ϱ^*, p^*, n, s^*, T^*, $Z_1, \ldots, Z_N$, $\tilde{\mu}_1^*, \ldots, \tilde{\mu}_N^*$) as algebraic functions of the other $1+N$. The stellar structure equations (3.11-8)-(3.11-11 $+N$), which include $Z_1 + \ldots + Z_N = 1$, are these three algebraic relations. Equation (3.11-12 $+N$) is the split of the density of mass-energy into rest mass plus internal energy, which we discussed in Sect. 2˙2.1. Equation (3.11-13 $+N$) is the expression for the average baryonic rest mass in terms of the nuclear abundances and rest masses.

3˙2.10. Opacity and conductivity relations. The radiative absorption coefficient, $\varkappa_R^*$, and the thermal conductivity, λ_c^*, depend upon local thermodynamic conditions, which are determined by two thermodynamic parameters (*e.g.* ϱ^* and T^*) and the nuclear aboundances, $Z_1, \ldots, Z_N$. The opacity and conductivity relations (3.11-14 $+N$) and (3.11-15 $+N$), which put this dependence in quantitative form, are discussed in all treatises on the Newtonian theory of stellar structure (see *e.g.*, SCHWARZSCHILD (1958), pp. 62-73; SCHATZMAN (1958), pp. 78-87; and COX (1965)).

For the purpose of computing stellar models the effects of opacity and conductivity are combined into the single absorption coefficient $\varkappa^*$ of eq. (3.11-7*a*). Perhaps the most accurate values of this combined absorption coefficient are those produced by a computer program which has been developed by COX and his collaborators at Los Alamos Scientific Laboratory (see *e.g.*, COX (1965)).

3˙2.11. Equations of thermonuclear energy generation. The reaction rates for thermonuclear transformations, like opacity and conductivity, depend upon local thermodynamic conditions. Equations (3.11-17 $+N$) through

(3.11-16 + 2N) are embodiments of this dependence. (*) For discussions of the specific reaction rates which are needed to make these equations quantitative see *e.g* SCHWARZSCHILD (1958), pp. 73-88; BURBIDGE (1963); REEVES (1965); BAHCALL (1964); BAHCALL and WOLF (1965*a*, *c*).

The remaining equations of thermonuclear energy generation, (3.11-16 + N) and (3.11-17 + 2N)–(3.11-16 + 3N), follow from the definitions of q^* and α_k^* (cf. Sect. 3·1.3).

This completes our discussion of the equations of stellar structure. We next turn our attention to the boundary conditions which must be imposed on the stellar-structure parameters at the center and surface of the star.

3·3. *Boundary conditions for stellar structure.* – Of the 16 + 3N equations of stellar structure (3.11), 7 are first-order differential equations with respect to the radial co-ordinate, r. Corresponding to these 7 differential equations are 7 boundary conditions on the stellar-structure parameters

$$(3.38a) \qquad a(0) = 0\,, \qquad m^*(0) = 0\,, \qquad L_r^*(0) = 0\,, \qquad L_r^{*(\nu)}(0) = 0\,,$$

$$(3.38b) \qquad \Phi(\infty) = 0\,,$$

$$(3.38c) \qquad p^*(R) = 0\,, \qquad T^*(R) = 0\,.$$

These boundary conditions can be understood as follows: a and m^* vanish at the center of the star by definition, since $a(r)$ is the number of baryons inside a sphere of area $4\pi r^2$ and $m^*(r)$ is the mass-energy inside that same sphere. The radial luminosities L_r^* and $L_r^{(\nu)*}$ vanish at the center because of spherical symmetry. The gravitational potential, Φ, is zero at radial infinity by definition—Φ is defined by the physics only up to an additive constant; the choice $\Phi(\infty) = 0$ corresponds to the demand that

$$(3.39) \quad (\text{co-ordinate time}, t) = \begin{pmatrix}\text{proper time as measured by an observer at rest}\\ \text{with respect to the star but very far away from it}\end{pmatrix}.$$

The boundary conditions at the surface of the star ($r = R$) are not so straightforward as those at the center and at infinity. Any star not at zero temperature possesses an atmosphere in which originate most of the photons that escape from the star. Although the atmospheric temperatures and pressures are definitely not zero, they are generally very small by comparison with interior temperatures and pressures. For this reason one can describe accurately all regions of a star except its surface layers and all properties of a star except the spectrum of its radiation by imposing the « zero-boundary conditions »

(*) α_N^* is fixed in terms of $\alpha_1^*, \ldots, \alpha_{N-1}^*$ by the relations $\sum Z_k = 1$ (one of eqs. [3.11-8]→ → [3.11-11 + N]) and $\mathrm{d}Z_k/\mathrm{d}t = e^{\Phi}\alpha_k^*$ (eqs. 3.11-17 + 2N]→ [3.11-16 + 3N]).

(3.38*c*). Since a relativistic theory of stellar atmospheres has not yet been developed, we shall confine ourselves to the zero-boundary conditions throughout these lectures (*).

3·4. *Construction of stellar models.*

3·4.1. External gravitational field. The equations of stellar structure (3.11) are easily solved in the region outside the star, yielding

$$\text{(3.40)} \qquad \begin{cases} m^*(r) = M^* \equiv m^*(R) \\ \Phi(r) \ = \frac{1}{2}\ln(1-2M^*/r) \end{cases} \qquad \text{for } r < R\,.$$

Consequently, the geometry of space-time outside the star is that first discussed by SCHWARZSCHILD (1961):

$$\text{(3.41)} \qquad ds^2 = (1-2M^*/r)\,dt^2 - (1-2M^*/r)^{-1}\,dr^2 - r^2(d\theta^2 + \sin^2\theta\, d\varphi^2)\,.$$

At distances $r \gg M^*$ this geometry represents a gravitational field which can be described accurately by the Newtonian gravitational potential

$$\text{(3.42)} \qquad U = -\Phi c^2 = M^* c^2/r = GM/r.$$

Hence, the quantity $M \equiv m(R)$ is the mass of the star as measured gravitationally by a distant observer; it is the mass which governs the Keplerian motion of distant planets about the star.

3·4.2. Internal structure of noncontracting stars. As in Newtonian theory, so also in general relativity, one can obtain physically interesting interior solutions to the equations of stellar structure only by numerical integration. In the case of noncontracting configurations (configurations in which the energy flux, L_r, is precisely balanced by thermonuclear energy generation) the time derivatives of eq. (3.11-5) (first equality) vanish. The equations of stellar structure then become 7 ordinary first-order radial differential equations (3.11-1)–(3.11-7) coupled to $9 + 2N$ (N being the number of different nuclear species present) algebraic relations (3.11-8)–(3.11-16 + $2N$) and to N first-order, time differential equations (3.11–17 + $2N$)–(3.11-16 + $3N$). There, are in all $16 + 3N$ equations for the $16 + 3N$ structure parameters (Φ, m^* a, ϱ^*, p^*, n, ε^*, s^*, T^*, L_r^*, $L_r^{(\nu)*}$, $\varkappa_R^*$, λ_c^*, q^*, $q_{(\nu)}^*$, μ_B^*, Z_1, ..., Z_N, $\bar{\mu}_1^*$, ..., $\bar{\mu}_N^*$, α_1^*, ..., α_N^*).

(*) For Newtonian discussions of stellar atmospheres see, *e.g.*, SCHWARSCHILD (1958), p. 89, and GREENSTEIN (1960). The general-relativity treatment should differ from the Newtonian treatment only as a result of red-shift effects, which will often be of negligible importance.

In order to construct a noncontracting stellar model and follow its subsequent evolution one might proceed in a manner similar to that used in Newtonian theory (see *e.g.* SCHWARZSCHILD (1958), pp. 97-101): 1) Specify *ab initio* the total number of baryons in the star, $A \equiv a(R)$, plus the initial nuclear abundances $Z_1, \ldots, Z_N$, as functions of the baryon-number co-ordinate, a. 2) Calculate the remaining $16 + 2N$ structure parameters by integrating the 7 differential equations (3.11-1)–(3.11-7) subject to the 7 boundary conditions (3.38) and coupled to the $9 + 2N$ algebraic relations (3.11-8)–(3.11-16 + 2N). The solution will be uniquely determined—aside from cases of mathematical degeneracy (*)— by these equations and boundary conditions. 3) Having now constructed the initial stellar model at time $t = 0$, use eqs. (3.11-17 + 2N)–(3.11-16 + 3N) to determine the nuclear abundances at a later time Δt

$$Z_k(a, \Delta t) = Z_k(a, 0) + \exp[\Phi(a, 0)]\alpha_k^*(a, 0)\Delta t\,, \qquad k = 1, \ldots, N\,. \tag{3.43}$$

In regions where convective transport occurs, correct (3.43) for convection by averaging over the convective zone the $Z_k(a, \Delta t)$ obtained from (3.43). 4) Next calculate the stellar configuration at time Δt by step 2). 5) Repeat steps 3) and 4).

In those phases of evolution characterized by rapid contraction or expansion of the star, this procedure must be replaced by that of the following Section in order to account for the internal energy changes caused by compression or expansion of the fluid.

3'4.3. Internal structure of stars in quasi-static contraction. Whenever the luminosity, L_r, is not precisely balanced by nuclear energy generation, the star must supply the required excess luminosity by quasi-static contraction and by changing its internal energy per baryon, ε^*/n. In order to construct a stellar model in quasi-static contraction (or expansion) and follow its evolution, one can proceed as follows: 1) Specify *ab initio* the total number of baryons, A, plus the initial nuclear abundances, $Z_1(a), \ldots, Z_N(a)$, plus the radial distribution of one thermodynamic variable—say $s^*(a)$ for definiteness. 2) Calculate the remaining $15 + 2N$ structure parameters by integrating the 6 radial differential equations (3.11-1, 2, 3, 4, 6, 7) subject to the 6 boundary conditions (3.38a, b) and $p^*(R)=0$, and coupled to the $9 + 2N$ algebraic relations (3.11-8)–(3.11-16 + 2N). (The boundary condition $T^*(R) = 0$ should be guaranteed by the specified value of $s^*(A)$ and the condition $p^*(R) = 0$.) The solu-

(*) Such cases do occasionaly arise, particularly for stars at the end point of thermonuclear evolution (see *e.g.* Sect. 5'4.1). For a discussion of the mathematical structure of the initial-value problem—which is the same in general relativity as in Newtonian theory—and of the uniqueness of the solution, see *e.g.* SCHWARZSCHILD (1958), p. 97.

tion will be uniquely determined aside from cases of mathematical degeneracy (*). 3) Having now constructed the initial stellar model at time $t = 0$, use eqs. (3.11-5) and (3.11-17 + 2N)–(3.11-16 + 3N) to determine the nuclear abundances and the distribution of entropy at time $t = \Delta t$

$$(3.44a) \qquad Z_k(a, \Delta t) = Z_k(a, 0) + \exp[\Phi(a, 0)]\alpha_k^*(a, 0)\Delta t\,, \qquad k = 1, \ldots, \mathrm{N}$$

$$(3.44b) \qquad s^*(a, \Delta T) = s^*(a, 0) - \frac{(1 - 2m^*/r)^{\frac{1}{2}} e^{-\Phi}}{4\pi r^2 n T^*} \frac{\mathrm{d}(L_r^* e^{2\Phi})}{\mathrm{d}r} \Delta t - \\ - T^{*-1} \sum \bar{\mu}_k^*(a, 0) \exp[\Phi(a, 0)]\alpha_k^*(a, 0)\Delta t\,.$$

4) Calculate the stellar configuration at time Δt by step 2) but with the initial condition $s^*(a) =$ (initial value of $s^*(a)$) replaced by (3.44b). 5) Repeat steps 3) and 4) until the assumption of quasi-static motion breaks down, *e.g.*, as the result of the onset of dynamical instabilities (cf. Sect. **4**), or until the star has cooled to zero temperature.

3·5. *Properties of nonrotating stars.* – We now turn our attention from procedures for constructing relativistic stellar models to some of the properties of such models. Our discussion will be based on the equations of stellar structure (3.11).

3·5.1. Geometry of space-time. For stars with mass M^* and radius R such that $2M^*/R \sim 1$, the geometry of space-time is far from Euclidean. Consequently, there is no *a priori* reason to expect that the surface area, $4\pi r^2$, of successive spheres about the center of such a star will be an always-increasing function of distance from the center. Indeed, in Sect. **7·3.7**, we shall see that $4\pi r^2$ can sometimes decrease (« bag of matter ») as one moves outward from the center of a gravitationally collapsing star. However, this peculiar radial decrease in $4\pi r^2$, and hence also in r, is limited to dynamical situations; *in any spherical configuration of hydrostatic equilibrium the radial co-ordinate, r, increases monotonically from 0 at the center of the star to ∞ at an infinite distance away.*

The monotonicity of r can be seen as follows: Introduce as a new radial co-ordinate proper distance, l, from the center of the star. By virtue of expression (3.1) for the geometry of space-time, l and r are related by

$$(3.45) \qquad \mathrm{d}r = \pm (1 - 2m^*/r)^{\frac{1}{2}} \mathrm{d}l\,.$$

Since r is zero at the center of the star and r is always nonnegative, r must at first increase with l as one moves outward from $l = 0$. $r(l)$ can later reach a maximum and start decreasing only at a point where $2m^*/r$ becomes unity

(*) See footnote (*) on p. 199.

(cf. eq. (3.45)). However, if $2m^*/r$ approaches unity in some region of the star, the pressure gradient (eq. (3.11-3)) becomes so large that the surface of the star, $p^* = 0$, is reached before $2m^*/r$ reaches one. After the surface of the star is passed, m^* remains constant and $2m^*/r$ decreases. Consequently, *$2m^*/r$ is always less than unity*; and $r(l)$ cannot have a maximum. QED. (For a more rigorous proof see BONDI (1964)).

The gravitational field of an equilibrium configuration is most easily visualized by means of an embedding diagram (Sect. **2**·3.1.) of the hypersurfaces of constant time. The geometry of these hypersurfaces is given by

$$d\sigma^2 = (1 - 2m^*/r)^{-1}\,dr^2 + r^2(d\theta^2 + \sin^2\theta\,d\varphi^2)\,. \tag{3.46}$$

In order to construct a surface with this geometry in Euclidean 3-space we must suppress one rotational degree of freedom; *i.e.* we must restrict ourselves to the 2-geometries

$$d\sigma^2 = (1 - 2m^*/r)^{-1}\,dr^2 + r^2\,d\theta^2 \tag{3.47}$$

of constant t and φ.

An embedding of this 2-geometry is most conveniently obtained by introducing into the Euclidean 3-space cylindrical co-ordinates $(\bar{r}, \bar{\theta}, \bar{z})$ and by taking as the embedded 2-surface

$$\bar{r} = r\,, \qquad \bar{\theta} = \theta\,, \qquad \bar{z} = \int_0^r [2m^*/(r - 2m^*)]^{\frac{1}{2}}\,dr\,. \tag{3.48}$$

That the intrinsic geometry of the 2-surface (3.48) in Euclidean 3-space is, indeed, identical to the geometry (3.47) of space around an equilibrium stellar configuration is easily verified as follows:

$$d\bar{\sigma}^2 = d\bar{z}^2 + d\bar{r} + \bar{r}^2\,d\bar{\theta}^2 = [2m^*/(r - 2m^*)]\,dr^2 + dr^2 + r^2\,d\theta^2 = \tag{3.49}$$
$$= (1 - 2m^*/r)^{-1}\,dr^2 + r^2\,d\theta^2 = d\sigma^2\,.$$

The embedded stellar geometry (3.48) for a typical equilibrium configuration is shown in Fig. 1.

The embedding diagram for any equilibrium configuration necessarily has the following properties: 1) The interior region is a bowl with a smooth bottom which opens outward and upward. 2) The exterior region is a paraboloid of the form

$$\bar{r} = 2M^* + (\bar{z} - \bar{z}_0)^2/8M^*\,, \qquad \bar{z}_0 = \text{const} < \bar{z} \text{ at surface of star}\,. \tag{3.50}$$

3) The interior and exterior regions join together smoothly. 4) The geometry

nowhere contains a radial bulge or neck (« bag of matter »); *i.e.* r is a monotonic increasing function of z.

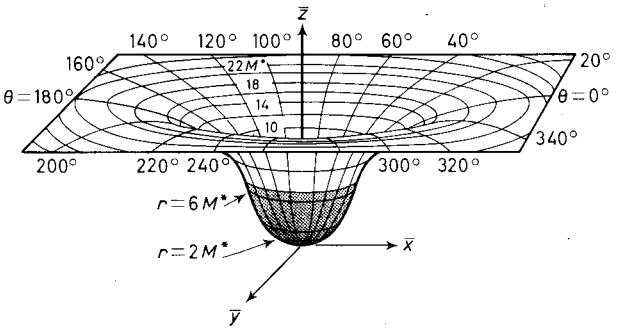

Fig. 1. – Embedding diagram for the geometry of the 2-surface $(t, \varphi) = \text{constant}$ of a nonrotating star in hydrostatic equilibrium. The co-ordinates (r, θ) intrinsic to this 2-surface are related to the co-ordinates $[\bar{r} = (\bar{x}^2 + \bar{y}^2)^{\frac{1}{2}}, \bar{\theta} = \mathrm{tg}^{-1}(\bar{y}/\bar{x}), \bar{z}]$ of the Euclidean embedding space by eqs. (3.48). The interior of the star is distinguished from the exterior by stippling. Because the rotational degree of freedom associated with φ has been suppressed from the diagram, regions of constant radius, r, are here circles of circumference $2\pi r$ about the center, $r = 0$. The 3-geometry of space around the star at a particular moment of time, t, can be visualized by mentally replacing the circles of constant r in this diagram with spheres of area $4\pi r^2$.

It must be emphasized that only points lying on the embedded 2-surface have physical significance so far as the stellar geometry is concerned; the 3-dimensional regions inside and outside the bowl of Fig. 1 are physically meaningless, as are the co-ordinates $(\bar{r}, \bar{z}, \bar{\theta})$ of the Euclidean embedding space. They merely permit us to visualize the geometry of space around the star in a convenient manner.

From the embedding diagram of Fig. 1 and also from eq. (3.46) it is clear that *the area, $4\pi r^2$, of a sphere about the center of the star is always less than $4\pi l^2$, where l is the proper radius of the sphere*

$$l = \int_0^r (1 - 2m^*/r)^{-\frac{1}{2}} \mathrm{d}r \,. \tag{3.51}$$

3·5.2. Distribution of pressure. From the TOV equation (3.11-3) of hydrostatic equilibrium it is evident that *pressure, p^*, decreases monotonically from the center of an equilibrium configuration to its surface.* Also, a comparison of the TOV equation with its Newtonian counterpart (3.18) reveals this, that at a radius r, inside of which is a mass m^*, *the pressure gradient is steeper than would be expected from Newtonian theory.* An increased pressure gradient is necessary

to counterbalance the relativistically enhanced gravitational acceleration (eq. (3.17)).

Two different types of relativistic nonlinearities enhance the gravitational acceleration, and hence the pressure gradient: 1) the « geometric » nonlinearity associated with the quantity $(1-2m^*/r)$ in the denominator of the TOV equation (3.11-3); and 2) « pressure-regenerative » nonlinearities associated with the two pressure terms in the numerator. In hot, supermassive stars, both geometric nonlinearities and pressure-regenerative nonlinearities are important; and they steepen the pressure gradient by $\lesssim 1\%$. Pressure-regenerative nonlinearities dominate and reach their extreme in (physically unrealistic) configurations of incompressible fluid—see, *e.g.*, HTWW Chapter 4, and WHEELER (1964*a*) pp. 222-225—where they enhance the pressure gradient by arbitrarily large amounts. In superdense stars near the endpoint of thermonuclear evolution (Sect. **5**) the two types of nonlinearities are equally important; they both enhance the pressure gradient by $\sim 10\%$.

3·5.3. Extremal mass-energy. A very important and intuitively satisfying property of equilibrium configurations is the following: Consider an arbitrary, momentarily static, spherical configuration of fluid which may or may not be in hydrostatic equilibrium. Adiabatically perturb this configuration in the radial direction by an amount $\xi(r) = \delta r$, and calculate the change, δM^*, in the total mass of the star which results from the perturbation. Then the original configuration was in hydrostatic equilibrium if and only if δM^* vanishes to first order in the amplitude of the perturbation, ξ. Put more briefly, *the total mass-energy, M^*, of an equilibrium configuration is an extremum with respect to adiabatic, radial perturbations* (*).

In Sect. **4**·2.1 we will see how this theorem of extremal mass-energy can be extended to determine the stability of an equilibrium configuration.

3·5.4. Orbits of freely falling bodies. The orbits of small bodies falling freely in the external gravitational field of a relativistic star have been studied in great detail by DARWIN (1959). We summarize here some of the most interesting results, assuming always that the surface of the star is inside the orbits under discussion.

(*) This theorem was first proved independently by COCKE (1965) and by THORNE and WHEELER (1965). (See also HTWW, p. 16 and 156). The proof in HTWW applies only to zero-temperature configurations, but it can be generalized to arbitrary configurations by simply replacing all ordinary derivatives ($dp^*/d\varrho^*$, $dn/d\varrho^*$, etc.) by isentropic partial derivatives $[(\partial p^*/\partial\varrho^*)_s$, $(\partial n/\partial\varrho^*)_s$, etc.]. COCKE actually proves the theorem, in an inverted but equivalent form; he shows that the total entropy, S, of an equilibrium configuration is extremized with respect to adiabatic, radial perturbations in which M^*—but not necessarily A—is kept fixed.

Orbits with perihelions at $r \gg M^*$ are Keplerian in form, except for the perihelion shift which is familiar in the case of Mercury. However, orbits which extend into the region $r \leqslant 10M^*$ have forms unexpected in Newtonian theory. For example, there is never a perihelion in the region $r < 3M^*$; any orbit which extends into this region necessarily hits the surface of the star. Circular orbits are allowed throughout the region $r \geqslant 3M^*$; but they are stable only for $r > 6M^*$. A particle in a circular orbit with $3M^* < r < 4M^*$, if perturbed, will escape to infinity or fall into the star. A circling particle with $4M^* < r < 6M^*$, if perturbed, will enter a spiraling orbit which eventually falls into the star. Circular orbits at $r = 3M^*$ are allowed only for photons or neutrinos since they can be maintained only by a particle moving with the speed of light.

The energy red-shift relation (3.3) plays a fundamental role in the study of particle and photon orbits.

3˙5.5. Gravitational red-shift. The energy red-shift relation (3.3) when applied to photons yields an expression for the gravitational red-shift of the wavelength of light. Consider a photon which is emitted at a point $(r_0, \theta_0, \varphi_0)$ in the gravitational field of a star and received at a point $(r_1, \theta_1, \varphi_1)$. Let the energy and wave length of the photon, as measured in the proper frames of observers at rest with respect to the star, be E and $\lambda = hc/E$. Then

$$Ee^{\Phi} = \big(hc/\lambda(r)\big) \exp[\Phi(r)] = \text{const}\,, \tag{3.52}$$

so that the red-shift factor is

$$z \equiv (\lambda_1 - \lambda_0)/\lambda_0 = \exp[\Phi(r_1) - \Phi(r_0)] - 1\,. \tag{3.53}$$

For a photon emitted from the surface of the star ($r = R$) and received at infinity this becomes (cf. eq. (3.40))

$$z = (1 - 2M^*/R)^{-\frac{1}{2}} - 1\,. \tag{3.54}$$

We found in Sect. **3**˙5.1 that $(1 - 2M^*/R)$ is necessarily greater than zero for a configuration of hydrostatic equilibrium. Consequently, the red-shift is never infinite. BONDI (1964, 1965), by a very careful and elegant analysis of the TOV equation of hydrostatic equilibrium, has put much more stringent limits on z. (See also BUCHDAHL (1959), a forerunner of Bondi's work.) For all configurations which are in principle physically realizable ($\varrho^* \geqslant p^* \geqslant 0$ everywhere; cf. end of Sect. **2**˙2.1). BONDI finds

$$M^*/R \leqslant 0.432\,, \qquad z \leqslant 1.71\,. \tag{3.55}$$

If, in order to avoid Taylor instabilities (see *e.g.* CHANDRASEKHAR (1961)), one imposes the additional restriction that ϱ^* be monotonic decreasing from the center of the star to the surface, then one obtains (BONDI (1964, 1965))

$$M^*/R \leqslant 0.390\,, \qquad z \leqslant 1.14\,. \tag{3.56}$$

In most realistic situations one actually has $p^* \leqslant \frac{1}{3}\varrho^*$ (cf. HTWW, Chapter 10) and an adiabatic or subadiabatic temperature gradient (cf. Sect. 3°2.8). When this is the case, Bondi's analysis yields the limits

$$M^*/R \leqslant 0.310\,, \qquad z \leqslant 0.63\,. \tag{3.57}$$

Although the red-shift of a photon originating at the *surface* of any equilibrium configuration is limited by $z < 1.63$, the red-shift of a photon—or, more realistically of a neutrino—which originates at the *center* can be arbitrarily large. An expression for the red-shift of such a neutrino is (cf. eqs. (3.53) and (3.11-3, 4))

$$z = (1 - 2M^*/R)^{-\frac{1}{2}} \exp\left[\int_0^R (\varrho^* + p^*)^{-1}(-\,\mathrm{d}p^*/\mathrm{d}r)\,\mathrm{d}r\right] - 1\,. \tag{3.58}$$

For configurations of arbitrarily high central pressure, this red-shift is arbitrarily large.

3°5.6. Spectrum of the stellar radiation. Having forgone any attempt to describe the stellar atmosphere (cf. Sect. 3°3), we have placed a barrier between ourselves and a *detailed* knowledge of the spectrum of the light radiated by a relativistic star. However, simple physical considerations, as well as astronomical observations, reveal that the spectrum is roughly that of a black body. By equating the total nonneutrino luminosity at the surface of the star, $L_r^*(R) - L_r^{(\nu)*}(R)$, to the integrated intensity, $4\pi R^2 \sigma^* T_e^{*4}$, of a black body of temperature T_e^* and surface area $4\pi R^2$, we obtain for the «effective temperature» which characterizes the star's black-body radiation

$$T_e^* = \left\{(L_r^* - L_r^{(\nu)*})_{r=R}/(4\pi R^2 \sigma^*)\right\}^{\frac{1}{4}}. \tag{3.59}$$

This is actually the effective temperature as seen by an observer near the surface of the star. For an observer very far away the light will be red-shifted by a factor

$$z \equiv \Delta\lambda/\lambda = \exp\left[-\,\Phi(R)\right] - 1 = (1 - 2M^*/R)^{-\frac{1}{2}} - 1\,. \tag{3.60}$$

This red-shift of wavelength preserves the (roughly) black-body form of the spectrum but lowers the temperature, which characterizes the spectrum, from

T_e to

$$(3.61)\qquad \left(\begin{matrix}\text{Black-body temperature}\\ \text{as seen at } r=\infty\end{matrix}\right)^* = T_e^*\left(1-\frac{2M^*}{R}\right)^{\frac{1}{4}} = \left\{\left[\frac{L_r^*-L_r^{(\nu)*}}{4\pi r^2\sigma^*}\right]_{r=\infty}\right\}^{\frac{1}{4}}.$$

To verify this, combine eqs. (3.11-5, 6) and (3.59) with the Planck distribution law for black-body radiation.

35.7. Injection energy and convection(*). Let an astrophysicist far from a stellar equilibrium configuration create δA baryons and drop them, along with an additional mass-energy W_0^*, down an idealized pipe, which is inserted into the star, to a colleague situated at radius r. Require that the nuclear abundances of the δA baryons be the same as the abundances at radius r in the star. Have the colleague at r: 1) catch the falling baryons, thereby extracting their kinetic energy of fall, $W_{\rm kin}^*$; 2) use the energy $W_0^* + W_{\rm kin}^*$ to compress and heat the δA baryons to the local thermodynamic conditions, and to insert them from the pipe into the star; 3) throw the excess mass-energy back up the pipe to the astrophysicist far away. The total mass-energy used up in this process, as measured by the distant astrophysicist, is called *the injection energy at r* and is equal to the change, δM^*, in the total mass-energy of the star which results from the addition of the δA baryons at r (conservation of total mass-energy). Let us calculate δM^*:

The total mass-energy which the distant astrophysicist drops down the pipe is $\mu_0^*\,\delta A + W_0^*$, where $\mu_{\rm B}^*$ is the average rest mass of the baryons created. When the colleague at r catches the δA baryons and excess mass W_0^*, they have a total energy of (cf. eq. (3.3))

$$W_{\rm total}^* \equiv \mu_{\rm B}^*\,\delta A + W_0^* + W_{\rm kin}^* = (\mu_{\rm B}^*\,\delta A + W_0^*)\exp[-\Phi(r)]\,.$$

Hence, the kinetic energy which he extracts is

$$W_{\rm kin}^* = (\mu_{\rm B}^*\,\delta A + W_0^*)(\exp[-\Phi]-1)\,.$$

The colleague at r uses $W_{\rm kin}^* + W_0^*$ to heat and compress the baryons to local thermodynamic conditions and to push aside enough fluid in the star to make room for the new baryons. Heating and compression require

$$W_{\rm heat}^* + W_{\rm compress}^* = [\varrho^*(r)/n(r) - \mu_{\rm B}^*]\,\delta A\,;$$

(*) The analysis of this Section is patterned after a similar analysis by WHEELER (HTWW, p. 20) for zero-temperature configurations.

while opening up a space in the star requires

$$W^*_{\text{open}} = p^*(r)[\delta A/n(r)] .$$

Hence, the excess energy which the colleague at r must throw back up the pipe is

$$W^*_{\text{excess at } r} = W^*_0 + W^*_{\text{kin}} - (W^*_{\text{heat}} + W^*_{\text{compress}} + W^*_{\text{open}}) = \\ = (W^*_0 + \mu^*_{\text{B}}\,\delta A)\,e^{-\Phi} - (\varrho^* + p^*)(\delta A/n)$$

According to the equation of energy red-shift (3.3) the colleague at r must convert a portion $(W^*_{\text{excess at } r})(1 - \exp[\Phi(r)])$ of this excess mass-energy into the kinetic energy of his throw in order to get the rest of the excess mass-energy back up to the distant astrophysicist. Thus, the distant astrophysicist receives an excess mass-energy of only

$$W^*_{\text{excess at } \infty} = W^*_{\text{excess at } r} \exp[\Phi(r)] = W^*_0 + \mu^*_{\text{B}}\,\delta A - (\varrho^* + p^*)\,n^{-1}\,e^{\Phi}\,\delta A .$$

The total mass-energy required to create the δA baryons and perform the injection process is thus

$$\delta M^* = W^*_0 + \mu^*_{\text{B}}\,\delta A - W^*_{\text{excess at } \infty}$$

$$\delta M^* = [\varrho^*(r) + p^*(r)][n(r)]^{-1} \exp[\Phi(r)]\,\delta A = (\partial\varrho^*/\partial n)_{s^*} \exp[\Phi(r)]\,\delta A . \tag{3.62}$$

This result has a simple interpretation: $(\partial\varrho^*/\partial n)_{s^*}\cdot\delta A$ is the local increase in mass-energy at r which results from adding δA baryons; and $\exp[\Phi(r)]$ is the fraction by which this mass-energy at r is red-shifted when it is brought out to radial infinity, where δM^* is measured.

The injection energy, δM^*, generally depends upon the radius, r, at which the δA baryons are injected. From the way in which we calculated injection energy, it is clear that δM^* *will be independent of* r if and only if baryons can be moved about freely in the star without any expenditure or release of energy —*i.e. if and only if the star is in marginal convective equilibrium.*

Let us verify that the condition $\delta M^* = \text{const.}$ is, indeed, equivalent to the adiabatic-gradient criterion (Sect. 3˙2.8.) for marginal convective equilibrium:

$$\delta M^* = \text{const} \Leftrightarrow [(\varrho^* + p^*)/n]e^{\Phi} = \text{const} \Leftrightarrow \ln(\varrho^* + p^*) - \ln n + \Phi = \text{const} ,$$

$$\Leftrightarrow (\varrho^* + p^*)^{-1}(\mathrm{d}\varrho^*/\mathrm{d}r + \mathrm{d}p^*/\mathrm{d}r) - n^{-1}\,\mathrm{d}n/\mathrm{d}r + \mathrm{d}\Phi/\mathrm{d}r = 0 ,$$

$$\Leftrightarrow (\varrho^* + p^*)^{-1}(\mathrm{d}\varrho^*/\mathrm{d}r + \mathrm{d}p^*/\mathrm{d}r) - n^{-1}\,\mathrm{d}n/\mathrm{d}r - (\varrho^* + p^*)^{-1}\,\mathrm{d}p^*/\mathrm{d}r = 0 ,$$

$$\Leftrightarrow \mathrm{d}\varrho^*/\mathrm{d}r = (\varrho^* + p^*)\,n^{-1}\,\mathrm{d}n/\mathrm{d}r \Leftrightarrow \mathrm{d}\varrho^*/\mathrm{d}r = (\partial\varrho^*/\partial n)_{s^*}\,\mathrm{d}n/\mathrm{d}r ,$$

$$\Leftrightarrow \text{the thermodynamic gradients are adiabatic.}$$

The value of the constant injection energy for a configuration which is everywhere isentropic (marginally convective) is most conveniently calculated at the star's surface

$$\delta M^* = \mu_B^*(R)[1 - 2M^*/R]_{\mathrm{II}}^{\frac{1}{2}} \delta A \,. \tag{3.63}$$

This completes our discussion of general properties of nonrotating equilibrium configurations. Before moving on to a discussion of stellar stability (Sect. **4**) and of specific stellar models (Sect. **5** and **6**), we shall describe briefly the little which is known about rotating, relativistic equilibrium configurations.

3·6. *Rotating equilibrium configurations.*

3·6.1. Rotation in general relativity. The relativistic gravitational field of an axially-symmetric rotating equilibrium configuration is conveniently described in terms of four gravitational potentials $\gamma(r, \theta)$, $K(r, \theta)$, $\omega(r, \theta)$, $N(r, \theta)$, which determine the geometry of space-time through the line element

$$\begin{aligned} \mathrm{d}s^2 = (N^2 - \omega^2 K^2 r^2 \sin^2\theta)\,\mathrm{d}t^2 - e^{2\gamma}\,\mathrm{d}r^2 - \\ - r^2 K^2(\mathrm{d}\theta^2 + \sin^2\theta\,\mathrm{d}\varphi^2) - 2\omega K^2 r^2 \sin^2\theta\,\mathrm{d}\varphi\,\mathrm{d}t \,. \end{aligned} \tag{3.64}$$

Here (t, r, θ, φ) are a particular, geometrically selected set of space-time co-ordinates which, for the special case of zero rotation, reduce to the spherical co-ordinates used to describe nonrotating equilibrium configurations.

The gravitational source equations and the equations of hydrostatic equilibrium for rotating configurations have been worked out by HARTLE and SHARP (1966) and by many others; but they are so complicated that no physically interesting solutions to them have yet been found.

Even the partial differential equations for the exterior gravitational field are almost unmanageable. Only one physically interesting solution to them is known—that of KERR (1963, 1965) (See also CARTER (1966) and BOYER and LINDQUIST (1966).) Kerr's solution is the external gravitational field for a limited class of rotating equilibrium configurations. BOYER (1965*a*, *b*) has studied some of the properties of those rigidly rotating equilibrium configurations which would generate Kerr's gravitational field, but the precise forms of the internal solutions are unknown (*). Other contributions to our understanding of the external gravitational fields of rotating configurations have come from PAPAPETROU (1953, 1966).

(*) DOROSHKEVICH, ZEL'DOVICH and NOVIKOV (1965) incorrectly argue that no rotating configuration could generate Kerr's gravitational field unless the fluid in its interior performed a circulatory motion in addition to rotating. Their argument is based upon the false belief that Kerr's metric contains nonremovable off-diagonal terms in addition to $g_{t\varphi}$. (Cf. BOYER and LINDQUIST (1966).)

Because the equations which govern rotating configurations are so intractable analytically, attempts to construct numerical solutions will soon be initiated. The construction of numerical solutions should not be too much more difficult in general relativity than in Newtonian theory because the number of independent variables is the same—two.

HARTLE and SHARP (1965, 1966) have recently constructed a mass-energy variational principle for rotating configurations, which is analogous to the variational principle of Sect. 3·5.3 for nonrotating configurations, and which may be of considerable value in the construction of numerical solutions to the equations of rotation. This variational principle states that *the equilibrium states of a uniformly rotating perfect fluid are those configurations which extremize the total mass-energy with respect to pertubations that a) are adiabatic, b) keep the total angular momentum fixed, and c) conserve the total number of baryons.*

As a special case of the Hartle-Sharp work on rotation, HARTLE (1966) has studied in some detail the effects of small amounts of rotation on relativistic configurations of hydrostatic equilibrium.

3·6.2. Rotation in the post-Newtonian approximation. The post-Newtonian approximation has been used frequently since 1925 to study the effects of rotation upon equilibrium configurations of perfect fluid and upon their external gravitational fields (see *e.g.* AKELEY (1931), CLARK (1947, 1948, 1950), CHANDRASEKHAR (1965*c*), FOWLER (1966), ROXBURGH (1965), DURNEY and ROXBURGH (1965)).

Those post-Newtonian studies which perhaps are most interesting from an astrophysical standpoint are the recent analyses by FOWLER (1966), by ROXBURGH (1965), and by DURNEY and ROXBURGH (1965) of the relationship between angular velocity, binding energy, and stability for rotating configutions; and the analysis by CHANDRASEKHAR (1965*c*) of the shapes of rotating configurations. Since Fowler's work is available in this volume, we shall describe only Chandrasekhar's results.

Consider a star with uniform density of mass-energy, ϱ^*, in uniform rotation about an axis of symmetry. Newtonian theory reveals that Maclaurin spheroids are possible equilibrium configurations for such a star. CHANDRASEKHAR has used his post-Newtonian tensor virial theorem to show that post-Newtonian gravitational forces will pull the equator of such a spheroid in toward its center. The order of magnitude of the reduction in eccentricity is indicated in Table II, where we compare the eccentricities expected from Newtonian theory with those predicted by post-Newtonian theory, for a spheroid with density of mass-energy ϱ, angular velocity ω, total mass-energy M, and equatorial radius R_{eq} (*). Note that the fractional post-Newtonian correction to the eccentricity

(*) For the precise physical meaning of the post-Newtonian quantities ω and R_{eq} (Ω and a_1 in Chandrasekhar's notation) see CHANDRASEKHAR (1965*b*, *c*).

is proportional to $2GM/c^2R_{eq} = 2M^*/R_{eq}$. This is a particular case of a frequent phenomenon in post-Newtonian theory: fractional post-Newtonian corrections to the Newtonian stucture of a star are usually proportioned to $2M^*/R$.

TABLE II. – *The effects of post-Newtonian gravitational forces on the eccentricity of a Maclaurin spheriod* [a].

$\omega^2/\pi G\varrho$	$2GM/c^2R_{eq}$	e_{Newton}	$e_{post\text{-}Newton}$
0.02146	0.01	0.20000	0.1996
0.02146	0.1	0.2000	0.196
0.27734	0.01	0.700	0.698
0.27734	0.1	0.70	0.68

[a] Based on an exact formula due to CHANDRASEKHAR (1965*c*).

3·7. *Summary.* – The principal conclusions from our discussion of equilibrium stellar configurations are these: The structure of a nonrotating equilibrium configuration is determined by $16 + 3N$ quantities, where N is the number of different nuclear species present: the gravitational potential, Φ; the mass-energy inside radius r, m^*; the number of baryons inside radius r, a; the density of mass-energy, ϱ^*; the pressure, p^*; the number density of baryons, n; the density of internal energy, ε^*; the entropy per baryon s^*; the temperature, T^*; the total luminosity (energy flux), L_r^*; the neutrino luminosity, $L_r^{(\nu)*}$; the radiative absorption coefficient, $\varkappa_R^*$; the thermal conductivity, λ_c^*; the rate of thermonuclear energy generation, q^*; the rate of energy release into neutrinos, $q_{(\nu)}^*$; the average baryonic rest mass, μ_B^*; the nuclear abundances, $Z_1, \ldots, Z_N$; the nuclear chemical potentials, $\bar{\mu}_1^*, \ldots, \bar{\mu}_N^*$; and the rates of change of nuclear abundances, $\alpha_1^*, \ldots, \alpha_N^*$. These quantities are all functions of a radial co-ordinate, r, defined such that $4\pi r^2$ is the surface area of a sphere about the center of the star. Equations (3.11) are $16 + 3N$ equations of stellar structure which uniquely determine the distributions of the $16 + 3N$ structural parameters once sufficient initial data are given. These equations also govern the evolution of relativistic stars.

Some important properties of nonrotating equilibrium configurations are the following: 1) The geometry of space-time about an equilibrium configuration, as given by the line element (3.1), can be represented pictorially by the bowl-like embedding diagram of Fig. 1. 2) This geometry (or gravitational field) causes a red-shift of photons emitted from the surface of the star. The red-shift is greater the more compact the star; but for no equilibrium configuration can it ever exceed $(\Delta\lambda/\lambda) = 1.71$. 3) The total mass-energy of an equilibrium

configuration is an extremum with respect to adiabatic, radial perturbations. 4) An equilibrium configuration has injection energy independent of radius if and only if it is in marginal convective equilibrium.

The relativistic theory of rotating equilibrium configurations has not yet been developed. However, it is known that 1) uniformly rotating configurations have extremal mass-energy; and 2) post-Newtonian gravitational forces tend to reduce the equatorial bulge of a rotating star.

4. – Stability of equilibrium configurations.

We now turn our attention from the theory of the structure of relativistic stellar models to the theory of their stability against small perturbations. We shall first discuss nonradial perturbations, about which very little is known; and then we shall review the extensively-developed theory of radial perturbations.

4·1. *Nonradial perturbations of nonrotating configurations.* – The analysis of small, nonradial motions of a star about its equilibrium configurations is so difficult that only recently has the Newtonian theory been developed into a fairly definitive form (LEDOUX and WALRAVEN (1958), CHANDRASEKHAR and LEBOVITZ (1964), CHANDRASEKHAR (1964*a*), and LEBOVITZ (1965*a*, *b*)); and the general relativity theory is as yet nonexistent. The relativistic theory, when it is developed, will be far more complicated than the Newtonian theory because, according to general relativity, a star in nonradial motion should emit gravitational waves.

One would like to gain some insight into the effects of general relativity on nonradial perturbations without becoming enmeshed in the complications of gravitational radiation theory. This can be done by going to the post-Newtonian approximation, where radiation is not present (cf. Sect. 2·3.5). CHANDRASEKHAR (1965*a*, *b*) has given a definitive post-Newtonian treatment of nonradial perturbations of equilibrium configurations. The most interesting and useful results of his analysis are these: As in Newtonian theory, so also in the post-Newtonian approximation 1) all of the nonradial normal modes of a star are stable if and only if the temperature gradient is everywhere subadiabatic; 2) there exist nonradial normal modes of zero frequency if and only if the temperature gradient is adiabatic over some finite region of the star; 3) there exists at least one unstable nonradial normal mode if and only if the temperature gradient is superadiabatic over some finite region; and when this is the case there is at least one unstable normal mode for each value, $l > 1$, of the spherical-harmonic index.

Because a superadiabatic temperature gradient is the criterion for convective instability, the above theorems state, in effect, that in post-Newtonian theory the instability of any nonradial normal mode of oscillation goes hand-in-hand with convective instability somewhere in the star. In most stars any convective instability which arises in the course of stellar evolution— and with it the associated dynamical instabilities— will be quickly removed by convective motions in the interior. Consequently, for most post-Newtonian configurations the only types of dynamical instability which are of any consequence are the radial instabilities discussed in the next Section.

Whether the remarkable Newtonian and post-Newtonian tie-up between dynamical, nonradial instabilities and convective instabilities holds also in general relativity is now unknown. It would not be surprising if this tie-up were to break down in the presence of very strong gravitational fields.

42. *Radial perturbations of nonrotating configurations* (*). – The theory of small radial motions of a star about its equilibrium configuration is unaffected by the complications of gravitational radiation because, just as a spherical charge distribution cannot radiate electromagnetically, so a spherical mass distribution cannot radiate gravitationally. The absence of gravitational waves has made possible a detailed development of the theory of radial perturbations of non-rotating, relativistic stellar models (ZEL'DOVICH (1963*b*), CHANDRASEKHAR (1964*b*, *c*), FOWLER (1964), WRIGHT (1964, 1965), HTWW (1965), BARDEEN (1965), COCKE (1965), BARDEEN, THORNE and MELTZER (1966)). We shall briefly describe that theory here.

There are two essentially different approaches to the study of the radial stability of relativistic configurations. There is a dynamical approach, which involves an analysis of the dynamics of radial oscillations; and there is a static approach, which requires only a comparison of the masses and radii of the members of a particular sequence of static, equilibrium configurations.

42.1. Dynamical approach to stability(**). Consider a star in small-amplitude, adiabatic, radial motion about its equilibrium configuration. Describe the motion by $\xi(r, t) \equiv \delta r(r, t)$, the radial co-ordinate displacement of the fluid element whose equilibrium radius is r, as a function of co-ordinate time, t. The total mass-energy of the perturbed star will differ from that of the equilibrium configuration by an amount δM^*, which can be divided into

---

(*) For a more detailed review of this topic see BARDEEN, THORNE and MELTZER (1966).

(**) Most of the results described in this section are due to CHANDRASEKHAR (1964*b*, *c*); but the present mass-energy derivation of them is due to THORNE (see HTWW, Appendix B). For a maximum-entropy derivation of these results see COCKE (1965).

a potential part, $\mathscr{P}^*$, plus a kinetic part, $\mathscr{K}^*$

$$\delta M^* = \mathscr{P}^*[\xi, \xi'] + \mathscr{K}^*[\dot{\xi}] . \tag{4.1}$$

A fairly straightforward calculation reveals (*)

$$\mathscr{P}^*[\xi, \xi'] = 2\pi \int_0^R \{P(r^2 e^{-\Phi}\xi)'^2 - Q(r^2 e^{-\Phi}\xi)^2\}\, \mathrm{d}r , \tag{4.2a}$$

$$\mathscr{K}^*[\dot{\xi}] = 2\pi \int_0^R W(r^2 e^{-\Phi}\dot{\xi})^2\, \mathrm{d}r , \tag{4.2b}$$

where $X' \equiv \partial X/\partial r$, $\dot{X} \equiv \partial X/\partial t$, Φ is the gravitational potential of eq. (3.1) for the equilibrium configuration, and P, Q, W are functions of the equilibrium configuration defined by

$$\begin{cases} P = e^{3\Phi}(1-2m^*/r)^{-\frac{1}{2}} r^{-2} \Gamma_1 p^* , \\ Q = -4e^{3\Phi}(1-2m^*/r)^{-\frac{1}{2}} r^{-3} p^{*\prime} - 8\pi e^{3\Phi}(1-2m^*/r)^{-\frac{3}{2}} r^{-2} p^*(\varrho^* + p^*) + \\ \qquad\qquad + e^{3\Phi}(1-2m^*/r)^{-\frac{1}{2}} r^{-2}(\varrho^* + p^*)^{-1} p^{*\prime 2} , \\ W = e^{\Phi}(1-2m^*/r)^{-\frac{1}{2}} r^{-2}(\varrho^* + p^*) . \end{cases} \tag{4.3}$$

Note that the mass-energy, δM^*, associated with the perturbation is quadratic in the amplitude of the perturbation. The vanishing of linear terms is in accordance with the theorem of extremal mass-energy for equilibrium configurations (Sect. 33.5.3). Note further that the expression for the kinetic energy can be rewritten

$$\mathscr{K}^*[\dot{\xi}] = \int_0^R \frac{1}{2}(\varrho^* + p^*)\big(\dot{\xi} e^{-\Phi}[1-2m^*/r]^{-\frac{1}{2}}\big)^2 e^{\Phi}\big(4\pi r^2[1-2m^*/r]^{-\frac{1}{2}}\,\mathrm{d}r\big) = \tag{4.2b'}$$

$$= \int \frac{1}{2}\begin{pmatrix}\text{inertial mass}\\ \text{per unit volume}\end{pmatrix} \times \begin{pmatrix}\text{velocity measured in}\\ \text{proper reference frame}\end{pmatrix}^2 \times$$

$$\times \begin{pmatrix}\text{gravitational}\\ \text{red-shift factor}\end{pmatrix} \times \mathrm{d}\begin{pmatrix}\text{proper}\\ \text{volume}\end{pmatrix} .$$

Expression (4.1) for δM^* can be taken as a foundation for the theory of small-amplitude, adiabatic, radial motions about equilibrium configurations. From

(*) See HTWW, Appendix B. The analysis in HTWW is for zero-temperature configurations, but it can be generalized to hot configurations by replacing all thermodynamic derivatives by the same derivatives at constant entropy $\mathrm{d}p^*/\mathrm{d}\varrho^* \to (\partial p^*/\partial \varrho^*)_{s^*}$, etc. Expressions (B.26) and (B.27) of HTWW for $\mathscr{P}^*$ and $\mathscr{K}^*$ contain an incorrect factor of $\exp[\nu_0(0)/2]$ ($\exp[\Phi(0)]$ in our notation).

it one can derive *a*) a potential-energy criterion for stability, *b*) the equation of motion which governs the time development of small, radial perturbations, and *c*) the frequencies and amplitudes of the normal models of radial motion.

a) *Potential-energy criterion for stability.* Because spherical motions cannot produce gravitational radiation, the total mass-energy of a radially perturbed configuration—and, hence, also δM^*—is a constant of its motion. Since the kinetic energy, $\mathscr{K}^*$, is positive definite and quadratic in the amplitude of the motion, the amplitude can grow large only for those $\xi(r, t)$ which make the potential energy negative. Hence, *an equilibrium configuration is stable against small radial perturbations if and only if the potential energy,* $\mathscr{P}^*[\xi, \xi']$, *associated with such perturbations is positive for all nonzero displacements,* $\xi(r)$. This criterion for stability is the analogue of the criterion that a particle in a potential $V(\boldsymbol{r})$ in is stable equilibrium if and only if it sits at a local minimum of V.

Although the potential-energy criterion for stability is conceptually simple, in numerical calculations it is considerably harder to apply and less reliable than the criteria which arise from the static analyses of Sect. **4**·2.2, **4**·2.3, and than the method of BARDEEN described near the end of this Section.

b) *Equation of motion for arbitrary perturbations.* – Consider an arbitrarily, but radially perturbed equilibrium configuration, the motion of which is described by $\xi = \xi(r, t)$. According to the Lagrangian formulation of mechanics, the difference between the kinetic and potential energies when integrated over time,

$$I^* \equiv \int \{\mathscr{K}^*[\dot{\xi}] - \mathscr{P}^*[\xi, \xi']\}\, \mathrm{d}t\,, \tag{4.4}$$

is extremized by the allowed modes of motion, ξ. The Euler-Lagrange equation

$$W r^2 e^{-\Phi} \ddot{\xi} = [P \cdot (r^2 e^{-\Phi} \xi)']' + Q r^2 e^{-\Phi} \xi\,, \tag{4.5}$$

which results from extremizing I^*, *is the equation of motion that governs the time-development of the arbitrary, adiabatic, radial perturbation.*

c) *Normal modes of radial oscillation.* An equilibrium configuration generally has a discrete set of normal modes of radial oscillation,

$$\xi(r, t) = \xi_n(r) \exp[i\omega_n^* t]\,, \tag{4.6}$$

which are distinguished from each other by the index $n = 0, 1, 2 \ldots$ (*). A par-

(*) Note that, because co-ordinate time, t, is measured in centimeters, the angular frequency, ω_n^*, which appears in eq. (4.6) is measured in cm^{-1}, *i.e.* it is « geometrized » as discussed in Sect. **1**.

ticular normal mode is stable (periodic oscillation) if its frequency, ω_n, is real, and unstable (exponential growth) if ω_n is imaginary. It is convenient to order the normal modes according to increasing squared frequency

$$\omega_0^2 < \omega_1^2 < \omega_2^2 < \dots , \tag{4.7}$$

so that *a star is stable against small radial perturbations if and only if its fundamental squared frequency, ω_0^2, is positive.*

The normal-mode amplitudes ξ_n, are governed by an eigenvalue equation which can be obtained by inserting expression (4.6) into the equation of motion (4.5):

$$[P\cdot(r^2 e^{-\Phi}\xi_n)']' + (Q + \omega_n^{*2} W) r^2 e^{-\Phi}\xi_n = 0 . \tag{4.8}$$

The normal modes of radial motion are those solutions to eq. (4.8) *which satisfy the boundary conditions*

$$\xi_n(r = 0) = 0 \tag{4.9a}$$

(center of star remains fixed during the motion), and

$$\Delta p^* = - e^{\Phi} r^{-2} \Gamma_1 p^* (r^2 e^{-\Phi}\xi_n)' \to 0 \text{ as } r \to R \tag{4.9b}$$

(pressure remains zero at the surface of the star during the motion). An equivalent formulation of the eigenproblem 4.8, 4.9), is the following variational principle due to CHANDRASEKAR (1964*b*, *c*): *Among all functions $\xi(r)$ which satisfy the boundary conditions* (4.9), *the normal-mode amplitudes are these that extremize the quantity*

$$\omega^{*2} \equiv \frac{\int_0^R [P(r^2 e^{-\Phi}\xi)'^2 - Q(r^2 e^{-\Phi}\xi)^2]\,\mathrm{d}r}{\int_0^R W(r^2 e^{-\Phi}\xi)^2\,\mathrm{d}r} = \frac{\mathscr{P}^*[\xi, \xi']}{\mathscr{K}^*[\xi]} ; \tag{4.10}$$

and the corresponding squared frequencies, ω_n^{*2}, are the extremal values of ω^{*2}.

The eigenvalue problem (4.8) (4.9) for the normal radiation modes is of the Sturm-Liouville type. Consequently, the powerful theorems of Sturm-Liouville theory (see *e.g.*, MORSE and FESHBACH (1953), pp. 719 ff.) are all applicable to the normal-mode problem. In particular, we can conclude that the amplitude, $\xi_n(r)$, of the n-th normal mode has precisely n nodes; and that between each pair of nodes of $\xi_n(r)$ there is at least one node of each higher-order amplitude, $\xi_k(r)$, $k > n$.

There are two useful methods for calculating the amplitudes and frequencies of the normal radial modes of a stellar model. One is to solve the eigen-

value problem (4.8, 4.9) by trial-and error integrations; the other is to apply Rayleigh-Ritz techniques (*see e.g.*, MORSE and FESHBACH (1953), pp. 1117 ff.; also GOERTZEL and TRALLI (1960), pp. 215-224) to the variation principle (4.10). As a third alternative, if one only wishes to know how many of the normal radial modes of a given model are unstable, one can use the following method due to BARDEEN (1965): Integrate differential equation (4.8) with $\omega_n^{*2} \equiv 0$ from the center of the star, where $\xi \sim r$, to the surface; and count the number, $N^{(0)}$, of nodes in the resultant function $\xi^{(0)}(r)$. By virtue of the relationship between the nodes of successive eigenfunctions, the stellar model has either $N^{(0)}$ or $N^{(0)}+1$ unstable normal radial modes. If the surface of the stellar model is a singularity of eq. (4.8)—*e.g.* if Γ_1 is finite and ϱ^*/p^* diverges at the surface—then the number of unstable modes is precisely $N^{(0)}$.

For a detailed discussion and comparison of these and other methods for studying normal radial modes see BARDEEN, THORNE, and MELTZER (1966).

Just as one can analyse the radial pulsation of an equilibrium configuration into normal modes

$$\xi(r, t) = \sum_n A_n \xi_n(r) \exp[i\omega_n^* t] , \tag{4.11}$$

so one can also analyse the pulsation energy into normal-mode components—at least so long as the configuration is stable. The total pulsation energy is equal to the kinetic energy $\mathscr{K}^*[\dot{\xi}]$ at a moment when $\xi(r, t) = 0$ (*i.e.* when $\mathscr{P} = 0$)

$$E_{\text{puls}} = \mathscr{K}^*[\dot{\xi}]|_{\xi=0} = 2\pi \sum_{k,n} A_k A_n \omega_k^* \omega_n^* \int_0^R W(r^2 e^{-\Phi} \xi_k)(r^2 e^{-\Phi} \xi_n)\, dr .$$

But according to the orthogonality theorem of Sturm-Liouville theory, the above integral vanishes unless $k = n$. Hence, the pulsation energy can be analysed into components

$$\begin{cases} E_{\text{puls}}^* = \sum_n A_n{}^2 E_{\text{puls}}^{(n)*} , \\ E_{\text{puls}}^{(n)*} \equiv 2\pi\omega_n^{*2} \int_0^R W(r^2 e^{-\Phi} \xi_n)^2\, dr . \end{cases} \tag{4.12}$$

42.2. Static approach to stability for zero-temperature stars (*). In certain cases of physical interest one can determine the precise number of

(*) The approach to stability described in this section is due to WHEELER (HTWW, p. 60), but the precise conditions under which it is valid are delineated for the first time here. See also BARDEEN, THORNE and MELTZER (1966); as well as MELTZER and THORNE (1966).

unstable normal radial modes for an equilibrium configuration without integrating the eigenvalue equation (4.8), and without using Chandrasekhar's variational principle (4.10). The « static analysis » which makes possible this counting of unstable modes is applicable in one form to zero-temperature stellar models, and in slightly different form to hot, isentropic models. Consider first the zero-temperature case.

The thermodynamic properties of matter at absolute-zero temperature are determined by a single equation of state (one degree of freedom)

$$p^* = p^*(\varrho^*, Z_1, \ldots, Z_N) \,. \tag{4.13}$$

In practice, in constructing zero-temperature stellar models one usually specifies the nuclear abundances $Z_1, \ldots, Z_N$ as functions of the density—*e.g.* by requiring that the matter be in its absolute lowest energy state — thereby putting the equation of state into the form

$$p^* = p^*\big(\varrho^*, Z_1[\varrho^*[, \ldots, Z_N]\varrho^*]\big) \equiv p^*(\varrho^*) \,. \tag{4.14}$$

The static approach to stability is applicable to those configurations with equations of state of this form for which no nuclear transformations occur as the density increases; *i.e.* for which

$$\mathrm{d}Z_1/\mathrm{d}\varrho^* = \mathrm{d}Z_2/\mathrm{d}\varrho^* = \ldots = \mathrm{d}Z_N/\mathrm{d}\varrho^* = 0 \qquad \text{at all } \varrho^* \,. \tag{4.15}$$

In the remainder of this Section we confine our attention to such configurations, while in the next Section and in Sect. 5·5.1 we generalize the static approach to other types of zero-temperature configurations.

As we shall see in Sect. 5·4.1, for matter obeying any given zero-temperature equation of state of the form (4.14) there is a one-parameter sequence of equilibrium configurations, which can be conveniently distinguished from each other by the central density, ϱ_c^*. The static approach to stability involves an analysis of the curve of mass, M^*, *vs.* radius, R, for this sequence of configurations. We adopt the convention that M^* be plotted upward and R be plotted to the right.

The key properties of the $M^*(R)$ curve for configurations in which (4.15) holds are these (see Fig. 2 for pictorialization in terms of a particular zero-temperature equation of state, that of SKYRME (1959), CAMERON (1959), and SAAKYAN (1963)):

a) One normal mode of radial oscillation changes stability at each peak or valley (« critical point ») in the $M^*(R)$ curve, and there are no changes of stability elsewhere. Proof: Configurations at which one radial mode changes stability are characterized by the fact that they possess a zero-frequency mode of radial

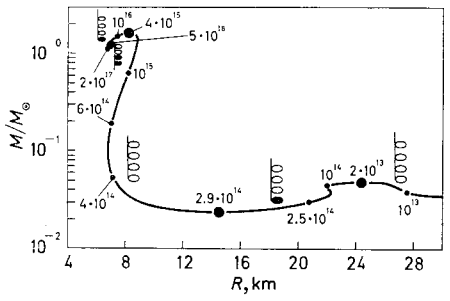

Fig. 2. – The $M^*(R)$ curve for the SKYRME (1959), CAMERON (1959), SAAKYAN (1963) equation of state for matter composed of pure neutrons. (For a specification of which version of the S-C-S equation of state is used here see MELTZER and THORNE (1966).) The curve is parametrized by central density, ϱ_c, in g/cm³. The critical points at which one normal radial mode changes stability are identified by large black dots. The normal radial modes are represented between each successive pair of critical points by a set of musical notes (ovals) with solid notes corresponding to unstable modes and open notes corresponding to stable modes. There are no critical points below $\varrho_c = 10^{13}$ g/cm³ (not shown in Figure); and we know from Newtonian theory that S-C-S configurations of $\varrho_c \sim 1$ g/cm³ are stable against all perturbations. Consequently, everywhere below $\varrho_c = 2\cdot10^{13}$ (first critical point) all normal radial modes are stable. At the first critical point the curve bends counterclockwise and one normal mode ($n = 0$) becomes unstable. At the second critical point ($\varrho_c = 2.9\cdot10^{14}$) the bend is clockwise, so the fundamental returns to stability. At the third critical point ($\varrho_c = 4\cdot10^{15}$) the bend is counterclockwise, so the fundamental mode becomes unstable again. At the fourth critical point ($\varrho_c = 2\cdot10^{17}$) the bend is counterclockwise so one more mode ($n = 1$) becomes unstable—and so it goes.

motion—*i.e.* they are characterized by the existence of other « near-by » equilibrium configurations into which they can transform themselves without the addition or removal of any baryons or of any mass-energy. Hence, configurations of changing stability are configurations which lie at extremal points in the curves $M^*(R)$ and $A(R)$. However, from expression (3.63) for the injection energy we see that an equilibrium configuration is extremal in $A(R)$ if and only if it is extremal in $M^*(R)$. Consequently, a necessary and sufficient condition for a configuration of changing stability is that $M^*(R)$ be extremal. QED.

b) At a critical point of the $M^*(R)$ curve for cold configurations the mode of changing stability is an even mode ($n = 0, 2, 4, \ldots$) if and only if the radius R decreases with increasing central density, $\mathrm{d}R/\mathrm{d}\varrho_c^* < 0$, in the neighborhood of the critical point; it is an odd mode ($n = 1, 3, 5, \ldots$) if and only if R increases, $\mathrm{d}R/\mathrm{d}\varrho_c^* > 0$. Proof: For a critical configuration the amplitude, $\xi_n(r)$, of the zero-frequency mode is identical to the motion, $\delta r(r)$, which carries the star from an equilibrium configuration on the low-density side of the critical point to one on the high-density side

$$\xi_n(r) \equiv \delta r(r) .$$

In such a motion across the critical point central density, ϱ_c, increases; *i.e.* the fluid moves inward near the center of the star. Hence, near $r = 0$ $\xi_n \equiv \delta r$ is negative. $\xi_n \equiv \delta r$ can be negative also at the surface ($\mathrm{d}R/\mathrm{d}\varrho_c < 0$) if and only if ξ has an even number of nodes—*i.e.*, if and only if $n = 0, 2, 4, \ldots$—; and it can be positive at the surface ($\mathrm{d}R/\mathrm{d}\varrho_c > 0$) if and only if ξ_n has an odd number of nodes ($n = 1, 3, 5, \ldots$). QED.

c) At a critical point of the $M^*(R)$ curve for cold configurations one mode becomes unstable with increasing ϱ_c if and only if the curve bends counterclockwise; and one mode becomes stable if and only if the bend is clockwise. Proof: This criterion for the direction of stability change follows from criterion *b)* above, plus the knowledge that at very low central densities—*e.g.* for a sphere of cold matter the size of a basketball—cold configurations are stable against small radial perturbations. To convince oneself that criterion *c)* is, indeed, equivalent to *b)*, one need only apply criterion *b)* to several hypothetical and as-pathological-as-desired $M^*(R)$ curves, and recognize that the results obtained are precisely those predicted by *c)*. QED.

Properties *a)* and *b)*, or *a)* and *c)* of the $M^*(R)$ curve enable one to calculate the precise number of unstable radial modes for each equilibrium configuration of any given zero-temperature equation of state for which nuclear abundances are independent of density (see, *e.g.* Fig. 2).

4·2.3. Generalizations of static approach to stability. The static approach to stability outlined in the last Section was derived under the rather restrictive assumption that the nuclear abundances which enter into the zero-temperature equation of state (4.14) are independent of density. This assumption was needed, for example, to allow the inference that at a critical point the zero-frequency amplitude, $\xi_n(r)$, is identical to the motion, $\delta r(r)$, which carries a star from an equilibrium configuration on the low-density side of the critical point to one on the high-density side.

The assumption that $\mathrm{d}Z_k/\mathrm{d}\varrho^* = 0$ is very severe; it is rarely satisfied in zero-temperature situations of physical interest. Consequently, in this Section we shall replace this assumption by others which are less restrictive.

We begin by noting that nuclear abundances never appear explicitly in the dynamical approach to stability (Sect. **4**·2.1). For zero-temperature configurations the dynamical approach depends only on the equation of state $p^* = p^*(\varrho^*)$, upon the adiabatic index Γ_1, and upon the laws of general-relativistic mechanics. Consequently, the assumption $\mathrm{d}Z_k/\mathrm{d}\varrho^* = 0$ cannot affect stability directly; rather, it can affect stability only through the restriction

$$\Gamma_1 = (\varrho^* + p^*)\, p^{*-1} (\mathrm{d}p^*/\mathrm{d}\varrho^*)_{\text{as given by equation of state (4.14)}} \tag{4.16}$$

which it imposes on the relation between the adiabatic index and the equation

of state. This reasoning allows us to conclude that *the static approach to stability* (properties *a*), *b*), and *c*) of the $M^*(R)$ curve as outlined in Sect. **4**·2.2) *is applicable to any family of zero-temperature configurations whose equation of state* (4.14) *and adiabatic index are related by* (4.16).

Assumption (4.16), like (4.15), is unnecessarily severe. The zero-temperature configurations of greatest current interest are configurations of matter catalyzed to the absolute endpoint of thermonuclear evolution—« cold, catalyzed matter ». (See Sect. **5**; also, HTWW.) Nuclear abundances in such configurations vary with density in such a manner as to keep the matter in its lowest-energy state; *i.e.* so as to minimize the total-mass energy per baryon, ϱ^*/n, subject to fixed baryon number density, n. For such configurations neither (4.13) nor (4.14) is valid; but, as we shall see in Sect. **5**·5.1, the static approach to stability is still applicable—albeit in slightly modified form

4·2.4. Static approach to stability for hot, isentropic configurations (*). A key point in the static analysis of the last Section is this, that the equilibrium configurations for any zero-temperature equation of state form a one-parameter family. By contrast, the equilibrium configurations for hot matter obeying a given fundamental equation

$$\varrho^* = \varrho^*(n, s^*, Z_1, \ldots, Z_N) \tag{4.17}$$

form an infinite-parameter family. (We saw in Sect. **3**·4.3 that to fix uniquely an equilibrium configuration one must specify in addition to the fundamental eq. (4.17) the total number of baryons, the nuclear abundances as functions of radius, and the radial distribution of the entropy.)

In order to develop an $M^*(R)$ analysis of stability for hot stars one must select a suitable one-paramenter family of configurations out of this infinite-parameter set. There are several one-parameter families for which an $M^*(R)$ analysis can be developed; but one particular family stands out as of greatest physical interest (**). This is the one-parameter family of isentropic (*i.e.* marginally convective) configurations with fixed total number of baryons and fixed, radially-invariant nuclear abundances. Such a family of configurations can be parametrized by the radially-constant entropy per baryon, $s(r) \equiv s_0$; or, more conveniently, by the central density, ϱ_c. Physically speaking, successive configurations in such a family represent successive states of a single, quasi-statically contracting configuration which *a*) is in marginal convective equilibrium, and *b*) is too cool for thermonuclear reactions to take place. Stel-

(*) The results of this Section are due to BARDEEN (1965) see also BARDEEN, THORNE and MELTZER (1966).

(**) For a discussion of other usable one-parameter families and of some which are not usable, see BARDEEN (1965).

lar models of this type play an important role in certain theories of quasi-stellar radio sources (FOWLER (1964), (1966)).

Consider the one-parameter family of isentropic configurations for a given fundamental equation (4.17), a given total number, A, of baryons, and given nuclear abundances. For this family construct a curve of minus the binding energy,

$$(4.18) \quad -E_B^* \equiv (\text{total mass-energy}) - (\text{rest mass}) \equiv M^* - M_0^* = M^* - \mu_B^* A \,,$$

vs. radius, R. This $-E_B^*(R)$ curve, like the $M^*(R)$ curve for zero-temperature configurations, plays a central role in the static analysis of stability. (We here use $-E_B^*[R]$ rather than $M^*[R]$ because the masses of the configurations in our sequence all differ only slightly from the constant rest mass M_0^*

$$M^*[R] = M_0^* + E_B^*[R] \approx M_0^* \,.)$$

The key properties of the $-E_B^*(R)$ curve which enter into the static analysis of stability are these (see Fig. 3 for pictorialization in terms of a hypothetical $-E_B^*[R]$ curve):

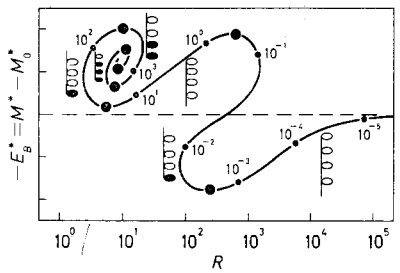

Fig. 3. – The $-E_B^*(R)$ curve for a hypothetical equation of state. The curve is parametrized by central density, ϱ_c. The critical points at which stability changes occur are indicated by large black dots. Between successive critical points each solid note represents one unstable normal radial mode and the open notes represent stable modes.

a) One normal mode of radial oscillation changes stability at each peak or valley (« critical point ») in the $-E_B^*(R)$ curve, and there are no changes of stability elsewhere.

Proof. The proof is similar to that of the analogous zero-temperature theorem. A point of changing stability on the $-E_B^*(R)$ curve corresponds to a configuration with a zero-frequency mode of motion. But a configuration in our one-parameter family can have a zero-frequency mode if and only if there are other, slightly different configurations to which it can be transformed by a motion with these properties: 1) the motion is adiabatic; *i.e.* $\delta s^*(a) = 0$; 2) the motion is irreversible—in particular, nuclear abundances do not change; 3) the motion conserves the total number of baryons; and 4) the motion leaves the total mass-energy unchanged. If the initial configuration is in our isentropic, fixed-A, fixed-nuclear abundances family, then these properties of the zero-frequency motion guarantee that the final configuration is also in our family. Hence, the theorem is proved if we only can show that, of all infinitesimal motions along the $-E_B^*(R)$ curve, those which occur at a peak or valley

(« critical point ») are motions with the above four zero-frequency properties. Property 4), conservation of mass-energy, guarantees that the zero-frequency motions occur at critical points. But do all motions across critical points have the 4 properties? They clearly satisfy properties 2), 3), and 4). That they also satisfy property 1) can be seen as follows: The change in total-mass energy in moving across a critical point is the negative of the heat radiated

$$0 = \delta M^* = -\delta Q^* = -\int_0^A \delta q^* e^{\Phi}\,\mathrm{d}a = -\int_0^A T^* \delta s^* e^{\Phi}\,\mathrm{d}a\,. \tag{4.19}$$

Here δq^* is the heat radiated per baryon, e^{Φ} is the red-shift factor ($\Phi[\infty] = 0$), and a is the number of baryons inside a given shell of matter. Because the initial and final configurations are both isentropic, δs^* is independent of radius and can be pulled out of the integral

$$0 = \delta s_0^* \int_0^A T^* e^{\Phi}\,\mathrm{d}a\,. \tag{4.20}$$

Equation (4.20) guarantees that $\delta s_0^* = 0$; hence, condition 1) is satisfied by motions across critical points. QED.

b) At a critical point of the $-E_{\mathrm{B}}^*(R)$ curve the mode of changing stability is even ($n = 0, 2, 4, \ldots$) if and only if the radius, R, there decreases with increasing central density, $\mathrm{d}R/\mathrm{d}\varrho_c^* < 0$; it is odd ($n = 1, 3, 5, \ldots$) if and only if R increases, $\mathrm{d}R/\mathrm{d}\varrho_c^* > 0$. The proof is identical to that for the zero-temperature case (Sect. 4·2.2).

c) At a critical point of the $-E_{\mathrm{B}}^*(R)$ curve one mode becomes unstable with increasing ϱ_c if and only if the curve bends clockwise there; one mode becomes stable if and only if the bend is counterclockwise. (That the correlation between stability and direction of bend is different here than in the zero-temperature case should not be disturbing; after all, the sequence of configurations considered here is very different in character from the zero-temperature sequence.) Proof of theorem: This criterion for the direction of stability change follows from criterion *b*), plus our knowledge that configurations of every low central density (very large radius; Newtonian theory applicable) are stable if they have $-E_{\mathrm{B}}^* < 0$ and unstable if $-E_{\mathrm{B}}^* > 0$. QED.

Properties *a*) and *b*), or *a*) and *c*) of the $-E_{\mathrm{B}}^*(R)$ curve enable one to calculate the precise number of unstable radial modes for each member of any sequence of isentropic equilibrium configurations which all have the same total number of baryons, A, and the same radially-invariant nuclear abundances. This method of diagnosing stability has been used quite extensively by FOWLER (1964, 1966) and by BARDEEN (1965).

4·3. *Stability properties of nonrotating configurations.* – Let us now turn our attention from the general theory of radial perturbations in relativistic stellar models to some of the more important results which have been obtained from that theory.

4·3.1. General relativity as a catalyzer of instabilities. A number of investigations of stellar stability have revealed that relativistic gravitational forces cause radial instabilities in stellar models which, according to Newtonian theory, would otherwise be stable. The most striking examples of general-relativistic instabilities come from the post-Newtonian approximation, where relativistic forces, which have a totally negligible effect upon the structure of a star, can make it unstable against small radial perturbations. FOWLER (1964, 1966) and CHANDRASEKHAR (1965*d*) have independently developed post-Newtonian criteria for the onset of general-relativistic instabilities. Chandrasekhar's analysis, which is based on the post-Newtonian limit of the variational principle (4.10), reveals this, that a post-Newtonian stellar model with adiabatic index, Γ_1, independent of radius is unstable if and only if its mass, M^*, and radius, R, satisfy

$$R < 2M^* K/(\Gamma_1 - 4/3). \tag{4.21}$$

Here K is a constant usually between 0.5 and 1.5, which depends only on the Newtonian structure of the star. Fowler's analysis, which is based not upon the dynamic approach to stability but on the static $-\frac{4}{1}E^*_B(R)$ approach, yields a similar result. This result plays an important role in Fowler's supermassive-star model for quasars (see lectures in this volume).

4·3.2. Manyfold instability of superdense stars. The $M^*(R)$ and $-E^*_B(R)$ curves of Fig. 2 and 3 both spiral in toward a limiting point as central density mounts toward infinity. This spiraling is a signal that the configurations of higher and higher central density are more and more unstable.

DMITRIEV and HOLIN (1963), HARRISON (1965) and WHEELER (HTWW, Chapter 5) have shown independently that such high-density spiraling of the $M^*(R)$ curve, and the consequent onset of higher- and higher-order instabilities, are characteristic of zero-temperature configurations for a wide range of equations of state. More particularly, for any equation of state which approaches the form

$$p^* = (\gamma - 1)\varrho^*, \qquad \gamma = \text{const}, \tag{4.22}$$

at high density, the $M^*(R)$ curve approaches the high-density spiral

$$\begin{cases} M^* - M^*_\infty = C_M \varrho_c^{*-\alpha/2} \cos\left[\frac{1}{2}\beta \ln \varrho_c^* + \delta_M\right], \\ R - R_\infty = C_R \varrho_c^{*-\alpha/2} \cos\left[\frac{1}{2}\beta \ln \varrho_c^* + \delta_R\right], \end{cases} \tag{4.23}$$

where C_M, C_R, δ_M, δ_R, α, and β are constants, and

$$\alpha = \frac{3}{2} - \frac{1}{\gamma}, \qquad \beta = \left[\frac{11}{\gamma} - \frac{9}{\gamma^2} - \frac{1}{4}\right]^{\frac{1}{2}}, \qquad \delta_M \neq \delta_R . \tag{4.24}$$

Similar formulae could be worked out for the $-E^*_B(R)$ curves of hot, isentropic stellar models.

The static approach to stability, when applied to formulae (4.23) for the spiraling $M^*(R)$ curve, tells us that zero-temperature configurations of high central density ($\varrho_c \geqslant 10^{19}$ g/cm^3; cf. Sect. **5**) have

$$\text{greatest integer less than } \{(\beta/2\pi)\ln(\varrho_c/\varrho_0)\} \tag{4.25}$$

unstable normal radial modes, where ϱ_0 is a constant. For realistic equations of state (Sect. **5**, Fig. 4)

$$\varrho_0 \sim 10^{16} \text{ g/cm}^3 . \tag{4.26}$$

Expression (4.25) for the number of unstable normal radial modes can also be derived by the dynamic approach to stability (see MELTZER and THORNE (1966) Sect. **3**-*d*).

4·4. *Stability of rotating stellar models.* – Thus far we have confined our attention to the stability of nonrotating stellar models. The only relativistic stability analyses performed to date on rotating stellar models are the post-Newtonian considerations of FOWLER (lectures in this volume), of ROXBURGH (1965), and of DURNEY and ROXBURGH (1965). The approaches used in these references are essentially generalizations of the post-Newtonian limit of the dynamic analysis of Section **4**·2.1.

4·5. *Summary.* – The principal conclusions from our discussion of stellar stability are these: The relativistic theory of radial perturbations of nonrotating equilibrium configurations is well understood. There are two approaches to radial stability—a dynamic approach, based on the equations of motion and energy properties of radial perturbations; and a static approach, based on mass-radius curves for certain sequences of equilibrium configurations. From each of these approaches one can obtain several different methods for studying the normal radial modes of a relativistic stellar model. The resultant methods were briefly described here and are catalogued and compared in detail by BARDEEN, THORNE, and MELTZER (1966). Applications of these methods reveal 1) that general relativity catalyzes radial instability in stellar models, and 2) that stellar models of very high central density have many unstable normal radial modes.

The relativistic theory of nonradial perturbations of nonrotating configurations has been developed only in the post-Newtonian approximation. In that approximation all nonradial dynamical instabilities are accompanied by convective instabilities and can be eliminated by efficient convection.

The only relativistic stability analysis of rotating configurations which has been performed to date is the post-Newtonian, « dynamic analysis » of FOWLER, ROXBURGH and DURNEY.

5. – White dwarfs, neutron stars, and hyperon stars.

We now have at our disposal all of the tools necessary to permit the detailed analysis of specific stellar models. There are two types of stellar configurations in which general relativity should play an important role: configurations near the endpoint of thermonuclear evolution (white dwarfs, neutron stars, hyperon stars); and supermassive configurations ($M \gtrsim 10^5 M_\odot$). This Section and the lecture by FINZI (1966) are concerned with the former type of configuration, while Sect. **6** and the lectures by FOWLER (1966) are concerned with the latter.

5·1. *Matter near the endpoint of thermonuclear evolution.* – In discussing configurations near the endpoint of thermonuclear evolution we begin with a brief description of the matter from which they are made. By « matter of baryon number density n, catalyzed to near the endpoint of thermonuclear evolution »—*catalyzed matter for short*—we mean matter at density n in which the nuclear abundances, $Z_1, \ldots Z_N$, are such as to absolutely minimize the total mass-energy per baryon, ϱ^*/n. Such matter is in thermonuclear equilibrium; no rest mass-energy can be converted into thermal energy by any nuclear reaction. This does not mean, however, that no energy can be extracted from a sample of such matter. There may be thermal energy in the sample; hence the phrase « ... catalyzed to *near* the endpoint of thermonuclear evolution ». When a sample of catalyzed matter does not contain any thermal energy it is called *cold catalyzed matter*. For a careful and comprehensive discussion of the concept of cold catalyzed matter see HTWW, Chapter 9.

5·1.1. Thermodynamics of catalyzed matter. In situations of interest to us here the density of thermal energy, ε_T^*, of a sample of catalyzed matter is always very much less than the density of total mass-energy

$$\varepsilon_T^* \ll \varrho^*; \tag{5.1}$$

and the thermal pressure is very much less than the pressure associated with the zero-point motion of the electrons and nuclei. Consequently, to a high degree

of approximation the equations of state $p^* = p^*(n, T^*, Z_1, ..., Z_N)$ and $\varrho^* = \varrho^*(n, T^*, Z_1, ..., Z_N)$ are independent of temperature. They are also independent of $Z_1, ..., Z_N$ since the nuclear abundances are uniquely fixed once the baryon number density, n, is given.

$$(5.2) \qquad \begin{cases} p^* = p^*(n, T^*, Z_1, \ldots Z_N) = p^*(n, 0, Z_1[n], ..., Z_N[n]) \equiv p^*(n) , \\ \varrho^* = \varrho^*(n, T^*, Z_1, \ldots Z_N) = \varrho^*(n, 0, Z_1[n], ..., Z_N[n]) \equiv \varrho^*(n) . \end{cases}$$

The simplified equations of state (5.2) are related by the first law of thermodynamics as embodied in the equation

$$(5.3) \qquad \mathrm{d}\varrho^*/\mathrm{d}n = (\varrho^* + p^*)/n .$$

(This relation follows from eq. (2.12) with $\mathrm{d}s^* = 0$, plus the relation $\sum \bar{\mu}_k^* \mathrm{d}Z_k = 0$. The latter relation is valid for all changes $[\mathrm{d}Z_1, \ldots, \mathrm{d}Z_N]$, in chemical composition, which are compatible with the conservation laws of elementary particle physics, because we are dealing with matter at the endpoint of thermonuclear evolution in which no nuclear reactions can release energy.)

Relation (5.3) *together with a single equation of state*—$\varrho^*(n)$, $p^*(n)$ or $p^*(\varrho^*)$—*uniquely fixes any two of the quantities* (ϱ^*, p^*, n) *in terms of the third.* Throughout our work we shall (arbitrarily) use $p^* = p^*(\varrho^*)$ as our « primary » equation of state.

Although temperature, T^*, has no (significant) effect on the density of mass-energy or on the pressure of catalyzed matter, it is a very important determinant of the density of thermal energy

$$(5.4) \qquad \varepsilon_T^* = \varepsilon_T^*(\varrho^*, T^*) \to 0 \qquad \text{when } T^* \to 0 .$$

In discussing stellar configurations of catalyzed matter we shall confine our attention to the thermodynamic parameters n, p^*, ϱ^*, T^*, and ε_T^*. If we wished we could also consider the entropy per baryon, s^*; the total internal energy, ε^*; the average baryonic rest mass, μ_B^*; the nuclear abundances, $Z_1, ..., Z_N$; the nuclear chemical potentials $\bar{\mu}_N^*, ..., \bar{\mu}_1^*$; and the *baryon chemical potential*, $\bar{\mu}^*$ which is defined by (cf. HTWW)

$$(5.5) \qquad \bar{\mu}^* \equiv \mathrm{d}\varrho^*/\mathrm{d}n = (\varrho^* + p^*)/n.$$

However, for clarity of presentation we shall exclude these supplementary parameters from discussion.

5.1.2. Equation of state of cold catalyzed matter. The equation of state of cold catalyzed matter, $p^* = p^*(\varrho^*)$,—which is also the equa-

tion of state of catalyzed matter (no temperature dependence)—has been calculated theoretically in various regions of density by a large number of workers including CHANDRASEKHAR (1935, 1939); OPPENHEIMER and SERBER (1938); OPPENHEIMER and VOLKOFF (1939); SCHATZMAN (1956); HARRISON, WAKANO and WHEELER (1958) see also HTWW, Chapter 10; CAMERON (1959); SALPETER (1960); AMBARTSUMYAN and SAAKYAN (1960); SAAKYAN (1963); SAAKYAN and VARTANYAN (1963*a*, *b*); SAAKYAN and CHUBARYAN (1963); TSURUTA (1964); TSURUTA and CAMERON (1965*b*, 1966*a*); GRATTON and SZAMOSI (1964); BARKER, BHATIA, and SZAMOSI (1966); BAHCALL and WOLF (1965*b*); and others.

The various calculated equations of state for cold catalyzed matter are in good qualitative agreement, but quantitatively there are some rather important differences, especially at densities $\varrho \gtrsim 10^{13}$ g/cm³. Crucial differences between the proposed equations of state are most clearly brought out not by curves of pressure *vs.* density, but by curves of the « adiabatic index »,

$$\gamma_{\text{eqn state}} \equiv (\varrho^* + p^*)\, p^{*-1} (\mathrm{d}p^*/\mathrm{d}\varrho^*)_{\text{as given by eqn. of state}} , \tag{5.6}$$

vs. density, ϱ^*. Such curves are shown in Fig. 4 for several of the more recent and plausible equations of state. (Ignore for the present the right half of Fig. 4.) The differences between the four curves of $\gamma_{\text{eqn state}}$ *vs.* ϱ^* are indicative of the present uncertainty in our knowledge of the equations of state of cold, catalyzed matter.

The equations of state of Fig. 4 can be understood by following the transformations which occur as an imaginary, small sample of cold catalyzed matter is compressed to higher and higher densities. At each stage in the compression all thermonuclear reactions in the sample must be catalyzed to their endpoints, and the resultant thermal energy must be removed.

At densities below $\varrho \sim 10^5$ g/cm³ only the H-W equation of state attempts to be accurate; no effort was taken to make the other three equations of state accurate here because such « low » densities are of little importance for superdense stellar configurations. In this low-density region our sample of cold, catalyzed matter is in the form of ^{56}Fe, the most tightly bound of all nuclei. At $\varrho = 7.86$ g/cm³ the pressure is zero, but the velocity of sound (cf. eq. (2.10))

$$v_s^* = p^*(\varrho^* + p^*)^{-1} \Gamma_1 = p^*(\varrho^* + p^*)^{-1} \gamma_{\text{eqn state}} \tag{5.7}$$

is finite. Consequently, $\gamma_{\text{eqn state}}$ is infinite. As the sample of matter is compressed from 7.86 g/cm³ to 10^5 g/cm³, the pressure is provided less and less by solid-state forces; more and more by the degenerate ^{56}Fe electrons. Consequently, $\gamma_{\text{eqn state}}$ decrease from ∞ toward $\frac{5}{3}$, the value for a *nonrelativistically* degenerate Fermi gas.

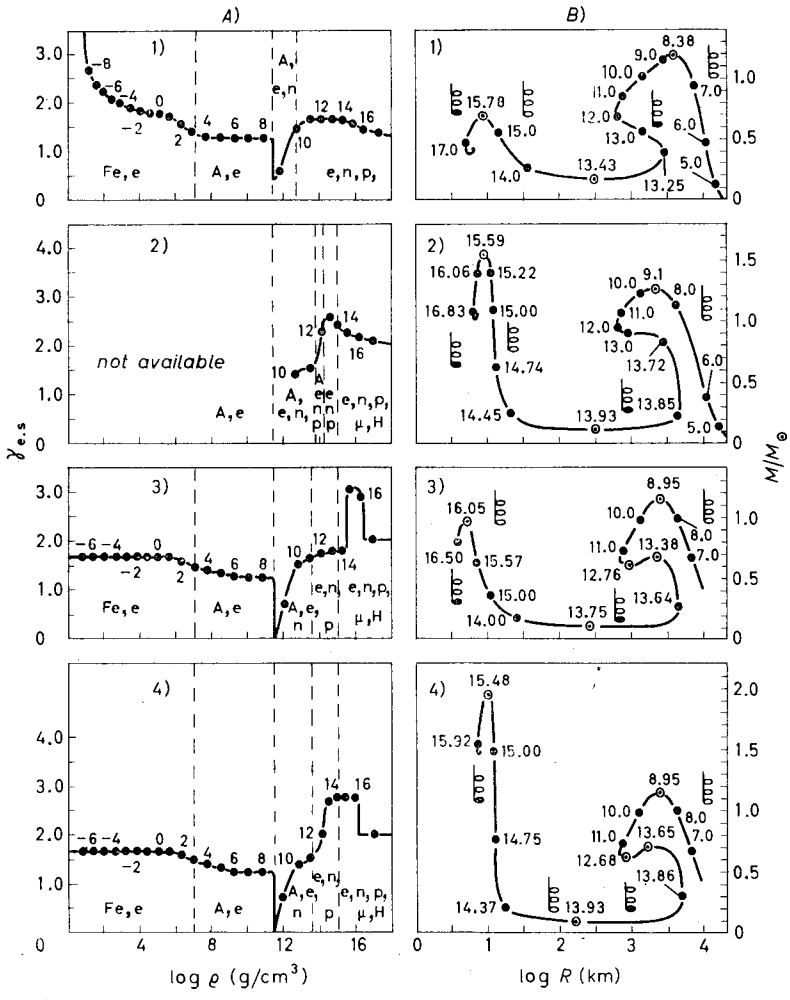

Fig. 4. – *A*) Several proposed equations of state for matter at or near the endpoint of thermonuclear evolution, and *B*) the corresponding equilibrium configurations. The four equations of state shown are 1) H-W: Harrison-Wheeler, see HARRISON, WAKANO and WHEELER (1958), also Chapter 10 of HTWW; 2) S-V: Saakyan-Vartanyan, see SAAKYAN and VARTANYAN (1963*a*, *b*; 1964), also SAAKYAN and CHUBARYAN (1963); 3) V_β and 4) V_γ: Levinger-Simmons, V_β, and V_γ see TSURUTA (1964), TSURUTA and CAMERON (1965*a*, 1966*a*). For each equation of state we plot the « adiabatic index » of eq. (5.6) against density of mass-energy, ϱ; and we parametrize each curve by p/c^2 measured in g/cm³. The nuclear constitution of the matter for each equation of state is indicated as follows: Fe, ^{56}Fe nuclei; *A*, nuclei more neutron rich than ^{56}Fe; e, electrons; n, free neutrons; p, free protons; μ, μ-mesons; H, hyperons. The Saakyan-Vartanyan equation of state is not available in the literature in tabular or analytic form for $\varrho < 3 \cdot 10^{12}$ g/cm³. For discussion of equations of state see Sect. 5˙1.2. The equilibrium configurations are represented by curves of total mass-energy, M^*, *vs.* (co-ordinate) radius, R. These $M^*(R)$ curves are parametrized by central density, ϱ_c, measured in g/cm³. The musical notes beside the $M^*(R)$ curves indicate stability against small radial perturbations: Each solid note represents one unstable normal radial mode while the open notes represent stable modes. One normal mode changes stability at each peak or valley (circled dots) of the $M^*(R)$ curves. For a discussion of the equilibrium configurations see Sect. 5˙4.1.

Above $\varrho = 10^5$ g/cm³ all four equations of state attempt to be accurate (*); and they are in good agreement up to $\sim 10^{13}$ g/cm³. Between 10^5 and 10^7 g/cm³ the pressure-providing electrons gradually become *relativistically* degenerate, and $\gamma_{\text{eqn state}}$ approaches $\frac{4}{3}$ in a manner first described by CHANDRASEKHAR (1935). Above $\varrho = 1.4 \cdot 10^7$ g/cm³ the rest mass of 62 $^{56}_{26}$Fe nuclei plus the rest mass of 44 electrons plus the rather large Fermi kinetic energy of 44 electrons exceeds the rest mass of 56 $^{62}_{28}$Ni nuclei. Consequently, as our sample of matter is compressed past $\varrho = 1.4 \cdot 10^7$ g/cm³ the nuclear reaction

$$62\ ^{56}_{26}\text{Fe} + 44\text{e}^- \rightarrow 56\ ^{62}_{28}\text{Ni} \tag{5.8}$$

must be catalysed to its endpoint. As the compression continues beyond this point, the rising electron Fermi energy induces new nuclear reactions similar to (5.8) but involving different nuclei. In these reactions more and more electrons are swallowed up to form new nuclei, which are more and more neutron rich. If electrons were not being swallowed up by nuclei, $\gamma_{\text{eqn state}}$ would hold steady at $\frac{4}{3}$ (relativistic Fermi gas) throughout the region $\varrho > 10^7$ g/cm³. However, the gradual removal of electrons causes pressure to increase more slowly with density than it would otherwise, and thereby keeps $\gamma_{\text{eqn state}}$ roughly constant, not at $\frac{4}{3}$, but at ~ 1.26. Such is the situation until the compression pushes our sample of matter up to $\varrho = 3 \cdot 10^{11}$ g/cm³. At this density the nuclei are so highly neutron rich ($^{122}_{39}$Y) that neutrons begin to drip off of them. When neutron drip is initiated at $\varrho = 3 \cdot 10^{11}$ g/cm³, most of the remaining electrons are suddenly swallowed up very rapidly with increasing density by the dripping nuclei. Consequently, as density increases through the region $\varrho \sim 3$ to $4 \cdot 10^{11}$ g/cm³, the degenerate electron pressure— and, hence, also the total pressure—remains almost constant; and $\gamma_{\text{eqn state}}$ plumets to ~ 0 and remains there. Above $\sim 4 \cdot 10^{11}$ g/cm³ the rising neutron degeneracy pressure becomes of the same order as the electron pressure, and then much larger. Consequently $\gamma_{\text{eqn state}}$ rises, reaching $\sim \frac{5}{3}$ (nonrelativistically degenerate neutron gas) at $\varrho \sim 10^{13}$ g/cm³.

In the density region above 10^{13} g/cm³ there are serious discrepancies among the equations of state of Fig. 4, and hence great uncertainties in our knowledge of the behaviour of cold catalyzed matter. Between 10^{13} and 10^{14} g/cm³ the few remaining nuclei all break up into their constituent nucleons—primarily neutrons—; and the sample of matter therefore becomes a mixture of degenerate neutron, proton, electron—and, at higher densities, muon and hyperon—gases interacting by nuclear and electromagnetic forces. Because nucleon-nucleon

(*) The S-V nuclear abundances in *this* density region are actually *not* those of cold, catalyzed matter; they are the slightly different abundances which one would expect of matter which has had only $\sim 10^{10}$ years to reach thermonuclear equilibrium. The effect upon the equation of state of this failure to be at the absolute endpoint of thermonuclear evolution is small.

interactions are only poorly understood, the equation of state of such a mixture is only poorly known. In the region $\varrho \geqslant 10^{13}$ g/cm^3 the four equations of state of Fig. 4 are based upon four different assumptions about the nature of nucleon-nucleon interactions:

The H-W assumption—which is probably incorrect—is that the effects of nucleon-nucleon interactions and of hyperon formation on the equation of state are negligible. Consequently, according to the H-W analysis, $\gamma_{\text{eqn state}}$ is $\frac{5}{3}$ (non-relativistically degenerate neutron gas) between $\varrho \approx 10^{13}$ and $\varrho \approx 10^{15}$ g/cm^3; and it drops toward $\frac{4}{3}$ (relativistic degeneracy) above 10^{15} g/cm^3.

The S-V equation of state assumes nucleon-nucleon interactions which are largely attractive below $\varrho \sim 3 \cdot 10^{13}$ g/cm^3 but very repulsive above this density. Consequently, the S-V value of $\gamma_{\text{eqn state}}$ is less than $\frac{5}{3}$ at $\varrho < 3 \cdot 10^{13}$ g/cm^3; but as the sample of matter is compressed beyond this density, $\gamma_{\text{eqn state}}$ shoots up to ~ 2.6 and then gradually falls back toward 2.0. At very high densities the S-V equation of state, $p^* = \varrho^*$ ($\gamma_{\text{eqn state}} = 2.0$) is the stiffest one compatible with the velocity of light (cf. eq. (5.7)) (*).

The V_β and V_γ equations of state, like S-V, involve nucleon-nucleon interactions which are at first mildly attractive, but then at higher densities, very repulsive. This explains the initially low ($< \frac{5}{3}$) values of $\gamma_{\text{eqn state}}$ in the region $\varrho > 10^{13}$ g/cm^3, and the subsequent sudden rise of $\gamma_{\text{eqn state}}$ to about 3.0. For V_β the repulsive nuclear forces occur at much higher densities (smaller nucleon-nucleon separations) than for S-V or V_γ. The empirically-derived V_β and V_γ nuclear interaction potentials are based upon faulty assumptions at $\varrho > 3 \cdot 10^{16}$ g/cm^3 and therefore lead to a speed of sound exceeding the speed of light. In order to avoid this conflict with causality the calculated equations of state are cut off when p^* becomes equal to ϱ^* ; and $p^* = \varrho^*$ ($\gamma_{\text{eqn state}} = 2.0$) is assumed from there on to the highest densities.

It should be emphasized that at densities $\varrho \geqslant 10^{16}$ g/cm^3 unsolved problems of-elementary-particle physics prevent us from having confidence in any proposed equation of state for cold catalyzed matter.

In his lectures in this volume SZAMOSI (1966) discusses in detail the formalism used to calculate equations of state in the region $\varrho \geqslant 10^{13}$ g/cm^3, the phenomenon of hyperon formation which occurs at $\varrho > 1.1 \cdot 10^{15}$ g/cm^3, and the details of several equations of state, including V_β and V_γ.

5·1.3. Density of thermal energy. For catalyzed matter at densities above $\sim 10^5$ g/cm^3, the thermal energy is concentrated partially in the

(*) Until recently it was generally believed that $p^* = \varrho^*/3$ ($\gamma_{\text{eqn state}} = \frac{4}{3}$) was the stiffest high-density equation of state compatible with the laws of physics. However, ZEL'DOVICH (1961) has shown that the equation of state $p^* = \varrho^*$ ($\gamma_{\text{eqn state}} = 2.0$; sound velocity = light velocity) is in principle attainable.

thermal tails of the Fermi energy distributions of the degenerate electron and baryon gases, and partially in the kinetic motion of the nondegenerate nuclei. From Fermi-Dirac theory one can show (cf. CHANDRASEKHAR (1939) p. 394) that the specific heat per particle, at constant volume, of a degenerate Fermi gas is

$$c_v = (\pi^2 k^2/\mu c^2)(\mu E_F/p_F^2)\, T\,. \tag{5.9}$$

Here k is Boltzman's constant, μ is the Fermion rest mass, p_F is the Fermi momentum at the top of the degenerate sea, and $E_F = (p_F c^2 + \mu^2 c^4)^{\frac{1}{2}}$ is the corresponding Fermi energy including rest mass. By integrating this specific heat per particle over temperature and summing over all of the Fermi gases present (electrons, neutrons, protons, muons, various hyperons), and by adding the thermal energy density of the nondegenerate nuclei, we obtain for the density of thermal energy as a function of total density of mass-energy and temperature (*)

$$\begin{cases} \varepsilon_T^*(\varrho^*, T^*) = \beta^*(\varrho^*)\, T^{*2} + \frac{3}{2} bn T^*\,, \\ \beta^*(\varrho^*) = [\pi^2/2] \sum_j n_j(\varrho^*)\, E_{F-j}^*(\varrho^*) [p_{F-j}^*(\varrho^*)]^{-2}\,. \end{cases} \tag{5.10}$$

Here $n_j(\varrho^*)$ is the number density of fermions of type j, while p_{F-j}^* and E_{F-j}^* are the corresponding Fermi momentum and total Fermi energy, and bn is the number density of nondegenerate nuclei. Equation (5.10) is expressed in geometrized units.

Corresponding to any proposed equation of state $p^*(\varrho^*)$ for cold, catalyzed matter there is a well-determined *thermal function* $\beta^*(\varrho^*)$, which can be calculated from eq. (5.10)

As density decreases from $\sim 10^5$ g/cm^3 toward 0, the orbital electrons of the iron nuclei gradually cease to form a degenerate Fermi gas, and eq. (5.10) gradually ceases to be correct. Since this low-density region is of physical interest only for descriptions of the very thin surface layers and atmospheres of superdense stars, and since the surface layers and atmospheres are actually not catalyzed to near the endpoint of thermonuclear evolution (see, *e.g.* TSURUTA and CAMERON (1966*b*)), we shall forgo any attempt to improve upon eq. (5.10) at low densities.

(*) GINZBURG and KIRZHNITS (1964) have suggested that the nucleon thermal excitation spectrum at high densities ($\varrho \gtrsim 10^{13}$ g/cm^3) might resemble a gas of superconducting electrons, rather than being continuous. If such is the case, then expression (5.10) will not describe correctly the density of thermal energy.

5·2. *Equations of stellar structure.* – Having completed our description of the theory of matter near the endpoint of thermonuclear evolution, we now turn our attention to the equations which govern the structure of stellar configurations of such matter. The lack of influence of temperature upon the equation of state, $p^*(\varrho^*)$, of catalyzed matter results in a separation of the $16 + 3N$ coupled equations of stellar structure (3.11) into three more or less independent groups:

The first group—the *primary structure equations*—consists of three coupled equations for density of mass-energy, ϱ^*, pressure, p^*, and mass, m^*, as functions of co-ordinate radius, r

$$p^* = p^*(\varrho^*)\,, \tag{5.11a}$$

$$m^* = \int_0^r 4\pi r^2 \varrho^* \,\mathrm{d}r\,, \tag{5.11b}$$

$$\frac{\mathrm{d}p^*}{\mathrm{d}r} = -\frac{(\varrho^* + p^*)(m^* + 4\pi r^3 p^*)}{r(r - 2m^*)}\,. \tag{5.11c}$$

Equation (5.11*a*) is the equation of state of catalyzed matter; (5.11*b*) is the mass equation (3.11-2); and (5.11*c*) is the TOV equation of hydrostatic equilibrium (3.11-3). In studying configurations of catalyzed matter one usually chooses a particular value of the central density, $\varrho_c^* = \varrho^*(r = 0)$ and then numerically integrates eq. (5.11) outward from $r = 0$ to the point at which p^* reaches zero, which is the surface of the star. The values of r and m^* at the termination point are the stellar radius, R, and the total mass-energy, M^*.

If, in addition to ϱ^*, p^*, and M^*, one is also interested in the gravitational potential, Φ, of eq. (3.1), the number density of baryons, n, or the number of baryons, a, inside radius r, he can calculate them by integrating the following *secondary structure equations* along with the primary equations (5.11):

$$\mathrm{d}\Phi/\mathrm{d}r = -(\varrho^* + p^*)^{-1}(\mathrm{d}p^*/\mathrm{d}r)\,, \qquad \Phi(r = R) = \ln(1 - 2M^*/R)^{\frac{1}{2}}\,, \tag{5.12a}$$

$$\mathrm{d}n/\mathrm{d}\varrho^* = n/(\varrho^* + p^*)\,, \tag{5.12b}$$

$$a = \int_0^r 4\pi r^2 n(1 - 2m^*/r)^{-\frac{1}{2}} \,\mathrm{d}r\,. \tag{5.12c}$$

Equation (5.12*a*) is the source eq. (3.11-4) for Φ; and its boundary condition, which is derived from eq. (3.40), is chosen so as to make $\Phi(r = \infty) = 0$. Equation (5.12*b*) we have met previously as (5.3); and (5.12*c*) is the baryon number equation (3.11-1). Note that equations (5.12*a*, *b*) can be integrated in terms

of the equations of state to give

$$\Phi(r) = \begin{cases} \ln(1-2M^*/R)^{\frac{1}{2}} - \int_0^{p^*(r)} (\varrho^* + p^*)^{-1}\,\mathrm{d}p^*\,, & r < R\,, \\ \ln(1-2M^*/R)^{\frac{1}{2}}\,, & r > R\,, \end{cases} \tag{5.12a'}$$

$$n = \frac{\varrho^* + p^*}{\mu_{\mathrm{B}}^*(0)} \exp\left[-\int_0^{p^*} \frac{\mathrm{d}p^*}{\varrho^* + p^*}\right] = \frac{(\varrho^* + p^*)\,e^{\Phi}}{\mu_{\mathrm{B}}^*(0)[1-2M^*/R]^{\frac{1}{2}}}\,. \tag{5.12b'}$$

Here $\mu_{\mathrm{B}}^*(0)$, the average baryonic rest mass at zero density, is $(1/56)\times$(the mass of an ^{56}Fe atom). Equation (5.12b'), when rearranged slightly, becomes a statement of the constancy of the injection energy for configurations of catalyzed matter (cf. eq. (3.62)) (*).

There is no mention whatsoever of temperature or of thermal energy in the primary or secondary structure equations (5.11), (5.12). If one is interested in the thermal properties of a configuration of catalyzed matter, he must integrate, in addition to eq. (5.11) and (5.12), the *thermal structure equations*:

a) Differential equations for thermal structure

$$\frac{\mathrm{d}(L_r^*\,e^{2\Phi})}{\mathrm{d}r} = -\frac{4\pi r^2\,e^{\Phi}}{(1-2m^*/r)^{\frac{1}{2}}}\left(\frac{\mathrm{d}\varepsilon_T^*}{\mathrm{d}t}\right), \tag{5.13a}$$

$$\frac{\mathrm{d}(L_r^{(\nu)*}\,e^{2\Phi})}{\mathrm{d}r} = \frac{4\pi r^2\,e^{2\Phi}}{(1-2m^*/r)^{\frac{1}{2}}}\,n q_{(\nu)}^*\,, \tag{5.13b}$$

$$\frac{\mathrm{d}(T^*e^{\Phi})}{\mathrm{d}r} = -\frac{3}{16\sigma^*}\,\frac{\varkappa^*\varrho^*}{T^{*3}}\,\frac{(L_r^* - L_r^{(\nu)*})\,e^{\Phi}}{4\pi r^2}\,(1-2m^*/r)^{-\frac{1}{2}} \approx \tag{5.13c}$$

$$\approx 0 \text{ in regions where electrons or baryons are degenerate,}$$

$$\frac{1}{\varkappa^*} = \frac{1}{\varkappa_R^*} + \frac{3\varrho^*\lambda_c^*}{16\sigma^* T^{*3}}\,,$$

$$U_T^* = \int_0^R \varepsilon_T^*\,e^{\Phi}\,4\pi r^2(1-2m^*/r)^{-\frac{1}{2}}\,\mathrm{d}r\,. \tag{5.13d}$$

(*) Strictly speaking, the injection energy is not quite constant unless the thermal energy, ε_T^*, is distributed isentropically—which it is not in highly conducting superdense stars. However, deviations from constant injection energy will be of the order of $\varepsilon_T^*/\varrho^*$ which is extremely small.

b) Gas characteristic relations

(5.14*a*) $\quad \varepsilon_T^* = \varepsilon_T^*(\varrho^*, T^*) = \beta^*(\varrho^*)\, T^{*2} + \frac{3}{2} bnT^*$,

(5.14*b*) $\quad \lambda_c^* = \lambda_c^*(\varrho^*, T^*) \approx \infty$ in regions where electrons or baryons are degenerate,

(5.14*c*) $\quad \varkappa_R^* = \varkappa_R^*(\varrho^*, T^*)$,

(5.14*d*) $\quad q_{(\nu)}^* = q_{(\nu)}^*(\varrho^*, T^*)$.

All of the quantities appearing here are defined and discussed in Sect. **3** except the density of thermal energy, ε_T^*, which was discussed in Sections **5**·1.1 and **5**·1.3; and U_T^*, the *total thermal energy of the configuration*. U_T^* is defined as the total mass-energy which observers at $r = \infty$ can collect from the star's photon and neutrino radiation, as the star cools from its present state to zero temperature.

Equations (5.13*a*, *b*) are the equations of thermal equilibrium (3.11-5,6) with q^* and $\mathrm{d}n/\mathrm{d}t$ set equal to zero (no thermonuclear energy release or change of density with temperature for catalyzed matter.) Equation (5.13*c*) is the equation of energy transport (3.11-7*a*) specialized to the case of no convection. Convection does not occur—except, perhaps, in the very thin, nondegenerate surface layer and atmosphere—because the high thermal conductivity of the degenerate electron and baryon gases maintains a temperature gradient well below the adiabatic limit. Expression (5.13*d*) for the total thermal energy is simply the integral, over the proper volume of the configuration, of the density of thermal energy red-shifted to account for the energy used up by photons and neutrinos as they climb out of the star's gravitational field. The gas characteristic relations (5.14) are expressions in terms of density and temperature for the thermal energy density, ε_T^*, the thermal conductivity, λ_c^*, the radiative absorption coefficient, $\varkappa_R^*$, and the rate, $q_{(\nu)}^*$, at which thermonuclear reactions convert thermal energy into outgoing neutrinos.

The thermal-structure equations (5.13), (5.14) are 8 coupled equations for the 8 quantities L_r^*, $L_r^{(\nu)*}$, T^*, U_T^*, ε_T^*, λ_c^*, $\varkappa_R^*$, and $q_{(\nu)}^*$. These equations must be subjected to the boundary conditions (cf. Sect. **3**·3)

(5.15) $\qquad L_r^*(0) = 0\,, \qquad L_r^{(\nu)*}(0) = 0\,, \qquad T^*(R) = 0\,.$

Note that in the equations of stellar structure (5.11)–(5.15) for configurations of catalyzed matter no mention is made of the parameters ε^*, s^*, q^*, $Z_1, \ldots, Z_N, \bar{\mu}_1^*, \ldots, \bar{\mu}_N^*, \alpha_1, \ldots, \alpha_N$, which enter into the more general structure equations (3.11). The parameters q^* and $\alpha_1, \ldots, \alpha_N$ are zero in catalyzed matter since no nuclear energy generation can occur there; the nuclear abundances $Z_1, \ldots, Z_N$ and chemical potentials $\bar{\mu}_1^*, \ldots, \bar{\mu}_N^*$, are not needed once the equation of state

$p^*(\varrho^*)$ and the thermal function $\beta^*(\varrho^*)$ have been calculated; the density of internal energy and the entropy per baryon, ε^* and s^*, are omitted because they play no important role in configurations of catalyzed matter.

5'3. *How to construct stellar models.* – To construct a model of a star near the endpoint of thermonuclear evolution and follow its subsequent thermal evolution one might proceed as follows: 1) Specify the central density, ϱ_c^*. 2) Integrate the primary and secondary structure equations (5.11) and (5.12) by the method described between those equations. 3) Take as the external gravitational field the Schwarzschild solution of Sect. **3'**4.1. 4) Specify an initial temperature distribution, $T^*(r)$, satisfying $T^*(r = R) = 0$. Solve the thermal equations (5.13) and (5.14) subject to boundary conditions (5.15) for the parameters L_r^*, $L_r^{(\nu)*}$, ε_T^*, $\mathrm{d}\varepsilon_T^*/\mathrm{d}t$, U_T^*, λ_c^*, $\varkappa_R^*$, $q_{(\nu)}^*$. This solution can be effected by a straighforward numerical integration from the center of the star to the surface. 6) Calculate a new value of the temperature at a later time, Δt, from

$$(5.16)\quad T^*(r, \Delta t) = T^*(r, 0) + \{2\beta^*(\varrho^*[r])\, T^*(r, 0) + \tfrac{3}{2} bn(r)\}^{-1}\{\mathrm{d}\varepsilon^*(r, 0)/\mathrm{d}t\}\Delta t$$

(cf. eq. (5.14*a*)). 7) Repeat steps 5) and 6) until the stellar model has cooled to zero temperature.

In practice this computational method cannot yield very reliable results for the thermal evolution of a superdense star, since it assumes that the pressure, $p^*(\varrho^*)$, is independent of temperature in the nondegenerate surface layers as well as in the main body of the star. A more nearly correct treatment (see, *e.g.*, SCHATZMAN (1958), and TSURUTA and CAMERON (1966*b*) for Newtonian versions) would treat the thin surface layers by means of a temperature-dependent equation of state and would make use of the theory of stellar atmospheres.

5'4. *Structure and properties of configurations of catalyzed matter.* – We now have at our disposal all the tools necessary to an analysis and discussion of the structure and properties of configurations of catalyzed matter. In the next few Sections we shall examine the hydrostatic structure, the thermal structure, and the stability of such configurations.

5'4.1. Hydrostatic structure. Aside from thermal properties, which are considered in the next Section, *to each proposed equation of state for catalyzed matter there corresponds a one-parameter family of equilibrium configurations.* Once the central density has been specified, an integration of the primary and secondary structure equations uniquely fixes a configuration's mass, radius, and gravitational field, and its distributions of pressure, density, and baryons (*).

(*) The uniqueness of this determination depends upon the assumption that the equation of state, $p^*(\varrho^*)$, is monotonic. That this is necessarily so is shown by HTWW, p 102-104.

The main features of the one-parameter family of equilibrium configurations for a given equation of state are most clearly depicted by a curve of total mass-energy, M^*, *vs.* radius, R, parametrized by central density, ϱ_c^*. Such curves are shown in Fig. 4 for the H-W, S-V, V_β, and V_γ equations of state. The rather uniform shape of these four $M^*(R)$ curves can be understood as follows:

Consider the transformations undergone by an imaginary configuration of cold catalyzed matter, as baryons are added to it or taken away in just the right manner to keep it at the endpoint of thermonuclear evolution. The process of adding and removing baryons could be accomplished, for example, by the idealized routine described in Sect. 33.7. Note that because of the constancy of the injection energy (*) it does not matter where in the equilibrium configuration the baryons are added; the addition of δA baryons is always accompanied by a mass increase of

$$\delta M^* = \mu_B^*(R)[1 - 2M^*/R]^{\frac{1}{2}}\delta A \,. \tag{5.17}$$

(Cf. eq. (3.63).) Here $\mu_B^*(R)$ is (1/56) × (mass of a ^{56}Fe atom).

At a central density of 7.86 g/cm^3 the equilibrium configuration which we wish to follow is a ball of ^{56}Fe, the size of an apple. As more and more ^{56}Fe atoms are added to the ball, its central density, mass, and radius become larger and larger, until a configuration of $\varrho_c = 3 \cdot 10^3$ g/cm^3, $M = 0.011 M_\odot$, and $R = 1.8 \cdot 10^4$ km is reached. (This configuration and all those of lower central density are too small to show up in Fig. 4.) At this point gravitational forces are becoming so strong that the addition of more ^{56}Fe nuclei causes the radius, R, to decrease rather than increase. This is roughly the beginning of the region of white dwarf stars (**).

As more ^{56}Fe nuclei are added to push the central density beyond $3 \cdot 10^3$ g/cm^3 and higher, the equilibrium configuration becomes more and more massive, its radius gets smaller and smaller, and internal gravitational forces become stronger and stronger. In the meantime, inside the configuration the orbital iron electrons become highly degenerate and begin to react with the ^{56}Fe nuclei

---

(*) See footnote (*) on p. 233.

(**) The white dwarfs which occur in nature are *not* catalyzed to near the endpoint of thermonuclear evolution because the reaction rates for the formation of neutron-rich nuclei at white dwarf temperatures and pressures are considerably slower than 10^{-10} per nucleus per year. However, the difference in nuclear composition between real white dwarfs and configurations of catalyzed matter has only a small effect on the equation of state. Consequently, realistic white dwarf models—as exemplified, *e.g.*, by the S-V configurations of Fig. 4 (cf. footnote (*) on p. 229)—are not too different from the configurations of catalyzed matter discussed here. For further discussion see, *e.g.*, SALPETER (1961), and HAMADA and SALPETER (1961).

to form neutron-rich nuclei (cf. Sect. 5·1.2). Eventually a critical point (first peak of $M^*[R]$ curve; $\varrho_c \approx 10^9$ g/cm^3; $M \approx 1.2\ M_\odot$, $R \approx 3000$ km; $A \approx \approx 1.4 \cdot 10^{57}$ baryons) is reached, at which point gravitational forces are so strong that the addition of one more baryon would force the configuration to collapse. This point is called the LHWW (Landau-Harrison-Wakano-Wheeler) *crushing point*; and the critical mass at this point is often called the *Chandrasekhar limit.*

Since the addition of one more baryon at the LHWW crushing point would induce gravitational collapse, one must now begin to *remove* baryons from the configuration in order to move it through equilibrium states of higher and higher central density. With the removal of baryons beyond the LHWW point the mass and radius decrease, the central density increases, and—according to the static approach to stability (Sect. 4·2.2 and 5·5.1)—the fundamental mode of radial pulsation of the configuration becomes unstable. The configuration remains unstable against small radial perturbations as more and more baryons are removed until the second critical point in the $M^*(R)$ curve is reached at $\varrho_c \sim 5 \cdot 10^{13}$ g/cm^3. (We ignore the two intermediate critical points for V_β and V_γ configurations, which signal the onset and removal of instability of the first harmonic of radial pulsation.) As baryons are removed and central density increases through the unstable region $10^9 \leqslant \varrho_c \leqslant 5 \cdot 10^{13}$, the cold catalyzed matter in the interior of the configuration is transformed from electrons plus neutron-rich nuclei into a mixture of degenerate neutron, proton, and electron gases. The peculiar behaviour of the equation of state as these nuclear transformations occur is largely responsible for the peculiar form of the $M^*(R)$ curve in this density region.

At the second critical point (minimum of $M^*(R)$ curve; « HWW*point* ») the removal of any additional baryons will force the configuration to explode or collapse. In order to move onward through equilibrium states of higher density one must now *add* baryons to the configuration; and this addition of baryons, according to the static analysis of stability, will make the fundamental mode of radial pulsation stable.

The stable equilibrium states through which the configuration now passes as baryons are added to it are called *neutrons stars* because the main constituents of the configuration are neutrons. (Because hyperons are also present in abundance for $\varrho_c > 10^{15}$ g/cm^3, the term hyperon stars is sometimes used as well.) The neutron stars extend from the HWW minimum of the $M^*(R)$ curve at $\varrho_c \approx 5 \cdot 10^{13}$ g/cm^3 the maximum at $\varrho_c \approx 5 \cdot 10^{15}$. This second maximum (third critical point) is called the « LOV *crushing point* » (LOV ≡ LANDAU, OPPENHEIMER, VOLKOFF). Here, as at the LHWW crushing point, one must cease adding baryons and begin to remove them, in order to avoid collapse and to move the configuration along the $M^*(R)$ curve toward still higher central densities.

As baryons are removed to compress the configuration beyond the LOV crushing point, the fundamental mode of radial pulsation becomes unstable. The continued removal of baryons brings the configuration to a fourth critical point—a minimum in $M^*(R)$—beyond which baryons must be added, and at which the first harmonic of radial pulsation becomes unstable. There follow an infinite sequence of critical points as the $M^*(R)$ curve spirals inward toward a limiting state of infinite central density but finite mass and radius. At each critical point one more mode of radial pulsation becomes unstable (counterclockwise spiral). In the region $\varrho_c \geqslant 10^{19}$ g/cm^3 the spiraling $M^*(R)$ curve is described analytically by eqs. (4.22)-(4.24).

Because the above behavior is common to all four $M^*(R)$ curves of Fig. 4, we have confidence that this behavior correctly describes configurations of matter near the endpoint of thermonuclear evolution. (In connection with this, see MISNER and ZAPOLSKY (1964).) However, there are several important differences among the four curves, which reflect gaps in our understanding of configurations of catalyzed matter. These differences occur primarily in and above the neutron star region, where uncertainty about the nature of nucleon-nucleon interactions makes our knowledge of the equation of state unreliable. Roughly speaking, the lower the density at which repulsive nuclear forces become important and the stronger those forces are, the larger are the typical and maximum masses for neutron stars. Widely differing assumptions about repulsive nuclear forces lead to masses at the LOV crushing point which vary from $\sim 0.65 M_\odot$ to $\sim 2.0 M_\odot$. In Table III we present the mass, radius, and central density of the most massive, stable neutron star (LOV point) as predicted by a number of different equations of state. The maximum mass of a stable neutron star is an important determinant of the fates of the collapsed cores of supernovae (cf. FINZI (1966), WHEELER (1966)). The larger the maximum mass, the more frequently neutron stars will be formed in supernova explosions. The smaller the maximum mass, the more frequently the cores of supernovae will undergo catastrophic gravitational collapse to a general-relativistic singularity (see Sect. 7).

Each equation of state for cold catalyzed matter proposed thus far has yielded only two regions of stable equilibrium configurations—the white-dwarf region and the neutron-star region. However, it is conceivable (J. A. WHEELER, private communication) that elementary-particle processes not now understood might lead to a third region of stability at central densities $\varrho_c \geqslant 10^{16}$ g/cm^3. Although such a possibility is conceivable, it seems unlikely. At these very high densities the adiabatic index required for stability against radial perturbations probably exceeds 2.0, whereas causality (speed of sound less than speed of light) demands that Γ_1 and $\gamma_{\text{eqn state}}$ be $\leqslant 2.0$ at these densities.

For a much more extensive discussion of the hydrostatic properties of stars near the endpoint of thermonuclear evolution see HTWW.

TABLE III. – *Characteristics of the neutron star of maximum mass* (L-O-V *crushing point*) *as predicted by various equations of state* [a].

Equation of state and references [b]	Central density, ϱ_c (g/cm^3)	Number baryons, $A/A_\odot$	Mass $M/M_\odot$	Radius R (km)
Ideal neutron gas (no hyperons or nuclear interactions): OPPENHEIMER and VOLKOFF (1939), INMAN (1965).	$3.9\cdot10^{15}$	0.738	0.712	9.27
Ideal neutron, proton, and electron gases (no hyperons or nuclear interactions). H-W: HARRISON, WAKANO, WHEELER (1958); HTWW.	$6.0\cdot10^{15}$	0.704	0.683	8.39
Ideal baryon gas (nucleons and hyperons but no nuclear interactions): AMBARTSUMYAN and SAAKYAN (1960, 1961).	$2.3\cdot10^{15}$	NA	0.634	11.0
Real nucleon gas (nuclear interactions but no hyperons):				
1) SKYRME (1959), CAMERON (1959), SAAKYAN (1963), INMAN (1965), TSURUTA (1964) [c]				
cut-off at $p^* = \varrho^*/3$	$4.5\cdot10^{15}$	1.98	1.61	8.2
cut-off at $p^* = \varrho^*$	$4.8\cdot10^{15}$	2.08	1.70	7.7
2) SALPETER (1960)	NA	NA	NA	NA
3) AMBARTSUMYAN and SAAKYAN (1960, 1961)	$8\cdot10^{15}$	NA	1.05	6.5
4) GRATTON and SZAMOSI (1964), PACINI (1965) [e]	$6\cdot10^{15}$	NA	0.85	8.1
5) INMAN (1965), case *c*.	$2.2\cdot10^{15}$	1.19	1.14	13.1
6) INMAN (1965), case *d*.	$2.0\cdot10^{15}$	1.71	1.60	13.0
Real baryon gas (nuclear interactions and hyperons):				
1) S-V: SAAKYAN and VARTANYAN (1963*a*, *b*; 1964)	$3.7\cdot10^{15}$	1.75	1.55	9.19
2) Levinger-Simmons V_β: TSURUTA (1964), TSURUTA and CAMERON (1966*a*) [c]				
cut-off at $p^* = \varrho^*/3$	$1.1\cdot10^{16}$	1.15 [d]	0.926	NA
cut-off at $p^* = \varrho$	$1.1\cdot10^{16}$	1.202 [d]	0.973	5.103
3) Levinger-Simmons V_γ: TSURUTA (1964), TSURUTA and CAMERON (1966*a*) [c]				
cut-off at $p^* = \varrho^*/3$	$2.9\cdot10^{15}$	2.28 [d]	1.914	NA
cut-off at $p^* = \varrho^*$	$3.0\cdot10^{15}$	2.317 [d]	1.953	9.8

[a] For comparison, at the LHWW crushing point (maximum white-dwarf mass) $\varrho_c \approx 1\cdot10^9$ g/cm^3; $A/A_\odot \approx M/M_\odot \approx 1.2$; $R \approx 3000$ km. In the table « NA » means not available.

[b] For discussions of equations of state see lectures by SZAMOSI (1966).

[c] Equation of state arbitrarily set to $p^* = \varrho^*/3$ or $p^* = \varrho^*$ when that point is reached so as to avoid velocity of sound exceeding velocity of light.

[d] This number is rest mass (cf. eq. (3.15)) in units of $M_\odot$, rather than $A/A_\odot$.

[e] These numbers are for hard-core nucleon-nucleon repulsion at $r_c = 0.4\cdot10^{-13}$ cm.

5·4.2. Thermal structure. In discussing the thermal structure of configurations of catalyzed matter, we shall concentrate our attention on stable configurations—white dwarfs and neutron stars.

General relativity has only negligible effects upon the structure, both hydrostatic and thermal, of white dwarf stars. For this reason white dwarfs are normally studied within the framework of the Newtonian approximation. For Newtonian treatments of the thermal structure of white dwarfs see, *e.g.*, SCHATZMAN (1958), SCHWARZSCHILD (1958), and MESTEL (1965).

The thermal structure of neutron and hyperon stars was first investigated by CHIU (1964), by CHIU and SALPETER (1964), and by MORTON (1964) in connection with the possibility that X-ray emission from young neutron stars might be observable at the earth. More recent studies have been made by ELLIS (1965), by BAHCALL and WOLF (1965*a*, *c*), by FINZI (1965*a*), and by TSURUTA and CAMERON (1965*a*, 1966*b*). *For a review see the lecture of* FINZI (1966).

In all of these studies Newtonian theory was used for simplicity, since the accuracy desired was less than the 5 to 30 % error which results from neglecting general relativity. However, in future calculations general-relativistic effects will probably be taken into account by means of the thermal-structure equations (5.13) (5.14), augmented by a more realistic analysis of the surface layers and atmosphere (cf. end of Sect. **5**·3), which are typically only a few meters thick.

5·5. *Stability and pulsations of configurations of catalyzed matter.* – We turn now from the equilibrium structure of stars near the endpoint of thermonuclear evolution to a discussion of their behavior under small radial perturbations, including: a « static » analysis of stability; numerical calculations of normal-mode frequencies and eigenfunctions; and the damping of pulsations. In this discussion of stability and pulsations we shall usually simplify matters by speaking in terms of *cold* catalyzed matter. This is allowable because the pulsation frequencies and eigenfunctions for configurations of catalyzed matter, like all other hydrostatic and hydrodynamic properties, are temperature-independent.

5·5.1. The static analysis of stability. The static, $M^*(R)$ approach to stability, as outlined in Sect. **4**·2.2 and **4**·2.3, is not applicable directly to configurations of cold, catalyzed matter because neither condition (4.15) nor (4.16) is satisfied by such configurations. In this Section we will modify slightly the $M^*(R)$ approach to stability to make it applicable to configurations of catalyzed matter. But before presenting the modified analysis, we must elucidate several key features of such configurations.

One key feature is this, that the adiabatic index Γ_1 for configurations of cold, catalyzed matter is not a unique function of density, ϱ^*. Rather, Γ_1 depends upon the frequency of the stellar pulsations, $|\omega|$, as well as upon ϱ^*. So long

as $1/|\omega|$ is large compared to the relaxation times, t_{relax}, of the nuclear reactions required to keep the pulsating matter at the endpoint of thermonuclear evolution, the nuclear reactions proceed to completion as rapidly as the density changes. Hence,

$$(5.18a)\qquad \begin{cases} \Gamma_1(|\omega|, \varrho^*) = \gamma_{\text{eqn state}}(\varrho^*) \\ \qquad\qquad \equiv (\varrho^* + p^*)p^{*-1}(\mathrm{d}p^*/\mathrm{d}\varrho^*)_{\text{as given by eqn of state}} \text{ when } |\omega|^{-1} \gg t_{\text{relax}} . \end{cases}$$

On the other hand, when $1/|\omega|$ is small compared to t_{relax}, nuclear reactions occur hardly at all. Consequently,

$$(5.18b)\quad \Gamma_1(|\omega|, \varrho^*) = \gamma_{\text{no reactions}}(\varrho^*) \equiv (\varrho^* + p^*)p^{*-1}(\partial p^*/\partial \varrho^*)_{\text{constant } Z_1, Z_2, \ldots Z_N} ,$$

when $|\omega|^{-1} \ll t_{\text{relax}}$.

In the intermediate case, where $1/|\omega|$ is of the same order as t_{relax}, Γ_1 is a complicated function of $|\omega|$, which might even be taken as complex—$\Gamma_1 = \Gamma_1^{(R)} + i\Gamma_1^{(I)}$—to account for pulsation damping by nuclear reactions. However, we shall temporarily ignore any imaginary part of Γ_1, leaving the discussion of pulsation damping to the end of this Section and to Sect. 5·5.3.

There is an important relationship between the values of Γ_1 for various frequencies: Consider a small sample of fluid at the endpoint of thermonuclear evolution. Let the volume of the sample be V_0 and its pressure be p_0. Compress the sample to volume $V_0 - \Delta V$, where $\Delta V \ll V_0$, at a rate of fractional volume change

$$\mathrm{d}(V/V_0)/\mathrm{d}t = -|\omega| .$$

According to the first law of thermodynamics the accompanying increase in total mass-energy of the sample is

$$(5.19)\qquad \Delta E^* = -\int_{V_0}^{V_0-\Delta V} p^* \mathrm{d}V = p_0^* \Delta V[1 + (\Gamma_1/2)(\Delta V/V_0) + \ldots] ,$$

where Γ_1 is the adiabatic index at density $\varrho_0^* = \varrho^*(p_0^*)$ and frequency $|\omega|$. The increase in mass-energy, ΔE^*, evidently depends by way of Γ_1 on the speed, $|\omega|$, with which the compression is performed. The slower the compression, the more nuclear reactions will proceed to completion; and, hence, the smaller will be ΔE^*. On the other hand, according to eq. (5.19), the smaller ΔE^* is, the smaller is Γ_1. These relations are possible only if $\Gamma_1(\varrho^*, |\omega|)$ is a non-decreasing function of $|\omega|$. Hence, Γ_1 must take on its minimum value at $|\omega| = 0$ and its maximum value at $|\omega| = \infty$.

$$(5.20)\qquad \gamma_{\text{eqn state}} \leqslant \Gamma_1(|\omega|, \varrho^*) \leqslant \gamma_{\text{no reactions}} .$$

Next consider a particular configuration at the endpoint of thermonuclear evolution. The squared angular frequency of its n-th normal mode, ω_n^2, can be calculated correctly from the *dynamical* approach to stability if and only if the correct adiabatic index, $\Gamma_1(|\omega|, \varrho^*)$, is used. If, instead, we were to use $\Gamma_1 = \gamma_{\text{eqn state}}$ or $\Gamma_1 = \gamma_{\text{no reactions}}$, we would obtain incorrect squared frequencies, ω_n^2 [eqn. state] or ω_n^2 [no reactions]. The inequality (5.20) between Γ_1, $\gamma_{\text{eqn state}}$, and $\gamma_{\text{no reactions}}$ imposes a similar inequality between the correct squared frequency, ω_n^2, and the incorrect ones:

$$\omega_n^2[\text{eqn state}] \leqslant \omega_n^2 \leqslant \omega_n^2[\text{no reactions}]\,. \tag{5.21}$$

Proof of inequality (5.21): Let $\omega_n^2[\gamma(\varrho^*)]$ be the squared frequency of the n-th normal mode of our particular configuration under the assumption that $\Gamma_1 = \gamma(\varrho^*)$. It is sufficient to show that, for any hypothetical adiabatic index $\gamma(\varrho^*)$ and some other *very slightly larger* index $\Gamma_1 = \gamma(\varrho^*) + \delta\gamma(\varrho^*)$, we necessarily have

$$\omega_n^2[\gamma + \delta\gamma] > \omega_n^2[\gamma]\,. \tag{5.22}$$

To prove this, we can apply standard, nondegenerate perturbation theory (*) to the eigenvalue eq. (4.8), thereby obtaining

$$\omega_n^{*2}[\gamma + \delta\delta\gamma] - \omega_n^{*2}[\gamma] = \frac{\int_0^R e^{3\Phi}(1 - 2m^*/r)^{-\frac{1}{2}} r^{-2} p^* \,\delta\gamma\,(r^2 e^{-\Phi}\xi_n)'^2\,\mathrm{d}r}{\int_0^R W(r^2 e^{-\Phi}\xi_n)^2\,\mathrm{d}r} + O[(\delta\gamma)^2]\,. \tag{5.23}$$

Here ξ_n is the eigenfunction corresponding to $\omega_n^2[\gamma]$. Because $\delta\gamma$ is very small and positive, the right-hand side of eq. (5.23) is positive. QED.

We now have the tools required for a proof that a modified form of the static approach to stability (Sect. 4·2.2) is applicable to the (one-parameter) family of configurations at the endpoint of thermonuclear evolution. Our proof is based upon Fig. 5, where we show two portions of the dependence upon central density, ϱ_c, of the n-th squared frequency, ω_n^2. If the adiabatic index $\Gamma_1(|\omega|, \varrho^*)$ were equal to $\gamma_{\text{eqn state}}$ (eq. (5.18a)) at all frequencies, ω_n^2 would have the ϱ_c-dependence shown by the curve labeled ω_n^2[eqn. state]; and if Γ_1 were always equal

(*) For an account of perturbation theory see, *e.g.* MATHEWS and WALKER (1964), Chapter 10. An alternative proof of (5.22), in which no infinite series such as (5.23) arise, can be based on the Rayleigh-Ritz method for solving the variational equation (4.10). For an account of the Rayleigh-Ritz method see BARDEEN, THORNE and MELTZER (1966).

to $\gamma_{\text{no reactions}}$ (eq. (5.18b)), ω_n^2 would follow the curve ω_n^2[no reactions]. However, Γ_1 varies with frequency between the limits $\gamma_{\text{eqn state}}$ and $\gamma_{\text{no reactions}}$, so according to eq. (5.21) ω_n^2 moves about in the region between the limiting curves

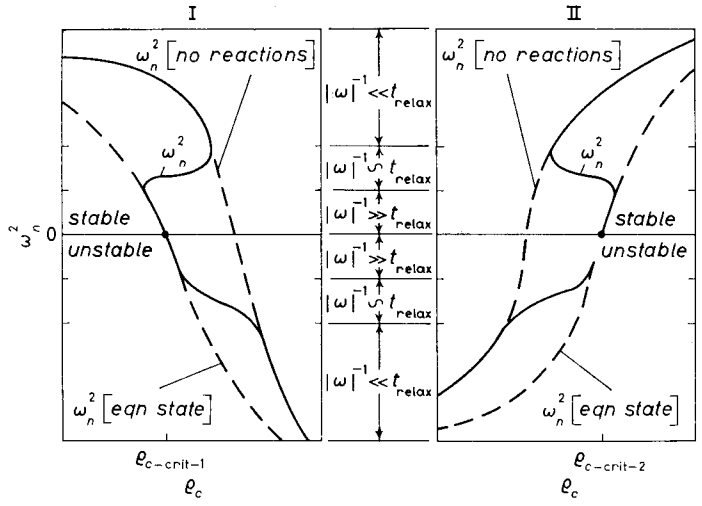

Fig. 5. – Stability behavior of the normal modes of radial pulsation of configurations of catalyzed matter near a critical point of the $M^*(R)$ curve. (Schematic.) The squared angular frequency, ω_n^2, of the mode of changing stability is shown as a function of central density, ϱ_c, in the neighborhoods of two typical critical points, $\varrho_{c\text{-crit-1}}$ and $\varrho_{c\text{-crit-2}}$. At $\varrho_{c\text{-crit-1}}$ the n-th normal becomes unstable with increasing central density. At $\varrho_{c\text{-crit-2}}$ it becomes stable. In the transition regions, $|\omega|^{-1} \sim t_{\text{relax}}$, pulsations are often damped extremely rapidly by nuclear reactions (*); and consequently, ω_n^2 is a complex function of ϱ_c, rather than real as idealized here.

ω_n^2(eqn. state) and ω_n^2[no reactions]. At low frequencies, where there is sufficient time for nuclear reactions to occur as the star pulsates, ω_n^2 coincides with ω_n^2[eqn. state]; at high frequencies it coincides with ω_n^2[no reactions]; and at intermediate frequencies it moves from one curve to the other.

At least this is the situation when pulsation damping has negligible effects upon the normal-mode eigenfunctions and frequencies. However, in the transition region, $|\omega_n|^{-1} \sim t_{\text{relax}}$,—and only there— the reactions which attempt to keep nuclear abundances at the endpoint of thermonuclear evolution can damp pulsations at a rate of the order of or larger than the pulsation frequency (*).

(*) The transition regions, $|\omega_n|^{-1} \sim t_{\text{relax}}$, of greatest physical interest occur near the LHWW point (maximum white-dwarf mass) and HWW point (minimum neutron-star mass), where the fundamental mode changes stability. (The LOV point is not of interest here because near that point ω_n^2 [no reactions] $= \omega_n^2$ [equation state].) Let $\omega_0 = \omega_0^{(R)} + i\omega_0^{(I)}$ in these transition regions, and for simplicity focus attention on the

Consequently, in the transition region ω_n is actually a complex function of ϱ_c, with an imaginary, damping part which may be large compared to the real part.

The static approach to stability, a generalization of which we wish to obtain, would be applicable if Γ_1 were equal to $\gamma_{\text{eqn state}}$ at all frequencies (cf. Sect. 4·2.3). Hence, the static approach predicts the stability behavior of the (incorrect) curve ω^2[eqn state]; it predicts that the n-th normal mode is stable for central densities $\varrho_c < \varrho_{c\text{-crit-1}}$ or $\varrho_c > \varrho_{c\text{-crit-2}}$ but unstable for $\varrho_c > \varrho_{c\text{-crit-1}}$ or $\varrho_c < \varrho_{c\text{-crit-2}}$ (cf. Fig. 5) The actual behaviour of the n-th normal mode is only slightly different from this prediction: For $\varrho_c < \varrho_{c\text{-crit-1}}$ or $\varrho_c > \varrho_{c\text{-crit-2}}$, the n-th mode is stable; but for $\varrho_c > \varrho_{c\text{-crit-1}}$ or $\varrho_c < \varrho_{c\text{-crit-2}}$, it is *both stable and unstable—i.e.* in these regions there are several normal radial modes of order n, corresponding to different adiabatic indices; and some of these modes are unstable, while others are stable.

These observations allow us to conclude that *the static approach to stability is applicable to the (one-parameter) family of configurations at the absolute endpoint of thermonuclear evolution if it is restated in the following slightly modified form*: Construct a curve of total mass-energy, M^*, plotted upward *vs.* radius, R, plotted to right. This curve has the properties *a*), *b*), and *c*) of Sect. 4·2.2; and, in addition, it has the following property: *d*) *In the neighborhood of a peak or valley (critical point) of the $M^*(R)$ curve the squared frequency, ω_n^2, of the mode of changing stability, behaves as indicated in Fig* 5. *A configuration near the critical point, $\varrho_{c\text{-crit}}$, may have several normal modes of order n. If the configuration*

---

stable side of the critical point. One can show by the following analysis that *at the center of these transition regions $\omega_0^{(I)}$, the damping rate, is much larger than $\omega_0^{(R)}$, the pulsation frequency*. The proof proceeds by contradiction: *Assume* that $\omega_0^{(I)} < \omega_0^{(R)}$ when $\omega_0^{(R)} \approx (t_{\text{relax}})^{-1}$. At this frequency pulsations will drive all nuclear reactions nearly to completion each time the star is in a state of maximum compression or expansion. In driving the reactions to completion the star converts

$$\Delta E^* \approx (A/2)\left[(p^*/n)(\gamma_{\text{no reactions}} - \gamma_{\text{eqn state}})(3\xi/r)^2\right]_{\text{avg over star}} \sim (p_c^*/\varrho_c^*)\, M^*\, [(\gamma_{\text{no reactions}} - \gamma_{\text{eqn state}})(\xi/r)^2]_{\text{avg over star}}$$

of its pulsation energy to heat and outgoing neutrinos (cf. eq. (5.19)). But the total pulsation energy is (cf. eq. (4.12))

$$E^*_{\text{puls}} \sim M^* \omega_0^{*2} R^2 [(\xi/r)^2]_{\text{avg over star}} .$$

Consequently,

$$\omega_0^{(I)}/\omega_0^{(R)} \sim \Delta E^*/E^*_{\text{puls}} \sim (p_c^*/\varrho_c^*)(ct_{\text{relax}}/R)^2\, (\gamma_{\text{no reactions}} - \gamma_{\text{eqn state}})_{\text{avg}} .$$

For configurations near the LHWW and HWW points we have (cf. Fig. 4 and Sect. 5·5.2) $(\gamma_{\text{no reactions}} - \gamma_{\text{eqn state}}) \gtrsim 0.01$, $(ct_{\text{relax}}/R)^2 \gtrsim 10^{17}$, $(p_c^*/\varrho_c^*) \gtrsim 10^{-4}$. Hence, $\omega_0^{(I)}/\omega_0^{(R)} \gtrsim 10^{11}$. But this contradicts the assumption that $\omega_0^{(I)} < \omega_0^{(R)}$ QED.

is on the stable side of $\varrho_{c\text{-crit}}$, *all of its modes of order n are stable*; *but if it is on the unstable side, at least one of its order-n modes is unstable.*

In Sect. 5·4.1 we discussed the implications of this $M^*(R)$ stability analysis for configurations of catalyzed matter. Our main conclusion was that there are only two types of stable configurations: white dwarfs and neutron stars.

5·5.2. Frequencies and eigenfunctions of normal radial modes. Although the « static » analysis has revealed to us the number of unstable normal radial modes of each configuration of cold catalyzed matter from $\varrho_c = 7.86$ g/cm³ to $\varrho_c = \infty$, it cannot tell us the frequencies or shapes of the normal modes, except at critical points of the $M^*(R)$ curve. To obtain such quantitative information between critical points one must use the « dynamic » approach to stability as described in Sect. 4·2.1.

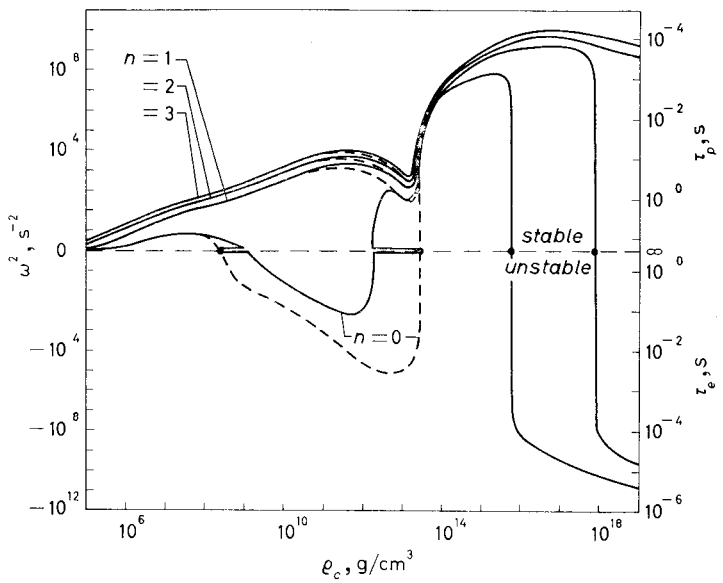

Fig. 6. – Squared angular frequencies as functions of central density for the lowest four normal radial modes of H-W-W configurations of catalyzed matter. (Based on MELTZER and THORNE (1966).) The right-hand vertical scale involves the pulsation period, $\tau_p = 2\pi/\omega$, for stable modes and the e-folding time, $\tau_e = 1/|\omega|$, for unstable modes. The solid curves represent the correct squared frequencies, while the thin dashed curves represent ω_n^2 [eqn. state] (cf. Sect. 5·5.1). The solid horizontal curves, which hug the $\omega^2 = 0$ axis between $2.5 \cdot 10^8$ and $1.3 \cdot 10^9$ g/cm³, represent the transition from ω_n^2 [no reactions] to ω_n^2 [eqn. state] and have amplitude-dependent periods and e-folding times $\gtrsim 10^{10}$ years. The horizontal curves between $2.1 \cdot 10^{12}$ and $2.7 \cdot 10^{13}$ g/cm³ have amplitude-dependent periods and e-folding times $\gtrsim 100$ days. In these transition regions pulsation-damping by nuclear reactions is very large (cf. footnote (*) on p. 243). At central densities below 10^8 g/cm³ and above 10^{14} g/cm³, ω_n^2 [no reactions] is very nearly equal to ω_n^2 [eqn. state].

MELTZER and THORNE (1966) have recently calculated, by the dynamical approach, the squared frequencies and eigenfunctions of the lowest four radial modes of the H-W-W configurations of cold catalyzed matter (cf. top Section of Fig. 4). The results of those calculations are shown in Fig. 6. Because the typical pulsation periods and e-folding times are much shorter than the relaxation times for nuclear reactions ($|\omega|^{-1} \ll t_{\text{relax}}$), the squared frequencies are almost everywhere equal to ω_n^2[no reactions]. Only very near the $\omega^2 = 0$ axis —at $|\omega| \leqslant 10^{-10}$/y for the white-dwarf region; $|\omega| \leqslant 1/100$ days for the neutron-star region—does ω_n^2 make the transition from ω_n^2[no reactions] to ω_n^2[eqn. state]. As a consequence, the unstable white dwarfs of $2.5 \cdot 10^8 < \varrho_c < 1.3 \cdot 10^9$ are actually *metastable*—but « molasseslike » because of pulsation damping (*)—with e-folding times $\geqslant 10^{10}$ years; and the neutron stars of $2.1 \cdot 10^{12} < \varrho_c < 2.7 \cdot 10^{13}$ are metastable but molasseslike, with e-folding times $\geqslant 100$ days. The periods and e-folding times of the metastable configurations are amplitude-dependent as a result of the dependence of nuclear reaction rates upon pulsation amplitude (cf. MELTZER and THORNE (1966), Appendix A).

According to Fig. 6 the period of the fundamental mode of a white-dwarf star is typically ~ 10 s, while the fundamental period of a neutron star—in the absence of nucleon-nucleon forces—is $\sim 10^{-3}$ s.When nucleon-nucleon forces are included in the equation of state, the neutron-star fundamental period is reduced to $\sim 0.3 \cdot 10^{-3}$ s (TSURUTA, WRIGHT, and CAMERON (1965); TSURUTA (1965); MELTZER and THORNE (1966)).

Figure 6 shows only the beginning of the high-density region, $\varrho_c \geqslant 10^{19}$ g/cm^3 in which more and more normal radial modes become unstable with increasing central density. Equation (4.25) for the number of unstable modes in this region, when adapted to the H-W equation of state, reads

$$(5.24)\quad \begin{cases} \text{number of unstable modes} = \\ \qquad = \text{greatest integer less than } \left\{ \dfrac{47^{\frac{1}{2}}}{8\pi \log_{10} e} \log \varrho_c - 9.3 \right\}, \\ \qquad = \text{greatest integer less than } \{0.63 \log \varrho_c - 9.3\}. \end{cases}$$

MELTZER and THORNE (1966) have calculated the eigenfunctions, $\xi_n(r)$, of the H-W-W normal radial modes corresponding to the frequencies of Fig. 6. In the white-dwarf region and in the upper neutron-star region ($\varrho_c \geqslant 1 \cdot 10^{15}$ g/cm^3) the fundamental mode is very nearly homologous,

$$(5.25)\qquad \xi_0(r) \propto r,$$

(*) See fotnote (*) on p. 243.

and the harmonics are somewhat sinusoidal. However, for most unstable configurations and for neutron stars of central density $\varrho_c \leqslant 3 \cdot 10^{14}$ g/cm^3($M \leqslant 0.4 M_\odot$) the normal-mode eigenfunctions are far from homologous or sinusoidal.

5.5.3. Pulsation energy and the damping of normal radial modes. A numerical evaluation of eq. (4.12) by MELTZER and THORNE (1966) reveals that, in the absence of nucleon-nucleon interactions, a stable neutron star pulsating in its nearly homologous fundamental mode will have a pulsation energy of

$$E_{\text{puls}} \approx 1 \cdot 10^{52} (\xi/r)^2 \text{ erg} . \tag{5.26}$$

Here (ξ/r) is the relative amplitude of pulsation. Nucleon-nucleon interactions, which increase the frequency of pulsation by a factor ~ 3, increase the pulsation energy by a factor $\sim 3^2 \approx 10$ (cf. eq. (4.12)). Hence, a more realistic estimate than (5.26) is

$$E_{\text{puls}} \approx 1 \cdot 10^{53} (\xi/r)^2 \text{ erg} . \tag{5.27}$$

For comparison, the total mass-energy of the sun is $M_\odot c^2 = 1.8 \cdot 10^{54}$ erg.

That the pulsation energy of a neutron star formed in a supernova explosion might be very large was originally reasoned from rough Newtonian considerations by HOYLE, NARLIKAR, and WHEELER (1964); by FINZI (1965*b*); and by CAMERON (1965*a*, *b*); and each of these physicists suggested astronomically observable consequences of such large pulsation energies. For a review, see the lecture by FINZI (1966); also WHEELER (1966).

Whether neutron-star pulsations are astrophysically important depends upon how rapidly and by what means they are damped. Among the mechanisms which may damp the pulsations are 1) the modified URCA reactions

$$\text{n} + \text{n} \rightarrow \text{n} + \text{p} + \text{e} + \bar{\nu} , \qquad \text{n} + \text{p} + \text{e} \rightarrow \text{n} + \text{n} + \nu , \tag{5.28}$$

which are driven by the rising and falling Fermi energies (FINZI (1965*b*, 1966); MELTZER and THORNE (1966); HANSEN (1966)); 2) reactions analogous to (5.28) involving μ^- and Σ^-; 3) shock waves generated in the stellar atmosphere by the pulsations (FINZI (1965*b*), CAMERON (1965*b*)); 4) hydromagnetic waves generated in the stellar magnetic field by pulsations (CAMERON (1965*a*, *b*)); 5) electromagnetic waves emitted by the vibrating magnetic field and the surrounding plasma (CAMERON (1965*b*)); 7) coupling of the normal radial modes to nonradial modes as a result of rapid stellar rotation, and the consequent damping by viscous forces and by gravitational radiation (ZEE and WHEELER (1966); WHEELER (1966)). The relative importance of these various mechanisms in stable neutron stars has yet to be determined for certain. However, the cal-

culations of ZEE and WHEELER (1966) and of WHEELER (1966) suggest that, unless the neutron star can get rid of most of its angular momentum during the first few hours after formation, gravitational radiation will damp the normal radial modes to negligible amplitudes in a time of the order of a day.

5·5.4. Nonradial pulsations of neutron stars. Thus far we have considered only the radial pulsations of neutron stars. Since the catastrophic collapse of the stellar core, which, according to present theory (cf. COLGATE and WHITE (1964, 1966)), initiates a supernova explosion, will rarely if ever be completely symmetric, the resultant neutron star will pulsate nonradially as well as radially. However, according to calculations of ZEE and WHEELER (1966), gravitational radiation will damp out the nonradial modes in a fraction of a minute, leaving only radial pulsations behind.

5·6. *Summary.* – In Sect. **5** we have applied the tools developed in earlier Sections to the study of configurations of matter catalyzed to near the endpoint of thermonuclear evolution. The equation of state of such matter, $p^*=p^*(\varrho^*)$, is independent of temperature under conditions of physical interest; and, as a consequence, the equations of stellar structure simplify considerably to the form (5.11)–(5.15). The hydrostatic structure of each solution to these equations is uniquely determined by a single parameter—*e.g.* the central density, ϱ_c; but the thermal structure evolves with time in a manner determined by the (arbitrary) initial temperature distribution.

The equation of state of cold, catalyzed matter and the corresponding equilibrium configurations are shown in Fig. 4. There are two types of stable configurations: white dwarfs, which are made of heavy nuclei plus a degenerate electron gas, and which have densities $\leqslant 10^9$ g/cm^3; and neutron stars, which are made of a mixture of interacting neutron, proton, electron, and hyperon gases and have densities between 10^{13} and 10^{16} g/cm^3. The maximum mass of a white-dwarf star is $\sim 1.2 M_\odot$, while that of a neutron star is not known for certain but lies between 0.7 and 2.0 $M_\odot$.

A modified form of the static approach to stability reveals that the normal modes of radial pulsation change stability in the strange manner of Fig. 5 at critical points of the $M^*(R)$ curve. The pulsation periods of white-dwarf stars are ~ 10 s, while those of neutron stars are $\sim 0.3 \cdot 10^{-3}$ s. Neutron stars can store a sizable fraction of their rest mass in the form of radial pulsations; but nonradial pulsations are damped out in a fraction of a minute by gravitational radiation.

Observational aspects of neutron star theory are reviewed in the lecture of FINZI (1966) and in the article of WHEELER (1966); and the equation of cold catalyzed matter at high densities is the subject of Szamosi's (1966) lectures.

6. – Nondegenerate stellar models.

The analysis of equilibrium configurations of catalyzed matter (Sect. 5) was considerably simplified over the general theory of stellar structure (Sect. 3) by the fact that the equation of state, $p^* = p^*(\varrho^*, T^*)$, for catalyzed matter is independent of temperature. When we turn our attention to configurations of nondegenerate matter, the assumption that $p^*(\varrho^*, T^*)$ is independent of T^* is no longer tenable; and, consequently, the equations of thermal structure do not decouple from the equations of hydrostatic structure.

Does this mean that, in order to learn something of the structure of nondegenerate stars in general relativity, one must integrate the $16 + 3N$ structure equations (3.11) coupled together into one grand differential system with singularities of the equations at both the center and the surface of the star? No; fortunately, a method which dates back to the nineteenth century and is associated with such names as LANE, RITTER, and EMDEN enables one, *under certain restrictive circumstances*, to decouple the hydrostatic and thermal equations from one another even in highly nondegenerate configurations. This method effects such great simplifications, and the alternative of working with the full structure equations is so formidable, that all studies of specific nondegenerate, relativistic stellar models performed to date have utilized it.

Here in Sect. 6 we shall present the general relativistic form of the method for decoupling the thermal and hydrostatic equations; and we shall briefly describe the various relativistic stellar models which have been constructed by means of it.

6·1. *Method for decoupling thermal and hydrostatic equations.* – Consider an equilibrium configuration made of matter which obeys the two equations of state

$$p^* = p^*(n, T^*, Z_1, \ldots, Z_N) , \qquad \varrho^* = \varrho^*(n, T^*, Z_1, \ldots, Z_N) . \tag{6.1}$$

The full equations of stellar structure (3.11) will determine the hydrostatic and thermal structure of the configuration once the gas characteristic relations (3.11-10)–(3.11-16 + 3N) and sufficient initial data (cf. Sect. 3·4) have been specified. However, one sometimes knows *ab initio* that the particular energy transport-mechanism at work in the star will produce a temperature distribution, $T^*(r)$, which is related in some well-determined way to the distribution of baryons, $n(r)$

$$T^*(r) = T^*[n(r)]; \tag{6.2}$$

and one knows that the nuclear abundances, $Z_1, \ldots, Z_N$, are related to the

number density of baryons in some particular way

$$Z_k(r) = Z_k[n(r)] \,. \tag{6.2'}$$

When such relations are known to hold, one can combine them with the equations of state (6.1) to obtain relations between pressure and mass density and between pressure and number density

$$p^* = p^*(\varrho^*) \,, \qquad n = n(p^*) \,. \tag{6.3}$$

Since the effects of temperature upon the « hydrostatic » parameters (p^*, ϱ^*, n) are thereby eliminated, the equations of stellar structure now separate cleanly into hydrostatic equations and thermal equations.

The hydrostatic equations, which can be integrated without any further considerations of temperature or of energy transport, and which have no singularity at the surface of the star, are nearly the same as those used for configurations of catalyzed matter. They are

a) Primary-structure equations

$$p^* = p^*(\varrho^*) \quad \text{(pressure-density relation (6.3))}, \tag{6.4a}$$

(6.4*b*, *c*) same as (5.11*b*, *c*).

b) Secondary-structure equations

$$n = n(p^*) \qquad \text{(relation (6.3))}, \tag{6.5b}$$

(6.5*a*, *c*) same as (5.12*a*, *c*).

Once the hydrostatic structure equations have been integrated, the temperature distribution, $T^*(r)$, is determined by eq. (6.2). The luminosity, $L^*(r)$, is then determined by the energy-transport equation (3.11-7) and by the equation of thermal equilibrium (3.11-5), which together must be compatible with the assumed temperature-density relation (6.2).

6.1.1. Configurations of perfect gas as an example. (Reference: TOOPER (1965).) For a perfect gas of constant average baryonic rest mass, μ_B^*, constant ratio of specific heats, Γ_4, and constant ratio, b, of number density of free particles to number density of baryons, the equations of state are

$$p^* = bn\,T^* \,, \qquad \varrho^* = \mu_B^* n + (\Gamma_4 - 1)^{-1} bn\,T^* \,. \tag{6.6}$$

In an equilibrium configuration of such a gas a mixture of convective and radiative transport will sometimes lead to the temperature-density relation

$$T^*/T_c^* = (n/n_c)^{1/N} \,, \tag{6.7}$$

where N is a constant, and where T_c^* and n_c are the central temperature and central density of baryons. For example, efficient convection would lead to the temperature distribution (6.7) with $N = (\Gamma_4 - 1)^{-1}$ (cf. eq. (3.37*b*), in which we here put $\Gamma_1 = \Gamma_2 = \Gamma_3 = \Gamma_4$). By combining (6.7) with (6.6) we obtain the relations

$$p^* = p_c^* (n/n_c)^{1+1/N} . \tag{6.8a}$$

$$\varrho^* = \mu_B^* n_c (p^*/p_c^*)^{N/(1+N)} + (\Gamma_4 - 1)^{-1} p^* , \tag{6.8b}$$

which permit the equations of hydrostatic structure to decouple from the equations of thermal structure.

6·2. *Relativistic polytropes.* – In the Newtonian theory of stellar structure the *polytropic* pressure-density relation,

$$p/p_c = (\varrho/\varrho_c)^{1+1/N} , \tag{6.9}$$

is a good approximation to many realistic situations. The most reasonable relativistic generalization of this relation is eq. (6.8*a*). The alternative possibility

$$p^*/p_c^* = (\varrho^*/\varrho_c^*)^{1+1/N} \tag{6.10}$$

is unacceptable for two reasons: 1) at very high densities (6.10) leads to a velocity of sound exceeding the velocity of light; and 2) realistic physical situations rarely lead to relations of the form (6.10), except in the Newtonian realm.

In Newtonian theory the polytropic relation (6.9), together with the hydrostatic equations

$$m = \int_0^r 4\pi r^2 \varrho \, dr , \qquad dp/dr = -G\varrho m/r^2 , \tag{6.11}$$

is sufficient to permit the computation of the hydrostatic structure of a stellar model. However, in general relativity the polytropic relation (6.8*a*), together with the hydrostatic equations (6.4*b*, *c*) and (6.5*a*, *c*), are not sufficient to determine the hydrostatic structure. One also needs a relation between p^* and ϱ^*. We shall here adopt the convention that, when p^* and ϱ^* are related by an equation of the form (6.8*b*), and when $p^*(n)$ has the polytropic form (6.8*a*), then the resultant equilibrium configurations will be called *relativistic polytropic models*— or *relativistic polytropes* for short.

Relativistic polytropes arise not only as equilibrium configurations for a perfect gas; they also arise in other contexts—*e.g.* as approximations to neutron

star configurations (GRATTON (1964*d*), TOOPER (1965)) and as approximations to certain massive stars in which radiation pressure is not negligible compared to gas pressure (IBEN (1963), BARDEEN (1965), GRATTON and GIANNONE (1965), TOOPER (1966)).

At first sight relativistic polytropic models appear to form a *five*-parameter family of equilibrium configurations; they depend upon the polytropic index, N, the adiabatic index, Γ_4, the ratio of central pressure to central rest-mass density,

$$\alpha^* = p_c^*/\mu_B^* n_c \,, \tag{6.12}$$

the central density of rest mass-energy, $\mu_B^* n_c$, and the baryonic rest mass, μ_B^*. In actuality only *three* of these five parameters —N, Γ_4, and α^*— enter into numerical integrations of polytropic models. The baryonic rest mass, μ_B^*, is easily removed from the equations of hydrostatic structure since it merely determines the constant ratio of the stellar rest mass to the total number of baryons, $M_0^*/A = \mu_B^*$, as well as the constant ratio of density of rest-mass energy to baryon number density, $\mu_B^* n/n = \mu_B^*$. The central density of rest mass-energy can also be removed from the structure equations, by choosing $(\mu_B^* n_c)^{-1}$ or some multiple of it as the unit of length in terms of which all other quantities are measured (*).

6·3. *Stellar models considered in the literature.* – Rather than present here the numerical solutions of the structure equation (6.4), (6.5) for relativistic polytropes and for other nondegenerate stellar models, we shall give a brief « guide » to some of the literature where such solutions can be found.

Relativistic polytropes have been studied by many physicists in several different contexts: BARDEEN (1965, 1966) has studied a number of particular polytropic models with various values of N, Γ_4, and α^* in connection with his interest in the relationship between binding energy and stability. TOOPER (1965) has presented a systematic treatment of isentropic polytropes—*i.e.* polytropes for which $\Gamma_4 = 1 + 1/N$. GRATTON (1964*a*, *b*, *c*, *d*; 1965), and GRATTON and GIANNONE (1965) have systematically studied polytropes with $\Gamma_4 = \frac{4}{3}$ in connection with the structures of neutron stars and of supermassive stars. TOOPER (1966)—see also FOWLER (1964, 1966) for the post-Newtonian approximation—has presented a complete account of polytropes of order $N = 3$ in connection with the theory of massive stars.

(*) As has been emphasized by BARDEEN (1965), the scale-invariance which permits one to eliminate $\mu_B^* n_c$ from the equations of hydrostatic structure is present whenever eqs. (6.3) can be put into the dimensionless form $p^*/\mu_B^* n_c = f(\varrho^*/\mu_B^* n_c)$ and $n/n_c = g(\varrho^*/\mu_B^* n_c)$. Here f and g are functions which may involve $\alpha^* = p_c^*/\mu_B^* n_c$ but must not involve p_c^*, ϱ_c^*, or n_c in any other way.

In addition to polytropes, several other nondegenerate, relativistic stellar models are treated in the literature: IBEN (1963) has studied massive hydrogen configurations with allowances in the equation of state for the effects of electron-positron pair formation. Iben's models are very nearly polytropes with $\Gamma_4 = \frac{4}{3}$. TOOPER (1964) has systematically treated the 3-parameter family of isentropic configurations for which

$$p^*/p_c^* = (\varrho^*/\varrho_c^*)^{1+1/N}\,, \qquad \mathrm{d}n/\mathrm{d}\varrho^* = n/(\varrho^* + p^*)\,. \tag{6.13}$$

A variation on these configurations of TOOPER, which is presented by GRATTON and GIANNONE (1965), avoids the difficulty of sound velocity exceeding light velocity at high densities. This variation is based upon the pressure-density relations

$$\begin{cases} p^* = \begin{cases} K\varrho^{*1+1/N} & \text{if } \varrho^* < (1/3K)^N\,, \\ \varrho^*/3 & \text{if } \varrho^* > (1/3K)^N\,, \end{cases} \\ \mathrm{d}n/\mathrm{d}\varrho^* = n/(\varrho^* + p^*)\,. \end{cases} \tag{6.14}$$

6·4. *Summary and commentary.* – The relativistic equations of stellar structure are greatly simplified by assuming that the mechanism of energy transport produces a temperature distribution related in some unique way to the distribution of baryons, $T^* = T^*(n)$. When such a relation is available, it can be used to eliminate temperature from the equations of state. The hydrostatic equations of stellar structure are then temperature-independent and can be integrated on a computer very easily.

This simplified method of studying stellar structure has been used in all investigations made until now of nondegenerate relativistic configurations. In Sect. 6·2 and 6·3 we presented a brief survey of the various models which have been studied to date.

Although this method of studying stellar structure may seem somewhat *ad hoc* and unphysical, it can often be used to obtain semiquantitative information about situations of interest. It was particularly useful during the pre-1940 period, when the foundations of the Newtonian theory of stellar structure were being laid; and it is performing a similarly valuable role today in the birth and infancy of the relatistic theory of stellar structure. However, we must emphasize that, one can rarely if ever place confidence in the quantitative details of (hopefully) realistic stellar models constructed by the above method, until after he has checked the details of those models by numerical integration of the full equations of stellar structure (3.11).

7. – Gravitational collapse to infinite density.

7·1. *Inevitability of collapse for massive stars. There is no equilibrium state at the endpoint of thermonuclear evolution for a star containing more than about twice the number of baryons in the sun* ($A > A_{\max} \sim 2A_{\odot}$). This is one of the surprising—and disturbing— consequences of the discussion in Sect. **5** of configurations of catalyzed matter (cf. especially Fig. 4). Stated differently: A star with $A > A_{\max} \sim 2A_{\odot}$ must eject all but $A_{\max}$ of its baryons—*e.g.*, through nova or supernova explosions — before settling down into its final resting state; otherwise there will be no final resting state for it to settle down into (*).

What is the fate of a star which fails to eject its excess baryons before nearing the endpoint of thermonuclear evolution? For example, after a very massive supernova explosion, what will become of the collapsed degenerate-neutron core, which contains more than $A_{\max}$ baryons? Such a supercritical mass cannot explode, since it is gravitationally bound and it has no more thermonuclear energy to release. Nor can it reach a static equilibrium state, since there exists no such state for so large a mass. There remains only one alternative; the supercritical mass must collapse, and collapse, and collapse, until it has reached infinite density and zero volume— or until the laws of classical general relativity break down and new, yet-to-be-discovered, quantum-gravitational forces halt the collapse.

The phenomenon of catastrophic gravitational collapse as described by classical general relativity will be the subject of this, the last major Section of these lectures. Throughout our discussion of collapse, except in the closing paragraphs, we shall ignore all quantum-gravitational effects.

7·2. *Hydrodynamic equations for a collapsing star.* – Because of the severe computational difficulties posed by nonspherical collapse, the hydrodynamic equations which govern relativistic collapse have been developed in explicit form only for situations with spherical symmetry. Within the framework of spherical symmetry PODURETS (1964*a*), MISNER and SHARP (1964*a*, *b*) BARDEEN (1964, 1965), and FIRMANI (1965) have all independently developed the equations for *adiabatic collapse* into forms suitable for numerical integration;

(*) The final resting state described here, being the lowest energy state for $A_{\max}$ baryons, is a nonrotating configuration. A *rotating* star, which has burned all its fuel and contains more than $A_{\max}$ baryons, can reach an equilibrium state, if its angular momentum is large enough, and if the magnetic field does not halt the rotation (HOYLE, NARLIKAR and WHEELER (1964)). However, the amount of rotation necessary to stabilize a star much larger than $A_{\max}$ is great enough that some, if not most of the supercritical stars in our universe are probably doomed to the catastrophic collapse which is described in the following pages.

MISNER (1965), and HERNANDEZ and MISNER (1966) have derived two alternative but equivalent forms for the equations of *collapse with escaping neutrinos*; MISNER and SHARP (1965, 1966) have derived the equations for *collapse with energy transport by photon diffusion, and with nuclear-energy generation*; and GINZBURG and OZERNOY (1964) have discussed *the behavior of a star's magnetic field during collapse*. In addition to this work on specifically spherical problems, the general-relativity theory of radiative transfer in more general dynamical situations has been developed by BARDEEN (1965) and by LINDQUIST (1966).

Thus far the exact equations of collapse, as analysed analytically in the above references and by numerical integrations elsewhere (PODURETS (1964*c*), BARDEEN (1965), FIRMANI (1965), and most extensively MAY and WHITE (1964), (1966)), have yielded little *new* insight into relativistic collapse. They have tended, instead, to confirm quantitatively the qualitative picture of collapse which was first brought to light by the pioneering work of OPPENHEIMER and SNYDER (1939). OPPENHEIMER and SNYDER discussed in detail the «free-fall» collapse of a spherical configuration in which gravitational forces completely overwhelm pressure forces. In the next few Sections we shall present a somewhat modernized version of the analysis of OPPENHEIMER and SNYDER, and we shall subsequently demonstrate that the qualitative features of this analysis cannot be modified by the presence of pressure forces inside the collapsing star.

7·3. *Free-fall collapse* (*).

7·3.1. Birkhoff's theorem. Before restricting our attention to the free-fall collapse of OPPENHEIMER and SNYDER, we must discuss an important feature of spherical collapse in general: *The geometry of space-time surrounding a collapsing, nonradiating, spherical configuration, like that around an equilibrium configuration* (Sect. **3·4.1** and **3·5.1**), *is the Schwarzschild geometry*

$$(7.1) \qquad ds^2 = (1 - 2M^*/r)\,dt^2 - (1 - 2M^*/r)^{-1}\,dr^2 - r^2(d\theta^2 + \sin^2\theta\,d\varphi^2)\,.$$

This result is called Birkhoff's theorem since it was first demonstrated by BIRKHOFF (1923) pp. 253-256. (For an alternative proof see TOLMAN (1934*a*), Sect. **99.**) Although Birkhoff's theorem is strictly valid only in the absence of radiation, it remains very nearly valid so long as the energy density in the radiation field is not strong enough to modify appreciably the geometry—*i.e.*, so long as the mass-energy radiated during the collapse is small compared to the star's total mass-energy (**).

(*) I am indebted to Prof. J. A. WHEELER for many enlightening discussions of the ideas in Sect. **7.3.**

(**) We shall delay until Sect. **7·5.1** a discussion of stars which radiate a large fraction of their mass as they collapse.

Birkhoff's theorem is easily understood on physical grounds: Consider an equilibrium configuration which is unstable against gravitational collapse and which, like all equilibrium configurations (cf. Sect. 3·4.1), has the Schwarzschild geometry as its external gravitational field. Perturb this equilibrium configuration in a spherically-symmetry way so that it begins to collapse radially. The perturbation and subsequent collapse cannot affect the external gravitational field because, just as Maxwell's laws prohibit monopole electromagnetic waves, so Einsteins' laws prohibit monopole gravitational waves. There is no possible way for any gravitational influence of the radial collapse to propagate outward.

7·3.2. Free-fall collapse as depicted in Schwarzschild co-ordinates. One most readily and directly confronts the novel aspects of relativistic collapse by examining the time evolution of the radius, R, of a freely collapsing configuration. (R is defined by $4\pi R^2 = [\text{surface area of collapsing star}]$; *i.e.*, R is the value of the Schwarzschild radial co-ordinate, r, at the surface.) Consider for definiteness a configuration with negligible internal pressure, which begins at Schwarzschild co-ordinate time $t = 0$ in a momentarily static state. Let the initial radius be R_i and the total mass be M^*. As the configuration collapses, its surface falls freely in the external Schwarzschild geometry. Consequently, the energy red-shift eq. (3.3) is applicable to any particle of matter on the surface of the star. When applied to such a particle, the red-shift equation yields the following relation between the velocity of collapse of the surface,

$$v_R^* = e^{-\Phi}(1 - 2M^*/R)^{-\frac{1}{2}}\,\mathrm{d}R/\mathrm{d}t = (1 - 2M^*/R)^{-1}\,\mathrm{d}R/\mathrm{d}t\,, \tag{7.2}$$

and the gravitation potential, $\Phi = \frac{1}{2}\ln(1 - 2M^*/R)$, at the surface:

$$(1 - v_R^{*2})^{-\frac{1}{2}} e^{\Phi} = \text{const} = \exp[\Phi(r = R_i)]\,. \tag{7.3}$$

By rearranging this equation, one obtains a differential equation for the radius of the freely collapsing configuration as a function of (co-ordinate) time, t

$$\frac{\mathrm{d}R}{\mathrm{d}t} = -\left(\frac{2M^*}{R_i - 2M^*}\right)^{\frac{1}{2}}\left(\frac{R_i}{R} - 1\right)^{\frac{1}{2}}\left(1 - \frac{2M^*}{R}\right). \tag{7.4}$$

The solution to this differential equation is most easily expressed in terms of a parameter η:

$$\begin{cases} R = (R_i/2)(1 + \cos\eta)\,, \\ t = 2M^* \ln\left[\dfrac{(R_i/2M^* - 1)^{\frac{1}{2}} + \operatorname{tg}(\eta/2)}{(R_i/2M^* - 1)^{\frac{1}{2}} - \operatorname{tg}(\eta/2)}\right] + \\ \qquad\qquad + 2M^*(R_i/2M^* - 1)^{\frac{1}{2}}[\eta + (R_i/4M^*)(\eta + \sin\eta)]\,. \end{cases} \tag{7.5a}$$

The Schwarzschild co-ordinate time, t, to which R is here related, is *not* the proper time which would be measured by the clock of an experimental astrophysicist standing on the surface of the collapsing star. Rather, the astrophysicist's comoving clock would read

$$\tau^* = \int_0^t [(1 - 2M^*/R)\,\mathrm{d}t^2 - (1 - 2M^*/R)^{-1}\,\mathrm{d}R^2]^{\frac{1}{2}};$$

i.e., it would read

(7.5*b*) $\quad \tau^* = (\text{proper time on surface of star}) = (R_i^3/8M^*)^{\frac{1}{2}}(\eta + \sin\eta)\,.$

Equations (7.5) for the radius of a freely collapsing star as a function of time have a strange behavior: one might have expected the star to collapse to zero volume ($R \to 0$) after the elapse of a finite Schwarzschild coordinate time, t. However, as t becomes larger and larger, $\mathrm{d}R/\mathrm{d}t$ gets smaller and smaller; and in the limit $t \to \infty$ [$\mathrm{tg}\,(\eta/2) \to (R_i/2M^* - 1)^{\frac{1}{2}}$], R decreases asymptotically to $2M^*$

$$R(t = \infty) = 2M^*\,. \tag{7.6}$$

Simultaneously, proper time as measured at the surface of the star approaches the *finite* value

$$\tau^*(t = \infty) = \left(\frac{R_i^3}{8M^*}\right)^{\frac{1}{2}} \cos^{-1}\left(\frac{4M^*}{R_i} - 1\right) + R_i\left(1 - \frac{2M^*}{R_i}\right)^{\frac{1}{2}}. \tag{7.7}$$

As proper time, τ^*, continues to increase beyond the value (7.7), the star continues to collapse (R decreases below $2M^*$), but the Schwarzschild co-ordinate time, t, now decreases rather than increases. Finally, after the elapse of a perfectly finite proper time,

$$\tau^*(R = 0) = \tau^*(\eta = \pi) = \pi(R_i^3/8M^*)^{\frac{1}{2}}\,, \tag{7.8}$$

the surface of the star has collapsed to a single point ($R = 0$). The corresponding final value of the co-ordinate time, t, is

$$t(R = 0) = 2\pi M^*(R_i/2M^* - 1)^{\frac{1}{2}}(1 + R_i/4M^*)\,. \tag{7.9}$$

This behavior of radius, R, as a function of co-ordinate time t, and proper time, τ^*, is exhibited graphically in the left half of Fig. 7 for a freely collapsing configuration of initial radius $R_i = 10M^*$. (Such an initial condition is representative of unstable, high-density configurations of catalyzed matter.)

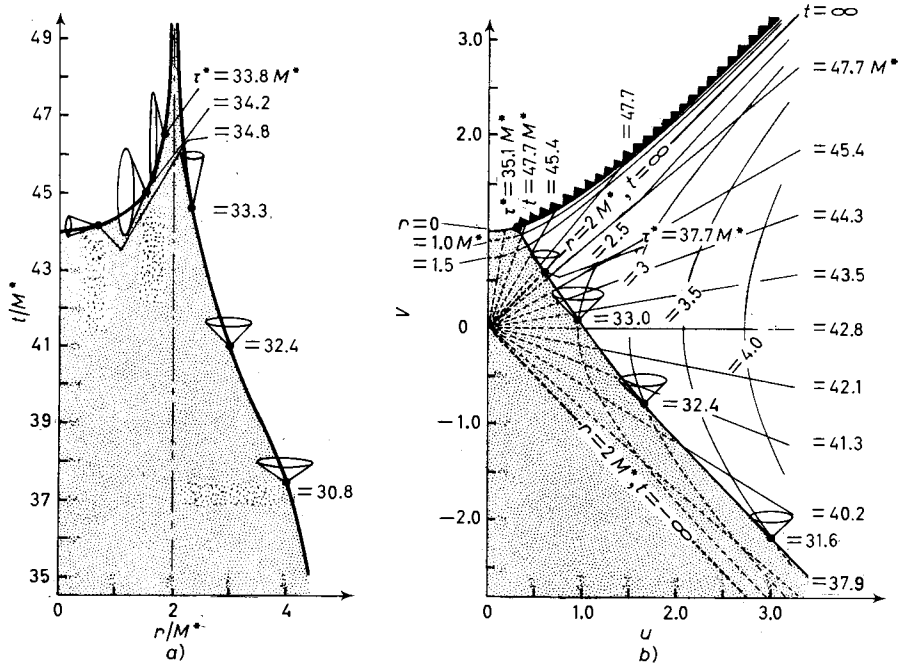

Fig. 7. – The free-fall collapse of a star of initial radius $R_i = 10M^*$ as depicted alternatively *a*) in Schwarzschild and *b*) in Kruskal co-ordinates. The region of space-time inside the collapsing star is stippled, while that outside is not. Only the geometry of the exterior region is that of Schwarzschild; for a discussion of the interior geometry see Sect. 7·3.6. The curve which separates the stippled and unstippled regions is the world line of the surface of the collapsing star. This world line is parametrized by proper time, τ^*, as measured by an observer who sits on the surface of the star; and light cones, as calculated from $ds^2 = 0$, are attached to it. Notice that, although the shapes of the light cones are not all the same relative to Schwarzschild co-ordinates, they are all the same relative to Kruskal co-ordinates. This is because light rays travel along 45 degree lines in the u-v plane ($dv = \pm du$), but they travel along curved paths in the r-t plane. The Kruskal space-time diagram shown here is related to the Schwarzschild diagram by eqs. (7.10) and (7.11*b*) *plus* a translation of Schwarschild time: $t \to t + 42.8\,M^*$. It is evident from these space-time diagrams that the free-fall collapse is characterized by a constantly diminishing radius, which drops from $R = R_i$ to $R = 0$ in a finite and short comoving proper time interval, $\Delta\tau^* = 35.1\,M^*$. The point $R = 0$ and the entire region $r = 0$ outside the star make up a physical « singularity » at which infinite tidal gravitational forces—according to classical, unquantized general relativity—can and do crush matter to infinite density.

7·3. Free-fall collapse as depicted in Kruskal co-ordinates. The above description of the collapse of a freely falling star is quite pathological in the neighborhood of ($R = 2M^*$, $t = +\infty$). Is the strange form of the Schwarzschild space-time diagram (left half of Fig. 7) at this point, and for $R < 2M^*$, an indication of some strange new force which acts upon the star here? Is space really as badly twisted up near ($R = 2M^*$, $t = \infty$) as the left

half of Fig. 7 would indicate? No. Physically speaking, there is nothing at all pathological about the geometry of space-time or the behavior of the star at ($R = 2M^*$, $t = \infty$). The pathology is all in the Schwarzschild co-ordinates (t, r, θ, φ) which we have used to describe the external gravitational field; and it is easily removed by transforming to a new, better-behaved co-ordinate system.

Several different co-ordinate systems have been used in the literature to describe in a reasonable manner the Schwarzschild space-time geometry which surrounds a collapsing star. The one most widely adopted in recent years is that of KRUSKAL (1960) (see also FULLER and WHEELER (1962)). Kruskal introduces new « time » and « radial » co-ordinates, v and u, which are related to the Schwarzschild t and r by

$$(7.10)\qquad \begin{cases} u = (r/2M^* - 1)^{\frac{1}{2}} \exp[r/4M^*] \cosh(t/4M^*) \\ v = (r/2M^* - 1)^{\frac{1}{2}} \exp[r/4M^*] \sinh(t/4M^*) \end{cases} \quad \text{for } r > 2M^*,$$

$$\begin{cases} u = (1 - r/2M^*)^{\frac{1}{2}} \exp[r/4M^*] \sinh(t/4M^*) \\ v = (1 - r/2M^*)^{\frac{1}{2}} \exp[r/4M^*] \cosh(t/4M^*) \end{cases} \quad \text{for } r < 2M^*.$$

In terms of Kruskal co-ordinates the Schwarzschild geometry (7.1) is described by

$$(7.11a)\qquad ds^2 = f^2(dv^2 - du^2) - r^2(d\theta^2 + \sin^2\theta\, d\varphi^2).$$

Here r is the Schwarzschild radial co-ordinate, which can be expressed in terms of $u^2 - v^2$ by

$$(7.11b)\qquad (r/2M^* - 1)\exp[r/2M^*] = u^2 - v^2;$$

and f^2 is defined in terms of r by

$$(7.11c)\qquad f^2 = (32M^{*3}/r)\exp[-r/2M^*].$$

In the right half of Fig. 7 the free-fall collapse of a star with initial radius $R_i = 10M^*$ is shown relative to the Kruskal co-ordinate system. Note how reasonably the world line of the star's surface behaves in this Kruskal space-time diagram. The co-ordinate pathologies at $r = 2M^*$ have been removed entirely.

Several features of the Kruskal diagram for free-fall collapse should be emphasized: 1) In the Kruskal u-v plane curves of constant Schwarzschild radius, r, are the hyperbolae $v^2 - u^2 = \text{const}$; while curves of constant Schwarzschild time, t, are the radial lines $v/u = \text{const}$. 2) The pathological « point » ($r = 2M^*$, $t = \infty$) of the Schwarzschild diagram becomes the null ($ds^2 = 0$) line $u = v$ in the Kruskal diagram. 3) Light rays travel along 45 degree lines—$du = \pm dv$—in the Kruskal diagram. In this sense the Kruskal diagram is a close analogue

of space-time diagrams of special relativity. 4) Although the Kruskal diagram is admirably suited to the description of the geometry of space-time near the surface of a collapsing star, it gives a somewhat pathological description of the region $r \gg M^*$ far from the star. In this far distant region, where space-time is very flat, one would like the u-v co-ordinate lines to form an inertial frame of reference (inertial in the sense of special relativity); but they do not. 5) Although it is possible for a man in a rocket ship to remain at a constant radius *outside* $r = 2M^*$ by pointing his rocket away from the star and firing his engines with an appropriate thrust, such a rocketeer cannot remain at a constant radius *inside* $r = 2M^*$. No matter how hard he fires his rockets, a rocketeer must always move along a timelike world line; but inside $r = 2M^*$ $(v > u)$ world lines of constant radius are spacelike. Hence, once a rocket ship follows the collapsing star in past $r = 2M^*$, it can never escape being pulled on in to $r = 0$. 6) This plight of the foolish rocketeer shows that, although the Schwarzschild geometry is static as seen by a certain family of observers (observers at fixed radius r) in the region $r > 2M^*$, there are no observers who see it as static in the region $r < 2M^*$.

Because of the key role played in the theory of collapse by the gravitational radius, $R_g = 2M^*$, of a star, it is of interest to examine the mean density of a collapsing star as it passes through its gravitational radius. Roughly speaking, the mean density at $R = R_g$ is

$$\bar{\varrho}^* \approx 3M^*/4\pi R_g^3 = 3/32\pi M^{*2}\,, \tag{7.12}$$

or, in conventional units,

$$\bar{\varrho} \approx 1.8 \cdot 10^{16} (M_\odot/M)^2 \text{ g/cm}^3\,. \tag{7.12'}$$

Note that, although this density at the gravitational radius is above nuclear densities for a one-solar-mass star, it is only 1 g/cm for a supermassive star of $M = 10^8 M_\odot$.

73.4. Nature of the singularity at $r = 0$. The region $r = 0$ of the Schwarzschild geometry, into which the surface of a collapsing star contracts, is called a « general-relativistic singularity ». That this singularity is not merely a co-ordinate pathology as was the region $r = 2M^*$ in the Schwarzschild picture can be verified by examining the plight of an experimental astrophysicist who stands on the surface of a freely falling star as it collapses to $R = 0$.

As the collapse proceeds toward $R = 0$ the various parts of the astrophysicist's body experience different gravitational forces. His feet, which are on the surface of the star, are attracted toward the star's center by an infinitely mounting gravitational force; while his head, which is farther away, is accelerated

downward by a somewhat smaller, though ever rising force. The difference between the two accelerations (« tidal force ») mounts higher and higher as the collapse proceeds, finally becoming infinite as R reaches zero. The astrophysicist's body, which cannot withstand such extreme forces, is stretched between head and foot to infinite length as R drops to zero.

But this is not all. Simultaneous with this head-to-foot stretching, the astrophysicist is pulled by the gravitational field into regions of space-time with ever-decreasing circumferential area, $4\pi r^2$. In order to accomplish this, tidal gravitational forces must compress the astrophysicist on all sides as they stretch him from head to foot. The circumferential compression is actually greater than the longitudinal stretching, so the astrophysicist, in the limit $R \to 0$, is crushed to zero volume and infinite length.

One can easily write down formulae to describe the stretching and compression of the astrophysicist after his body forces are overwhelmed by the gravitation forces. In this last stage of collapse each baryon in the astrophysicist's body falls freely toward $r = 0$ along a path which, in the Schwarzschild space-time diagram (left half of Fig. 7) has almost constant Schwarzschild time coordinate, t. The astrophysicist's feet touch the star's surface at one particular value of t—say $t = t_f$—while his head moves along the curve $t = t_h > t_f$. Consequently, the length of the astrophysicist's body increases according to the formula

$$(7.13a) \qquad l_{\text{Astroph}} = [-g_{tt}(R)]^{\frac{1}{2}}[t_h - t_f] = [2M^*/R]^{\frac{1}{2}}[t_h - t_f] \propto R^{-\frac{1}{2}} \propto (\tau_{\text{collapse}} - \tau)^{-\frac{1}{3}} .$$

Here $\tau = [-c^{-1}\int (g_{rr})^{\frac{1}{2}} \mathrm{d}r + \text{const}]$ is proper time as it would be measured by the astrophysicist if he were still alive. The gravitational field also constrains the baryons of the astrophysicist's body to fall along world lines of constant θ and φ during the final stages of collapse. Consequently, his cross-sectional area decreases according to the law

$$(7.13b) \qquad A_{\text{Astroph}} = [g_{\theta\theta}(R) g_{\varphi\varphi}(R)]^{\frac{1}{2}} \Delta\theta \Delta\varphi \propto R^2 \propto (\tau_{\text{collapse}} - \tau)^{\frac{2}{3}} .$$

By combining eq. (7.13a, b) we see that the volume of the astrophysicist's body decreases, during the last few moments of collaspe, according to the law

$$(7.13c) \qquad V_{\text{Astroph}} = l_{\text{Astroph}} A_{\text{Astroph}} \propto R^3 \propto (\tau_{\text{collapse}} - \tau).$$

This crushing of matter to infinite density by infinitely large tidal gravitational forces can occur not only at the surface of the collapsing star; it can also occur at any other point along the $r = 0$ singularity of the external gravitational field. Hence, any foolish rocketeer who ventures below the radius $r = 2M^*$ of the external gravitational field is doomed to destruction.

In Sect. 7·7 we shall discuss briefly the modifications which quantum-gravi-

tational effects may impose on this classical picture of the crushing of matter to infinite density by tidal gravitational forces.

7'3.5. Free-fall collapse as seen by an external observer. Now that we have examined relativistic collapse as seen by an experimental astrophysicist on the surface of a collapsing star, let us next analyse it from the point of view of an astronomer who observes the collapse from a great distance. Suppose that the astrophysicist on the star sends a series of uniformly spaced signals to the astronomer to inform him of the progress of the collapse. These signals propagate along lightlike 45 degree lines in the Kruskal u-v space-time diagram of Fig. 8. The signals originate on the world line of the stellar surface and they are received by the distant astronomer when they intersect his hyperbolic world line, $r = \text{const} \gg M^*$. As the star collapses closer and closer to its gravitational radius, $R = 2M^*$, the signals, which are sent at regularly spaced intervals according to the astrophysicist's clock, are received by the astronomer at more and more widely spaced intervals. The astronomer does not receive a signal emitted just before the gravitational radius, $R = 2M^*$, is reached until after an infinite amount of time has elapsed; and he never receives signals emitted after the gravitational radius has been passed. Those signals, like the astrophysicist who sends them, get caught and destroyed in the singularity at $r = 0$.

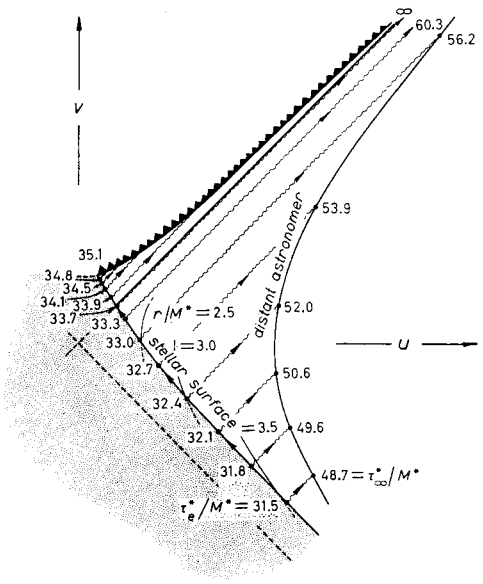

Fig. 8. – Kruskal diagram of the communication between a collapsing star of initial radius $R_i = 10\,M^*$ and a distant astronomer. As in Fig. 7, the interior of the star is stippled, but the exterior, Schwarzschild region is not. The wavy 45 degree lines represent the paths of radial light rays sent by an astrophysicist on the star's surface to the distant astronomer. The world lines of the stellar surface and of the astronomer are parametrized by the proper times at which the light rays are emitted and received. Light rays emitted after the star collapses through $R = 2\,M^*$ get caught in the singularity at $r = 0$.

Hence, to the distant astronomer, the collapsing star appears to slow down as it approaches its gravitational radius, light from the star becomes more and more red-shifted, and clocks on the star appear to run more and more slowly. It takes an infinite time for the star to reach its gravitational radius; and, as seen by the distant astronomer, the star never gets beyond there.

From the Kruskal diagram and eqs. (3.52) and (7.10), one can calculate the red-shift of radially travelling photons received from the center of the star's disk by the distant astronomer during the very late stages of collapse. One finds that the ratio of wavelength received to wavelength emitted is

$$\lambda_\infty/\lambda_e = \text{const} \times \exp[\tau^*_\infty/4M^*] , \tag{7.14}$$

where τ^*_∞ is proper time as measured by the very distant astronomer. Notice how short the e-folding time is

$$\tau_{e\text{-folding}} = 4GM/c^3 = 1.968 \cdot 10^{-5}(M/M_\odot)\ \text{s} . \tag{7.15}$$

Formulae (7.14) and (7.15) are valid not only for a freely collapsing star, but also for a collapsing star of large internal pressure; and they are valid not only for radially travelling photons emitted from the surface of the star, but also—with a different multiplication constant—for neutrinos emitted from the star's center (*).

Neutrinos from the star's center all travel radially outward along paths which are not bent by the gravitational field. Consequently, the neutrino luminosity during the late stages of collapse decays according to the law

$$L^{(\nu)} = \text{const} \times \exp[-\tau^*_\infty/2M^*] . \tag{7.16}$$

One factor of $\exp[\tau^*_\infty/4M^*]$ comes from the red-shift of each neutrino, and the other comes from the increasing time interval between arrival of neutrinos. This formula was first derived by ZEL'DOVICH and PODURETS (1964).

The luminosity decay of light from the surface of the collapsing star is not so easily calculated. In addition to the red-shift and the increase in time between photons, which entered into eq. (7.16), one must consider :1) the bending of nonradial light rays in the star's gravitational field; 2) the aberration of light rays not emitted precisely radially; 3) the inability of a photon to escape from the star's gravitational field to infinity unless it is emitted from the star's surface within an angle

$$\theta_{\max} \propto (R/2M^* - 1) \tag{7.17}$$

of the vertical, as seen in the proper reference frame of a man standing on the star's surface; and 4) the fact that a photon emitted in a nonradial direction requires longer to reach the astronomer than one emitted radially. Effects 1)-3) tend to increase the rate of luminosity decay, while effect 4) tends to decrease

(*) For a more detailed discussion of most of the material in the remainder of this Section see the review by ZEL'DOVICH and NOVIKOV (1964).

the decay rate. PODURETS (1964*b*), who has examined all these effects, finds that 4) outweighs 1)–3) and thereby results in a decay of light from the star's surface of

$$L^{(\mathrm{ph})} = \mathrm{const} \times \exp\left[-\frac{4}{3\sqrt{3}}\frac{\tau^*_\infty}{2M^*}\right], \tag{7.18}$$

which is more gentle than the decay (7.16) of neutrinos from the star's center.

In any realistic collapse situation the decaying photon luminosity from the collapsing star would probably be masked by light from the lagging or exploding stellar atmosphere. However, predictions such as the above could be tested quite easily by a physicist in a space-ship near a collapsing star many thousands —or millions or billions— of years after the collapse was initiated. By this time the star would be a very black sink for photons and matter, observable only by virtue of its gravitational field. The physicist, having discovered such an invisible sink, could determine whether it was a collapsing star or a cold, dead neutron star by dropping a radio transmitter *radially* into the gravitational field. If the transmitter stopped functioning abruptly at a frequency red-shift of $\sim 10\,\%$, the physicist would know it had hit the surface of a neutron star. On the other hand, if the received intensity died out and was red-shifted exponentially with time, the object would be a collapsing star. During the late stages of fall the red-shift would be governed by eq. (7.14), while the intensity decay would obey

$$L^{(\mathrm{radio})} = \mathrm{const} \times \exp[-\tau^*_\infty/M^*], \tag{7.19}$$

(cf. ZEL'DOVICH and NOVIKOV (1964), eq. (15.11)). This intensity decay is steeper than $L^{(\nu)}$ of eq. (7.16) by virtue of the effects of 1) and 2) (cf. preceding Section) upon photons emitted very nearly, but not quite, radially. Such photon are received by the detection antenna because of its finite size.

73.6. Interior of a freely collapsing star. Thus far we have concentrated all of our attention on the surfaces of collapsing stars and on their external gravitational fields. We now turn to an examination of the interior regions. Rather than calculate from scratch the time evolution of the interior, we shall limit ourselves to a description of the results of such calculations for a particularly simple case: that of a freely collapsing star of initially uniform density. The collapse of such a configuration was originally analysed by OPPENHEIMER and SNYDER (1939), but the description presented below is due primarily to BECKEDORFF and MISNER (1962) and to BECKEDORFF (1962) (*). As the de-

(*) For descriptions of this homogeneous interior solution from different points of view, and of other *inhomogeneous* interiors, see TOLMAN (1934*b*), DATT (1938), KLEIN (1961), ZEL'DOVICH (1962, 1963*a*), HOYLE, FOWLER, BURBIDGE and BURBIDGE (1964), MCVITTIE (1964), CALLAN (1964), and HTWW, pp. 125-134.

scription which follows requires a prior familiarity with Friedmann's closed cosmological model, we shall begin with a brief review of it. For further details see, *e.g.* TOLMAN (1934*a*) parts III and IV, especially pp. 426-7; also LANDAU and LIFSCHITZ (1962), pp. 375-384.

The Friedmann universe has the space geometry of a 3-sphere. (A 3-sphere is the analogue in one higher dimension of the *surface* of an ordinary sphere.) In terms of hyperspherical co-ordinates (χ, θ, φ) and a time coordinate η, the Friedmann geometry is described by

$$ds^2 = a^2(\eta)[d\eta^2 - d\chi^2 - \sin^2\chi(d\theta^2 + \sin^2\theta\, d\varphi^2)] . \tag{7.20}$$

Einstein's field equations demand that the radius, a, of the Friedmann universe be the following function of time:

$$a = (a_0/2)(1 + \cos\eta) . \tag{7.21}$$

The density of mass-energy in the Friedmann universe is uniform and is related to the time-dependent radius by

$$\varrho^* = 3/(8\pi a^2) . \tag{7.22}$$

The material particles in the Friedmann universe always remain fixed with respect to the hyperspherical co-ordinates (χ, θ, φ), and the pressure always remains zero. Only the radius and density of the universe vary with time. Notice from eqs. (7.21) and (7.22) that the universe begins ($\eta = -\pi$) in a singular state of zero radius, zero volume, and infinite density. As co-ordinate time, η, increases from $-\pi$ to 0, the universe expands to a maximum radius, $a = a_0$; and as η increases on past 0 to $+\pi$, it recontracts to a singular state of infinite density. Proper time as measured by a clock attached to the stationary matter is related to co-ordinate time by

$$\tau^* = \int a(\eta)\, d\eta = (a_0/2)(\eta + \sin\eta) . \tag{7.23}$$

Consequently, the total proper-time lapse from the creation of the universe to its destruction is $\tau^*(\pi) - \tau^*(-\pi) = \pi a_0$. The time evolution of the Friedmann universe could be illustrated by a series of embedding diagrams of the hypersurfaces of constant co-ordinate time, η. If one rotational degree of freedom —φ for example—were suppressed from the embedding diagrams, they would be simply a succession of ordinary spherical surfaces, which begin with radius $a = 0$, expand to $a = a_0$, and then contract back to $a = 0$.

To see the intimate relationship between a freely collapsing star of initially uniform density and the Friedmann universe, imagine the following surgical

operation: 1) Take a Friedmann universe of radius $a = a_0$ at its moment of maximum expansion, $\eta = 0$; and slice off and discard the region $\chi_0 < \chi \leqslant \pi$, where χ_0 is some angle less than $\pi/2$. 2) Take a Schwarzschild geometry of mass $M^* = (a_0/2)\sin^3\chi_0$ at the moment $t = 0$; and slice off and discard the region $r < R_i = a_0 \sin\chi_0$. 3) Glue the retained pieces of Friedmann and Schwarzschild geometry together smoothly along their cut surfaces. The resultant object will be a momentarily static star of uniform density

$$\varrho_{0]}^* = 3/(8\pi a_0^2)\,, \tag{7.24a}$$

of mass

$$M^* = (a_0/2)\sin^3\chi_0\,, \tag{7.24b}$$

and of radius

$$R_i = a_0 \sin\chi_0\,. \tag{7.24c}$$

An embedding diagram for this momentarily static, initial configuration is shown in Fig. 9 (curve A-A'-A'' of history A-B-C-D, rotated about its vertical axis). The spherical cup, A-A', of this embedding diagram is the interior of the star and comes from the truncated Friedmann universe. The parabolic funnel, A'-A'', which is capped by the spherical cup, is the external gravitational field and comes from the truncated Schwarzschild geometry.

Suppose that our patched-together star is released from its momentarily static state at $\eta = 0$ and allowed to collapse. How will its geometry and density distribution evolve with time? According to the calculations of OPPENHEIMER and SNYDER *the interior, truncated Friedmann universe and the exterior, truncated Schwarzschild geometry evolve just as though they had never been cut up and patched together.* In the interior region, the geometry as a function of η is described by eqs. (7.20) and (7.21), and the density remains uniform, increasing with time in accordance with eq. (7.22). The surface of the star, $\chi = \chi_0$, at which the join to the exterior Schwarzschild geometry is made, moves through the Schwarzschild space-time along the curve (7.5), which we have already discussed in great detail. Note that the time co-ordinate, η, which is used to describe the Friedmann interior (eqs. (7.20) and (7.21)) is identical to the parameter, η, used in describing the motion of the star's surface in the Schwarzschild geometry (eq. (7.5)).

In Fig. 9 we exhibit a space-time diagram for a freely collapsing star of $R_i/M^* = 2/\sin^2\chi_0 = 3$. This space-time diagram makes use of two co-ordinate patches: a Friedmann patch for the interior region, and a Kruskal patch for the exterior region. A photon, α, is emitted from the surface of the star and another, β, is emitted from the center just before collapse begins; and they both travel radially outward to $r = \infty$. A third photon, γ, is emitted radially from

the center of the star at the last possible instant before it would be doomed to be caught in the singularity. Photon γ travels radially outward through the star and crosses its collapsing surface at the moment when $R = 2M^*$. γ then remains at $r = 2M^*$ forever, since it cannot move quite rapidly enough to escape

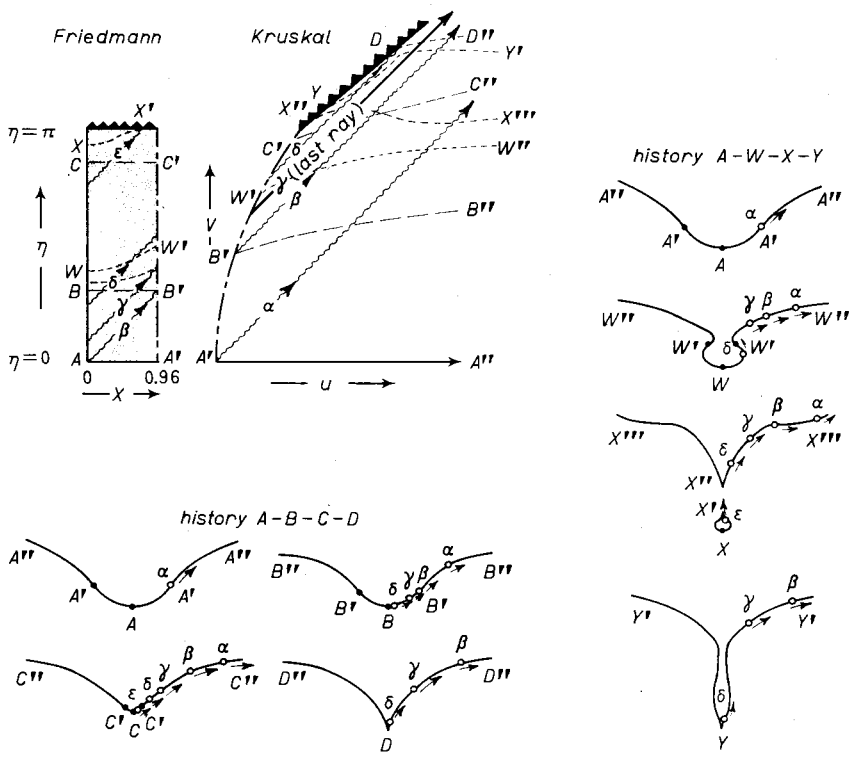

Fig. 9. – Space-time diagram and embedding diagrams for a freely collapsing star of uniform density with initial radius $R_i = 3M^*$. The space-time diagram consists of two co-ordinate patches: a Friedmann patch to cover the interior of the star and a Kruskal patch to cover the exterior. The join between the Friedmann and Kruskal patches, as regulated by eqs. (7.5) and (7.10), is indicated at several points by the letters A', B', W' and C'. The paths of several light rays, which are emitted from the center of surface of the star as it collapses, are shown as wavy 45 degree lines labeled with Greek letters. The $r = 0$ singularity into which the star collapses is indicated by saw teeth. Embedding diagrams are shown corresponding to 2 different ways of viewing the star's collapse—history A-B-C-D and history A-W-X-Y. These embedding diagrams are skeletonized in that they must be rotated about their vertical axes in order to become 2-dimensional surfaces analogous to Fig. 1. The several photons emitted from the center or surface of the star are indicated in the embedding diagrams by small circles. Notice that the hypersurfaces of which embedding diagrams are given intersect the singularity only tangentially. We do not consider *here* hypersurfaces which intersect the singularity at a finite angle in the u-v plane because such spacelike hypersurfaces cannot be embedded in a Euclidean space. Instead, a Minkowskian space (indefinite metric) must be used. For a discussion of embedding diagrams in Minkowskian spaces see THORNE (1965*a*).

from the star's gravitational field, nor quite slowly enough to be pulled into the singularity. A fourth photon, δ, and a fifth, ε, are emitted from the center of the star after the moment of no escape. Photon δ emerges from the star before being crushed, but it gets pulled into the singularity shortly thereafter. Photon ε, on the other hand, cannot even reach the star's surface before being crushed.

73.7. Embedding diagrams for free-fall collapse. Thus far we have described the geometry of space-time around and inside a collapsing star primarily in co-ordinate-dependent terms. Let us now use the technique of embedding diagrams to picture that geometry in a co-ordinate-independent manner.

We will need a sequence of embedding diagrams, each corresponding to the geometry of a spacelike hypersurface to the future of the preceding one, in order to describe the time development of the collapse geometry. But how are the hypersurfaces to be chosen? In Newtonian theory or special relativity, and also in the case of a general-relativistic equilibrium configuration (Sect. **3**5.1) one chooses hypersurfaces of constant time. But in dynamical regions of a curved space-time no naturally perferred time co-ordinate exists. This situation forces one to make a totally *arbitrary* choice of hypersurfaces for use in visualizing the time development of geometry, and to keep in mind how very arbitrary that choice was.

In Fig. 9 we use two very different choices of hypersurfaces to depict the time development of the geometry of a particular freely collpasing star. In both of these representative histories the initial configuration, A-A'-A'', is the one which we constructed by patching together momentarily static Friedmann and Schwarzschild geometries. History A-B-C-D depicts the time development of this initial 3-geometry as sampled by a succession of hypersurfaces which have constant Friedmann time, η, in the interior region. As depicted in this history, the interior region remains always a spherical cup of half angle χ_0, but it contracts from radius $R = a_0 \sin\chi_0$ to $R = 0$ as time increases. The matter in the star is all crushed to infinite density simultaneously when R reaches zero, and the external Schwarzschild « funnel » develops a cusplike singularity at that point. As time increases further, this cusp pulls the region $r < 2M^*$ of the funnel into $r = 0$ at such a fast rate that the outward-traveling photon δ is gobbled up and crushed.

The collapse geometry as sampled by hypersurfaces A-W-X-Y looks quite different from that revealed by A-B-C-D. As time passes, a neck develops in the geometry just outside the surface of the star. This neck becomes tighter and tighter and then pinches off, leaving the star completely isolated from the rest of the universe, and leaving a deadly cusplike singularity in the exterior geometry where the star used to be. The isolated star, in its own little closed universe, continues to contract until it is crushed to infinite density; while the

external geometry begins to develop another neck, and the cusp quickly gobbles up photon δ.

The extreme difference between histories *A-B-C-D* and *A-W-X-Y* serves as a warning that only a small part of the dynamics of collapse can be captured by embedding diagrams or by an examination of representative 3-geometries. The dynamics is four dimensional; but embedding diagrams only sample two- or at best three-dimensional projections of it.

7·4. *Spherical collapse with internal pressure forces.* – So far as the external gravitational field is concerned, the only difference between a freely collapsing star and a collapsing, spherically-symmetric star with internal pressure is this, that the surfaces of the two stars move along different world lines in the exterior Schwarzschild geometry. Because the exterior geometry is the same in both cases, *the qualitative aspects of free-fall collapse as described in Sects.* **7**·3.1 *through* **7**·3.5 (and also the quantitative equations (7.1), (7.6), and (7.10)–(7.19)) *can be carried over directly to the case of nonnegligible internal pressure.* For example, the vast difference between what is seen and experienced by a man on the surface of the collapsing star and what is seen by a distant observer is preserved.

An important and fascinating question to ask is this: Can large internal pressures in any way prevent a collapsing star from being crushed to infinite density by infinite tidal gravitational forces? From the Kruskal diagram of Fig. 8 it is evident that, once a star has passed inside its gravitational radius ($R < 2M^*$), no internal pressures, regardless of how large they may be, can prevent the star's surface from being crushed in a singularity. The surface must move along a timelike world line, and all such world lines inside $r = 2M^*$ hit $r = 0$. BARDEEN (private communication) has shown that, for spherical collapse, inside the gravitational radius pressure forces are not only powerless to prevent *the star's surface* from being crushed; they also cannot prevent *any part of the interior* from being crushed. The *entire* star is doomed once it has passed the gravitational radius.

The interior dynamics of spherically collapsing stars with pressure are not so well understood as the exterior dynamics. However, major advances in our understanding of the interior dynamics are now being made by means of numerical computations and analytic analyses (for references see Sect. **7**·2); and in these computations and analyses no surprising new features have been encountered which did not occur in the simple, uniform-density, free-fall collapse of Sect. **7**·3.6 and **7**·3.7.

7·5. *Collapse in totally realistic situations.* Until recently it was often argued (see, *e.g.*, LIFSCHITZ and KHALATNIKOV (1963)) that the general-relativistic singularity at $r = 0$ was a feature peculiar to spherically symmetric collapse, so that small deviations from spherical symmetry could prevent a singularity

from arising and could thus save a collapsing star from being crushed to infinite density. Recent analyses have revealed, however, that those arguments were incorrect: General-relativistic singularities are an essential and (almost) unavoidable aspect of gravitational collapse once the collapse has proceeded past the gravitational radius, $R = 2M^*$, or past the analogue of $R = 2M^*$ for non-spherical bodies. Let us review the analyses which lead to this conclusion, and make the conclusion more precise.

7.5.1. Trapped surfaces and the evolution of singularities. In spherically-symmetric collapse the external, Schwarzschild gravitational field is divided into two regions of very different character by the « event horizon » $r = 2M^*$. The region inside $r = 2M^*$ can be distinguished from the exterior region by either of two properties. The first, a *global property*, is this, that after the surface of a collapsing star has passed into the region $r < 2M^*$, the star's surface cannot escape being crushed in a singularity of infinite tidal gravitational forces. The second distinguishing property of $r < 2M^*$ is a *local* (or *quasi-local*) *property*: A bundle of radial light rays inside $r = 2M^*$ is convergent (the light rays move closer together as they propagate) whether it is an « outgoing » bundle or an « ingoing » bundle (cf. Fig. 8). Is the global property of the evolution of a singularity related in any intimate way to the local property of convergent outgoing and ingoing light rays? By posing this question and answering it affirmatively, PENROSE (1965) has made one of the greatest contributions in the history of general relativity.

PENROSE begins by generalizing the property of convergent outgoing and ingoing light rays to asymmetric regions of space-time. His generalization is motivated by a close examination of the 2-dimensional, spherical surfaces

$$(7.25) \qquad (r = \text{const} < 2M^*,\ t = \text{const}) \equiv (u = \text{const},\ v = \text{const} > u)$$

in the Schwarzschild geometry. When related to these 2-surfaces the property of convergent light rays states: *Light rays emitted from one of these 2-surfaces in the perpendicular, outward direction converge toward each other as they propagate; and inward light rays perpendicular to the 2-surface also converge.* PENROSE calls any closed 2-surface, spherically symmetric or not, which has this property a *trapped surface*; and he suggests that asymmetric regions of space-time which contain trapped surfaces are analogous to the region $r < 2M^*$ of the Schwarzschild geometry.

The analogue between regions of space-time containing trapped surfaces and the Schwarzschild region $r < 2M^*$ is made explicit by the following theorem, which is Penrose's most important result (we state the theorem in more physical, but less precise language than that of Penrose): *Consider a star undergoing completely realistic gravitational collapse* (*i.e.*, asymmetric collapse with rotation,

radiation, magnetic fields, shock waves, etc.) *in a universe which has the following properties*:

1) *The universe is open*; *i.e.*, on some initial spacelike hypersurface it has infinite area (*).

2) *Along every timelike world line in the universe the future direction is uniquely distinguished from the past.*

3) *At each point of spacetime the density of mass-energy as measured by an arbitrary observer in his own proper reference frame is nonnegative.*

4) *General relativity is the correct theory of gravitation.*

If a trapped surface evolves during stellar collapse in such a universe, then either or both of the following must occur subsequently:

a) *A general relativistic singularity evolves.* This singularity need not be characterized by an infinite density of mass-energy, but it must be a region beyond which either photons or matter—and probably both—cannot continue to exist (**)

or

b) another universe suddenly attaches itself to the star's universe. (Equivalently, but in more mathematical terms, the star's universe does not possess an initial Cauchy hypersurface) (***).

This theorem establishing the intimate connection between trapped surfaces and singularities is extremely powerful. Only two modifications would be needed to enable us with confidence to infer that singularities *necessarily* follow the evolution of a trapped surface in our own universe: the elimination of condition 1) and the elimination of possibility *b*) as an alternative to *a*). PENROSE (private communication) believes that it may, indeed, be possible to eliminate 1) by a reformulation of the proof of the theorem; but he is not optimistic about eliminating *b*) as an alternative to *a*).

(*) This assumption was not stated explicitly in Penrose's (1965) paper, but he points out in a private communication that it is necessary to his proof.

(**) For examples of particularly strange types of singularities see SHEPLEY (1964; 1965*a*, *b*), as well as the description by TAUB and MISNER (1966) of the join between the Taub universe and the NUT universe. For discussions of the ways in which magnetic fields in collapsing bodies affect the structure of the singularities, see KHALATNIKOV (1965) and THORNE (1964).

(***) For examples in which *both b*) and *a*) follow the evolution of a trapped surface see the extension by GRAVES and BRILL (1960) of the Reisner-Nordstrom solution, and the extension by BOYER and LINDQUIST (1966) and by CARTER (1966) of the Kerr solution.

7·5.2. Small deviations from spherical symmetry. According to the analysis of Penrose, the evolution of a trapped surface during gravitational collapse is a key indicator that something strange will subsequently happen to the geometry of spacetime—that either a singularity will halt the collapse, or that another universe will attach itself to ours, or both. Hence, at this point in the discussion we should ask whether trapped surfaces are a typical feature of stellar collapse, or whether they are peculiar to the case of spherical symmetry.

That trapped surfaces are somewhat typical has been shown recently by DOROSHKEVICH, ZEL'DOVICH, and NOVIKOV (1965) by means of an analysis of small perturbations of a collapsing star from spherical symmetry. Their argument, in rough outline, is as follows: In the idealized case of spherical symmetry a collapsing star feels no special or peculiar forces as it passes through its gravitational radius $R = 2M^*$. Consequently, there should be no peculiar forces available at $R = 2M^*$ to magnify enormously small initial deviations from spherical symmetry; the deviations, if sufficiently small initially, will remain small until after $R = 2M^*$ is passed. But small perturbations in the neighborhood of $R = 2M^*$ cannot prevent the evolution of a trapped surface (for proof see DOROSHKEVICH *et al.*). Hence, *a collapsing star, which is initially nearly spherical and has only a little angular momentum, generates trapped surfaces during the late stages of collapse.*

DORESHKEVICH *et al.* not only prove that trapped surfaces evolve during slightly aspherical collapse; they also discuss the evolution of nonspherical and rotational perturbations during the collapse. Most interesting of all is their discovery that, as the star approaches its gravitational radius, all multipole perturbations in the gravitational field seen by an *external* observer die away to zero; whereas rotational perturbations remain finite.

7·6. *Gravitational collapse to a singularity in other contexts.* – According to general-relativity theory, gravitational collapse to a singularity is not a phenomenon confined to massive and supermassive stars. Rather, it is a phenomenon which easily can occur in any large aggregate of matter—in galactic nuclei, in quasi-stellar sources, in the universe as a whole, etc. For example, collapse to a singularity—or the time-reversed explosion from one— is a feature common to almost all relativistic cosmological models (see, *e.g.*, SHEPLEY (1964, 1965*a*, *b*), HAWKING and ELLIS (1965), HAWKING (1965, 1966), GEROCH (1966)). That there is an intimate relationship between the collapse of a cosmological model and the collapse of a star is hinted at by the analysis of Sect. 7·3.6. (See also HTWW, pp. 137-141.)

Gravitational collapse to a singularity can occur, in principle, in small agglomerations of matter as well as in large ones. However, when the mass of a configuration is less than $M_{\text{LOV}} \sim 1.5 M_\odot$, the collapse must be initiated not by classical processes, but by the quantum-mechanical tunneling of a potential

barrier. For a discussion of this phenomenon and of the fantastically slow rates associated with it, see HTWW.

Collapse to a singularity can occur even in the absence of matter if space-time is sufficiently curved intrinsically, or if it contains enough gravitational radiation. For a discussion see WHEELER (1964*b*).

7·7. *The issue of the final state* (*). – The crushing of matter to infinite density by infinite tidal gravitational forces is a phenomenon with which one cannot live comfortably. From a purely philosophical standpoint it is difficult to believe that physical singularities are a fundamental and unavoidable feature of our universe. On the contrary, when faced with a theory which predicts the evolution of a singular state, one is inclined to discard or modify that theory rather than accept the suggestion that the singularity actually occurs in nature. Such was the case with Rutherford's theory of the atom, which was needed to explain α-scattering experiments, but which predicted the evolution of a physical singularity—the spiraling of orbital electrons into the atomic nucleus as a result of radiation reaction. It was to avoid this singularity and thereby explain atomic spectra that BOHR suggested quantizing the energy states available to orbital electrons. Just as quantization of classical mechanics prevented physical singularities from evolving in Rutherford's atom, so quantization of general-relativity theory may prevent physical singularities from evolving in gravitational collapse.

That quantum-gravitational effects must play an important role in the very late stages of collapse is evident on two grounds: 1) When densities in excess of 10^{49} g/cm^3 are reached, the radii of curvature of space-time become smaller than the Compton wave lengths of elementary particles (cf. Sect. 2·1); and, consequently, the intrinsic properties of elementary particles are modified by tidal gravitational effects. 2) The gravitational field, like all fields, must undergo quantum fluctuations; and the characteristic size of gravitational fluctuations is the Planck length

$$L^* = (\hbar G/c^3)^{\frac{1}{2}} = 1.616 \cdot 10^{-33} \text{ cm} \tag{7.26}$$

(see WHEELER (1962) pp. 76-77). Surely such fluctuations in the geometry of space-time will have a profound effect upon the dynamics of collapse when the collapse has proceeded so far that the radii of curvature of space-time are of the order of L^*! Note that this stage of collapse occurs at a density of

$$\begin{cases} \varrho^{*-\frac{1}{2}} \sim (\text{radii of curvature}) \sim L^* , \\ \varrho \quad \sim 10^{93} \text{ g/cm}^3 . \end{cases} \tag{7.27}$$

(*) The ideas in the first three and the last two paragraphs of this section are due primarily to J. A. WHEELER; see WHEELER (1964*b*) and HTWW, pp. 138-147.

In what manner will quantum gravitational effects modify the classical picture of collapse to a singularity? This question cannot be answered with confidence until the foundations of the quantum theory of gravitation are well understood. However, it seems probable, in analogy with familiar quantum-mechanical scattering problems, that *the quantum theory of catastrophic collapse will be characterized, not by a singular final state as is the classical theory, but by a probability amplitude for this, that, or another physically reasonable outcome.*

Already in the development of the quantum theory of gravitation, highly idealized calculations by DEWITT (1966) and his students indicate that this probability-amplitude picture of collapse is reasonable: DEWITT *et. al.* have partially solved, in two different ways, the problem of quantizing the gravitational field of the Friedmann universe, and both of their partial solutions suggest that the probability amplitude for the contracting universe to « bounce » in this, that, or another manner, rather than be crushed to infinite density, is very high—perhaps unity. However, because the quantum effects which cause the bounce do not become important until a density of the order of 10^{93} g/cm^3 is reached, little or no information could be transmitted from the collapsing phase of the universe, through the quantum bounce, and into the re-expanding phase.

From these results of DEWITT *et. al.* it seems reasonable—though far from necessary!—to expect that the transformation of catastrophic collapse into catastrophic explosion may be a general feature of the quantum theory of gravitation. If so, does this mean that an external observer, who watches a star collapse toward its gravitational radius and then waits sufficiently long, will see the star suddenly explode back out? No! There is a large region of space-time separating the event horizon, $r = 2M^*$, of the Schwarzschild geometry from the quantum region

$$r \lesssim r_{\text{quantum}} \sim 10^{-20}(M/M_\odot)^{\frac{1}{3}} \text{ cm} . \tag{7.28}$$

(Note: $r \lesssim r_{\text{quantum}}$ is the region where the radii of curvature of space-time, $(r^3/M^*)^{\frac{1}{2}}$, are of the order of or small compared to the Planck length, $L^* = 1.616 \cdot 10^{-33}$ cm.) In the region $r_{\text{quantum}} \ll r < 2M^*$ stellar dynamics are governed by the familiar laws of classical general relativity. However (cf. Fig. 8), a star cannot explode outward from the quantum region, through this classical region of trapped surfaces, and into the outside universe, except by reversing its direction of motion in time; and a time-reversed, exploding star would appear to an external observer to be a collapsing antistar (whatever that is). Consequently, it is difficult to understand how a quantum-mechanical reversal of collapse in the region $r \lesssim r_{\text{quantum}}$ could cause a star to explode (in the conventional sense of the word « explode ») back out, through the event horizon $r = 2M^*$ which swallowed it in the collapsing phase. More reasonable is the suggestino

that quantum effects cause a collapsing star to bounce and then re-explode, not back to where it came from, but into another region of the universe (multiply-connected space-time geometry; difficulties with causality), or into some other universe (*). However, the peculiar and ill-understood nature of quantized space-time may well invalidate any description such as this of the outcome of collapse.

The above considerations are indicative of the deep problems of principle posed by the phenomenon of gravitational collapse. Some of the other issues raised by this confrontation between classical gravitation theory and the fundamental principles of quantum theory are discussed by Wheeler (1964*b*, 1965) and by HTWW (especially pp. 138-147). These quantum-gravitational issues include: the breakdown of the classical concepts of space and time; the question of whether the law of baryon conservation has any meaning within the context of collapse; the phenomenon of dynamical changes in the topology of space-time; and the relationship between elementary-particle physics and the quantum theory of gravitation.

In the words of Wheeler (1964*b*), p. 501. « There have been few occasions in the history of physics when one could surmise more surely than he does now, in the case of gravitational collapse, that he confronts a new phenomenon, with a mysterious nature of its own, waiting to be unraveled. »

(*) For further discussions along this line see NOVIKOV (1964).

BIBLIOGRAPHY

AKELEY, E. S., 1931, *Phil. Mag.*, **11**, 330.

AMBARTSUMYAN, V. A. and G. S. SAAKYAN, 1960, *Astr. Žur.*, **37**, 193; English translation in *Soviet Astronomy, A. J.*, **4**, 187.

AMBARTSUMYAN, V. A. and G. S. SAAKYAN, 1961, *Astr. Žur.*, **38**, 785; English translation in *Soviet Astronomy, A. J.*, **5**, 601.

BAHCALL, J. N., 1964, *Ap. J.*, **139**, 318.

BAHCALL, J. N. and R. A. WOLF, 1965*a*, *Phys. Rev. Letters*, **14**, 343.

BAHCALL, J. N. and R. A. WOLF, 1965*b*, *Phys. Rev.*, **140**, B 1445.

BAHCALL, J. N. and R. A. WOLF, 1965*c*, *Phys. Rev.*, **140**, B 1452.

BARDEEN, J. M., 1964, paper presented at the *Second Texas Symposium on Relativistic Astrophysics*, Austin, Texas, December, 1964; proceedings to be published by University of Texas Press.

BARDEEN, J. M., 1965, unpublished *Ph. D. Thesis*, Caltech, available from University Microfilms, Inc. (Ann. Arbor, Michigan).

BARDEEN, J. M., K. S. THORNE and D. W. MELTZER, 1966, *Ap. J.*, **145**, 505.

BARKER, B. M., M. S. BHATIA and G. SZAMOSI, 1966, submitted for publication.

BECKEDORFF, D. L., 1962, *Terminal Configurations of Stellar Evolution*, unpublished *A. B. Senior Thesis*, Princeton University.

BECKEDORFF, D. L. and C. W. MISNER, 1962, unpublished.

BIRKHOFF, G. D., 1923, *Relativity and Modern Physics* (Cambridge, Mass.).

BONDI, H., 1964, *Proc. Roy. Soc. London*, A **282**, 303.

BONDI, H., 1965, chapters in *Lectures on General Relativity*, vol. 1 of proceedings of 1964 Brandeis Summer Institute in Theoretical Physics (Englewood Cliffs, N. J.).

BOYER, R. H., 1965*a*, *Proc. Camb. Phil. Soc.*, **61**, 527.

BOYER, R. H., 1965*b*, *Proc. Camb. Phil. Soc.*, **61**, 531.

BOYER, R. H. and R. W. LINDQUIST, 1966, *Journ. Math. Phys.*, in press.

BUCHDAHL, H. A., 1959, *Phys. Rev.*, **116**, 1027.

BURBIDGE, G. R., 1963, chapter in *Star Evolution, Proceedings S.I.F.* vol. XXVIII, p. 95.

BURBIDGE, G. R., E. M. BURBIDGE, and A. R. SANDAGE, 1963, *Rev. Mod. Phys.*, **35**, 947.

CALLAN, C. G., jr., 1964, unpublished *Ph. D. Thesis*, Princeton University, available from University Microfilms, Inc. (Ann Arbor, Michigan).

CALLEN, H. B., 1960, *Thermodynamics* (New York).

CAMERON, A. G. W., 1959, *Ap. J.*, **130**, 884.

CAMERON, A. G. W., 1965*a*, *Nature*, **205**, 787.

CAMERON, A. G. W., 1965*b*, *Nature*, **206**, 1342.

CARTER, B., 1966, *Phys. Rev.*, **141**, 1242.

CHANDRASEKHAR, S., 1935, *M. N.*, **95**, 207.

CHANDRASEKHAR, S., 1939, *Introduction to the Study of Stellar Structure* (Chicago).

CHANDRASEKHAR, S., 1961, *Hydrodynamic and Hydromagnetic Stability* (Oxford).

CHANDRASEKHAR, S., 1964*a*, *Ap. J.*, **138**, 185.

CHANDRASEKHAR, S., 1964*b*, *Phys. Rev. Letters*, **12**, 114, 437.

CHANDRASEKHAR, S., 1964*c*, *Ap. J.*, **140**, 417.

CHANDRASEKHAR, S., 1965*a*, *Phys. Rev. Letters*, **14**, 241.

CHANDRASEKHAR, S., 1965*b*, *Ap. J.*, **142**, 1488.

CHANDRASEKHAR, S., 1965*c*, *Ap. J.*, **142**, 1513.

CHANDRASEKHAR, S., 1965*d*, *Ap. J.*, **142**, 1519.

CHANDRASEKHAR, S. and N. R. LEBOVITZ, 1964, *Ap. J.*, **140**, 1517.

CHIU, H. Y., 1964, *Annals of Physics*, **26**, 364.

CHIU, H. Y. and E. E. SALPETER, 1964, *Phys. Rev. Letters.*, **12**, 412.

CLARK, G. L., 1947, *Proc. Cambridge Phil. Soc.*, **43**, 164.

CLARK, G. L., 1948, *Phil. Mag.*, **39**, 747.

CLARK, G. L., 1950, *Proc. Roy. Soc. London*, A **201**, 510.

COCKE, W. J., 1965, *Ann. Inst. Henri Poincaré*, **2**, 283.

COLGATE, S. A. and R. H. WHITE, 1964, *The Hydrodynamic Behavior of Supernova Explosions*, University of California Lawrence Radiation Laboratory Report UCRL-7777.

COLGATE, S. A. and R. H. WHITE, 1966, *Ap. J.*, **143**, 626.

COX, A. N., 1965, chapter 3 of *Stellar Structure*, L. H. ALLER and D. B. MCLAUGHLIN, ed., (Chicago).

CURTIS, A. R., 1950, *Proc. Roy. Soc. London*, A **200**, 248.

DARWIN, C., 1959, *Proc. Roy. Soc. London*, A **249**, 180.

DATT, B., 1938, *Zs. f. Phys.*, **108**, 314.

DEWITT, B., 1966, submitted for publication.

DICKE, R. H., 1964, *Experimental Relativity* (New York).

DICKE, R. H., P. J. E. PEEBLES, P. G. ROLL and D. T. WILKINSON, 1965, *Ap. J.*, **142**, 414.

DMITRIEV, N. A. and S. A. HOLIN, 1963, chapter in *Voprosi Kosmogonii*, **9** (Moscow).

DOROSHKEVICH, A. G., YA. B. ZEL'DOVICH and I. D. NOVIKOV, 1965, *Žurn. Èksp. Teor. Fiz.*, **49**, 170; English translation in *Soviet Physics-JETP*, **22**, 122 (1966).

DURNEY, B. and I. ROXBURGH, 1965, *Nature*, **208**, 1304.

EINSTEIN, A., 1956, *The Meaning of Relativity* (Princeton, N. J.).

ELLIS, D. G., 1965, *Phys. Rev.*, **139**, B 754.

FAIRBANK, H. W. and C. W. F. EVERITT, 1966, work in progress.

FINZI, A., 1965*a*, *Phys. Rev.*, **147**, B 472.

FINZI, A., 1965*b*: *Phys. Rev. Letters*, **15**, 599.

FINZI, A., 1966, this volume p. 302.

FIRMANI, C., 1965, unpublished *Ph. D. Thesis*, University of Rome.

FOWLER, W. A., 1964, *Rev. Mod. Phys.*, **36**, 545, 1104.

FOWLER, W. A., 1966, this volume p. 313.

FULLER, R. W. and J. A. WHEELER, 1962, *Phys. Rev.*, **128**, 919.

GEROCH, R., 1966, *Phys. Rev. Letters*, **17**, 445.

GINZBURG, V. L. and D. A. KIRZHNITS, 1964, *Žurn. Èksp. Teor. Fiz.*, **47**, 2006; English translation in *Soviet Physics-JETP*, **20**, 1346 (1965).

GINZBURG, V. L. and L. OZERNOY, 1964, *Žurn. Èksp. Teor. Fiz.*, **47**, 1030; English translation in *Soviet Physics-JETP*, **20**, 689 (1965).

GOERTZEL, G. and N. TRALLI, 1960, *Some Mathematical Methods of Physics* (New York).

GRATTON, L., 1964*a*, chapter in *Padova Symposium on Cosmology* (Florence).

GRATTON, L., 1964*b*, *Rend. Acc. Lincei*, **37**, 222.

GRATTON, L., 1964*c*, *Rend. Acc. Lincei*, **37**, 354.

GRATTON, L., 1964*d*, paper presented at the *Second Texas Symposium on Relativistic Astrophysics*, Austin, Texas, December 1964, proceedings to be published by University of Texas Press.

GRATTON, L., 1965, *Rend. Acc. Lincei*, **38**, 25.

GRATTON, L. and P. GIANNONE, 1965, *Mem. Soc. Astr. Ital.*, **36**, 445.

GRATTON, L. and G. SZAMOSI, 1964, *Nuovo Cimento*, **33**, 1056.

GRAVES, J. C. and D. R. BRILL, 1960, *Phys. Rev.*, **120**, 1507.

GREENSTEIN, J. L., 1960, *Stellar Atmospheres* (Chicago).

HAMADA, T. and E. E. SALPETER, 1961, *Ap. J.*, **134**, 683.

HÄMEEN-ANTTILA, K. A. and E. ANTTILA, 1966, *Annales Academiae Scientiarum Fennicae*, A. VI, 191.

HANSEN, C. J., 1966, *Nature*, **211**, 1069.

HARRISON, B. K., 1965, *Phys. Rev.*, **137**, B 1644.

HARRISON, B. K., K. S. THORNE, M. WAKANO and J. A. WHEELER, 1965, *Gravitation Theory and Gravitational Collapse* (Chicago). Cited in text as HTWW.

HARRISON, B. K., M. WAKANO and J. A. WHEELER, 1958, chapter in Onzième Conseil de Physique Solvay, *La structure et l'évolution de l'univers* (Brussels).

HARTLE, J. B., 1966, *Bull. Am. Phys. Soc.*, **11**, 340.

HARTLE, J. B. and D. H. SHARP, 1965, *Phys. Rev. Letters*, **15**, 909.

HARTLE, J. B. and D. H. SHARP, 1966, *Ap. J.*, in press.

HAWKING, S. W., 1965, *Phys. Rev. Letters*, **15**, 689.

HAWKING, S. W., 1966, *Phys. Rev. Letters*, **17**, 444.

HAWKING, S. W. and G. F. R. ELLIS, 1965, *Physics Letters*, **17**, 246.

HERNANDEZ, W. C. and C. W. MISNER, 1966, *Ap. J.*, **143**, 452.

HILL, H. and C. ZANONI, 1966, work in progress.

HOYLE, F., W. A. FOWLER, E. M. BURBIDGE and G. R. BURBIDGE, 1964, *Ap. J.*, **139**, 909.

HOYLE, F., J. V. NARLIKAR and J. A. WHEELER, 1964, *Nature*, **203**, 914.

IBEN, I., 1963, *Ap. J.*, **138**, 1090.

INMAN, C. I., 1965, *Ap. J.*, **141**, 187.

KERR, R. P., 1963, *Phys. Rev. Letters*, **11**, 522.

KERR, R. P., 1965, chapter in *Quasi-Stellar Source and Gravitational Collapse*, I. ROBINSEN, A. SCHILD and E. SCHUCKING, eds. (Chicago).

KHALATNIKOV, E. M., 1965, *Žur, Eksp. Teor. Fiz.*, **48**, 261; English translation in *Soviet Physics-JETP*, **21**, 172 (1965).

KIPPENHAHN, R., 1963, *Proc. S.I.F.* Course XXVIII p. 330.

KLEIN, O., 1961, in *Werner Heisenberg und die Physik unserer Zeit* (Braunschweig).

KRUSKAL, M. D., 1960, *Phys. Rev.*, **119**, 1743.

LANDAU, L. D. and E. M. LIFSCHITZ, 1962, *The Classical Theory of Fields* (Reading, Mass.), second edition.

LEBOVITZ, N. R., 1965*a*, *Ap. J.*, **142**, 229.

LEBOVITZ, N. R., 1965*b*, *Ap. J.*, **142**, 1257.

LEDOUX, P. and TH. WALRAVEN, 1958, *Handbuch der Physik*, **51**, 458, S. FLÜGGE, ed. (Berlin).

LIFSCHITZ, E. M. and I. M. KHALATNIKOV, 1963, *Usp. Fiz. Nauk*, **80**, 391; English translation in *Soviet Physics-Uspekhi*, **6**, 495 (1963).

LINDQUIST, R. W., 1966, *Annals of Physics*, **37**, 487.

MCVITTIE, G. C., 1964, *Ap. J.*, **140**, 401.

MATHEWS, J. and R. L. WALKER, 1964, *Mathematical Methods of Physics* (New York).

MAY, M. M. and R. H. WHITE, 1964, paper presented at *Second Texas Symposium on Relativistic Astrophysics*, Austin, Texas, December 1964; proceedings to be published by University of Texas Press.

MAY, M. M. and R. H. WHITE, 1966, *Phys. Rev.*, **141**, 1232.

MELTZER, D. W. and K. S. THORNE, 1966, *Ap. J.*, **145**, 514.

MESTEL, L., 1965, chapter 5 of *Stellar Structure*, L. H. ALLER and D. B. MCLAUGHLIN, ed. (Chicago).

MISNER, C. W., 1965, *Phys. Rev.*, **137**, B 1360.

MISNER, C. W. and D. H. SHARP, 1964*a*, *Phys. Rev.*, **136**, B 571.

MISNER, C. W. and D. H. SHARP, 1964*b*, paper presented at *Second Texas Symposium on Relativistic Astrophysics*, Austin, Texas, December 1964; proceedings to be published by University of Texas Press.

MISNER, C. W. and D. H. SHARP, 1965, *Physics Letters*, **15**, 279.

MISNER, C. W. and D. H. SHARP, 1966, paper in preparation.

MISNER, C. W. and H. S. ZAPOLSKY, 1964, *Phys. Rev. Letters*, **12**, 635.

MORSE, P. M. and H. FESHBACH, 1953, *Methods of Theoretical Physics*, 2 volumes (New York).

MORTON, D. C., 1964, *Ap. J.*, **140**, 460.

NOVIKOV, I. D., 1964, *Astr. Žur.*, **41**, 1075; English translation in *Soviet Astronomy-AJ*, **8**, 857.

OPPENHEIMER, J. R. and R. SERBER, 1938, *Phys. Rev.*, **54**, 530.

OPPENHEIMER, J. R. and H. SNYDER, 1939, *Phys. Rev.*, **56**, 455.

OPPENHEIMER, J. R. and G. VOLKOFF, 1939, *Phys. Rev.*, **55**, 374.

PACINI, F., 1965, *Mem. Soc. Astron. Ital.*, **36**, 323.

PAPAPETROU, A., 1953, *Ann. der Physik*, **12**, 309.

PAPAPETROU, A., 1966, *Ann. Inst. Henri Poincaré*, in press.

PENROSE, R., 1965, *Phys. Rev. Letters*, **14**, 57.

PODURETS, M. A., 1964*a*, *Astr. Žur.*, **41**, 28; English translation in *Soviet Astronomy-AJ*, **8**, 19.

PODURETS, M. A., 1964*b*, *Astr. Žur.*, **41**, 1090; English translation in *Soviet Astronomy-A.J.*, **8**, 868.

PODURETS, M. A., 1964*c*, *Doklady Acad. Nauk USSR*, **154**, 300; English translation in *Soviet Physics-Doklady*, **9**, 9 (1964).

POUND, R. V. and J. L. SNIDER, 1964, *Phys. Rev. Letters*, **13**, 539.

REEVES, H., 1965, chapter 2 of *Stellar Structure*, L. H. ALLER and D. B. MCLAUGHLIN, eds. (Chicago).

ROBINSON, I., A. SCHILD and E. SCHUCKING, 1965, *Quasistellar Sources and Gravitational Collapse* (Chicago).

ROSS, D. K. and L. I. SCHIFF, 1966, *Phys. Rev.*, **141**, 1215.

ROXBURGH, I. W., 1965, *Nature*, **207**, 363.

SAAKYAN, G. S., 1963, *Astr. Žur.*, **40**, 82; English translation in *Soviet Astronomy-A.J.*, **7**, 60 (1963).

SAAKYAN, G. S. and E. V. CHUBARYAN, 1963, *Soobshch. Byurakan. Obs.*, **34**, 99.

SAAKYAN, G. S. and YU. L. VARTANYAN, 1963*a*, *Soobshch. Byrakan Obs.*, **33**, 55.

SAAKYAN, G. S. and YU. L. VARTANYAN, 1963*b*, *Nuovo Cimento*, **30**, 82.

SAAKYAN, G. S. and YU. L. VARTANYAN, 1964, *Astr. Žur.*, **41**, 193; English translation in *Soviet Astronomy-A.J.*, **8**, 147 (1964).

SALPETER, E. E., 1960, *Ann. of Phys.*, **11**, 393.

SALPETER, E. E., 1961, *Ap. J.*, **134**, 669.

SCHATZMAN, E., 1956, *Astr. Žur.*, **33**, 800.

SCHATZMAN, E., 1958, *White Dwarfs* (New York).

SCHIFF, L. I., 1960, *Proc. Nat. Acad. Sci. USA*, **46**, 871.

SCHIFF, L. I., 1966, lectures in *Proceedings of the American Mathematical Society* 1955 *Summer Seminar on Relativity and Astrophysics*, to be published.

SCHWARZSCHILD, K., 1916, *Berl. Ber.*, p. 189.

SCHWARZSCHILD, M., 1958, *Structure and Evolution of the Stars* (Princeton, N. J.).

SCIAMA, D., 1966, this volume, p. 418.

SHAPIRO, I. I., 1964, *Phys. Rev. Letters*, **13**, 789.

SHAPIRO, I. I., 1966*a*, *Phys. Rev.*, **141**, 1219.

SHAPIRO, I. I., 1966*b*, *Phys. Rev.*, **145**, 1005.

SHEPLEY, L. C., 1964, paper presented at the *Second Texas Symposium on Relativistic Astrophysics*, Austin, Texas, December 1964; proceedings to be published by University of Texas Press.

SHEPLEY, L. C., 1965*a*, unpublished *Ph. D. Thesis*, Princeton University, available from University Microfilms, Inc. (Ann Arbor, Michigan).

SHEPLEY, L. C., 1965*b*, *Proc. Nat. Acad. Sci. U.S.A.*, **52**, 1403.

SKYRME, T. H. R., 1959, *Nuclear Physics*, **9**, 665.

SYNGE, J. L., 1960, *Relativity: The General Theory* (Amsterdam).

SZAMOSI, G., 1966, this volume p. 281.

TAUB, A. H., 1948, *Phys. Rev.*, **74**, 328.

TAUB, A. H. and C. W. MISNER, 1966, paper in preparation.

THORNE, K. S., 1964, paper presented at *Second Texas Symposium on Relativistic Astrophysics*, Austin, Texas, December 1964; proceedings to be published by University of Texas Press.

THORNE, K. S., 1965*a*, chapter 7 of *Quasi-Stellar Sources and Gravitational Collapse*, I. ROBINSON, A. SCHILD and E. SCHUCKING, eds. (Chicago).

THORNE, K. S., 1965*b*, unpublished *Ph. D. Thesis*, Princeton University, available from University Microfilms, Inc. (Ann Arbor, Michigan).
THORNE, K. S., 1965*c*, *Science*, **150**, 1671.
THORNE, K. S., 1966, *Ap. J.*, **144**, 201.
THORNE, K. S. and J. A. WHEELER, 1965, *Bull. Am. Phys. Soc.*, **10**, 15.
TOLMAN, R. C., 1934*a*, *Relativity, Thermodynamics and Cosmology* (Oxford).
TOLMAN, R. C., 1934*b*, *Proc. Nat. Acad. Sci. U.S.A.*, **20**, 169.
TOLMAN, R. C., 1939, *Phys. Rev.*, **56**, 364.
TOOPER, R. F., 1964, *Ap. J.*, **140**, 434.
TOOPER, R. F., 1965, *Ap. J.*, **142**, 1541.
TOOPER, R. F., 1966, *Ap. J.*, **143**, 465.
TSURUTA, S., 1964, unpublished *Ph. D. Thesis*, Columbia University.
TSURUTA, S., 1965, *Nature*, **207**, 364.
TSURUTA, S. and A. G. W. CAMERON, 1965*a*, *Nature*, **207**, 364.
TSURUTA, S. and A. G. W. CAMERON, 1965*b*, *Canadian J. Phys.*, **43**, 2056.
TSURUTA, S. and A. G. W. CAMERON, 1966*a*, *Canadian J. Phys.*, **44**, 1895.
TSURUTA, S. and A. G. W. CAMERON, 1966*b*, *Canadian J. Phys.*, **44**, 1863.
TSURUTA, S., J. P. WRIGHT and A. G. W. CAMERON, 1965, *Nature*, **206**, 1137.
WEBER, J., 1964, section in *Relativity, Groups and Topology*, C. DEWITT and B. DEWITT, eds. (New York).
WHEELER, J. A., 1962, *Geometrodynamics* (New York).
WHEELER, J. A., 1964*a*, chapter 10 of *Gravitation and Relativity*, H. Y. CHIU and W. F. HOFFMANN, eds. (New York).
WHEELER, J. A., 1964*b*, chapter in *Relativity, Groups and Topology*, C. DEWITT and B. DEWITT, eds. (New York).
WHEELER, J. A., 1965, lecture presented at Deutsche Akademie der Wissenschaften zu Berlin, November 1965; to be published.
WHEELER, J. A., 1966, article in *Annual Reviews of Astronomy and Astrophysics*, vol. **4**, L. GOLDBERG, ed. (Palo Alto, Cal.).
WRIGHT, J. P., 1964, *Phys. Rev.*, **136**, B 288.
WRIGHT, J. P., 1965, *Nature*, **208**, 65.
ZEE, A. and J. A. WHEELER, 1966, paper in preparation.
ZEL'DOVICH, YA. B., 1961, *Žurn. Eksp. Teor. Fiz.*, **41**, 1609; English translation in *Soviet Physics-JETP*, **14**, 1143 (1962).
ZEL'DOVICH, YA. B., 1962, *Žur. Eksp. Teor. Fiz.*, **43**, 1037; English translation in *Soviet Physics-JETP*, **16**, 732 (1963).
ZEL'DOVICH, YA. B. 1963*a*, *Usp. Fiz. Nauk*, **80**, 357; English translation in *Soviet Physics-Uspekhi*, **6**, 475.
ZEL'DOVICH, YA. B., 1963*b*, *Voprosi Kosmogonii*, **9**, 157, proceedings of the *Theoretical Seminar on Major Problems of Astrophysics*, Tarta, 7-13 July 1962 (Akademii Nauk SSSR, Moscow).
ZEL'DOVICH, YA. B. and I. D. NOVIKOV, 1964, *Usp. Fiz. Nauk*, **84**, 377; English translation in *Soviet Physics-Uspekhi*, **7**, 763 (1965).
ZEL'DOVICH, YA. B. and I. D. NOVIKOV, 1965, *Usp. Fiz. Nauk*, **86**, 447; English translation in *Soviet Physics-Uspekhi*, **8**, 522 (1966).
ZEL'DOVICH, YA. B. and M. A. PODURETS, 1964, *Doklady Acad. Nauk SSSR*, **156**, 57; English translation in *Soviet Physics-Doklady*, **9**, 373.